Dynamic Analysis of Harmonics in Electrical Systems

Möllerstedt, Erik

2000

Document Version:
Publisher's PDF, also known as Version of record

Dynamic Analysis of Harmonics in Electrical Systems

Erik Möllerstedt

Automatic Control

Dynamic Analysis of Harmonics in Electrical Systems

Dynamic Analysis of Harmonics in Electrical Systems

Erik Möllerstedt

Lund 2000

Till Anna

Department of Automatic Control
Lund Institute of Technology
Box 118
SE-221 00 LUND
Sweden

ISSN 0280–5316
ISRN LUTFD2/TFRT--1060--SE

Printed in Sweden by Bloms i Lund Tryckeri AB.
Lund 2000

Contents

Acknowledgments

In Cambridge you have to state that your dissertation does not includes anything which is the outcome of work done in collaboration. Guess I am lucky that this thesis is to be defended in Lund. There are many people, without whom this thesis would never have been in your hand.

First I would like to thank my supervisor Bo Bernhardsson, who has a unique blend of theoretical knowledge and practical know-how. He is also a very pedagogical inspirer and is extremely helpful in times of short deadlines. My second supervisor Anders Rantzer has also played an important role in the writing of this thesis. The project was initiated by Sven Erik Mattsson but, unfortunately, he left the department after I had finished my licentiate thesis.

One of the persons who have meant the most for my time at the department is Henrik Olsson. He was the one who convinced me to start my PhD studies when he was a most inspiring teaching assistant in the course in adaptive control. He also saw the need for our methods in the analysis of converter locomotives, and established invaluable contacts with Daimler-Chrysler, Adtranz, and ABB Corp. Research.

Many thanks goes to my PAL Johan Eker for helping me out with all sorts of computer problems, and for filling my ears with such lovely music.

I would also like to thank all colleagues at the department for six fantastic years. Especially I would like to mention Karl Johan Åström, Björn Wittenmark, and Per Hagander, for making every possible effort to make all of us to get on well. Not to mention the fifth floor babes. What would the world be like without you? I would also like to thank Leif Andersson for excellent computer support.

Many thanks to Henrik Sandberg for long-desired collaborations, and for giving me the possibility to leave everything half-finished, and to Andrey Ghulchak for many valuable comments on the manuscript.

During the years of this project I have always appreciated the help I have received from the people at IEA. Especially I would like to thank Olof Samuelsson, who always have time for discussions and has read numerous manuscripts during the years.

I would like to thank Alec Stothert for a very nice and interesting stay at ABB Corp. Research in Baden-Dättwil, and Markus Meyer at Adtranz, Zürich, for good collaborations.

I also want to mention my dear friends who looked after Albin during my first stumbling weeks on paternity leave; Kerstin, Loffe, Johan, Mor, Matti, Ingrid, Johan, Linda, Amalia, and Ingela.

My PhD studies have been financed within the Elektra project by Svenska Elföretagens Forsknings- och Utvecklings- Elforsk- AB, Statens Energimyndighet, and the Swedish National Board for Industrial and Technical Development (NUTEK).

Finally, thanks to all my friends and family who have encouraged me during all years. Most precious of all, however, has been, and will always be, my wife Anna, whose patience and support seem to be never-ending, and Hugo and Albin. I guess I am the luckiest man on earth!

Erik

1

Introduction

1.1 Motivation

Economical and environmental reasons force a more efficient use of the power networks. Improved network operation has been made possible with the introduction of active power electronic components for power conditioning, protection, and conversion. Characteristic for power electronics is that they have switching dynamics, and that they are highly dependent on control. The switching nature of power electronics results in increased harmonic injection into the grid.

The common approach to steady state stability analysis and control design, however, assumes sinusoidal conditions. This assumption is based on conditions in traditional power systems, where the amount of harmonics is neglectable. Even though harmonics exist, they are believed not to affect the stability of the system. Hence, harmonics are not considered in stability analysis. With an increasing amount of switching components attached to the grid, this picture has to change. Harmonics can lead to unpredicted interaction between components, which in worst case can lead to instability. To guarantee stable network operation, the dynamic aspects of the harmonics have to be considered. A problem is that such analysis is complicated, and as power systems are very large and complex, one has to rely on simplified analysis and simulations.

This thesis describes a method to combine the continuous dynamics of the power system with the switching power electronics. The idea is to linearize the system around the periodic steady-state operating point, which normally can be derived by assuming a sinusoidal grid voltage. The result is a linear time periodic (LTP) model, which captures the coupling between different frequencies that arise due to the periodic dynamics. A frequency domain framework is developed, and it is shown that many

results developed for common linear time invariant (LTI) systems can be generalized to time periodic systems. Hence, many existing results on robustness analysis, robust controller design and model reduction can be directly applied.

1.2 Contributions of the Thesis

A frequency domain framework for modeling and analysis of electrical systems with a mix of continuous and discrete dynamics is developed. This is an infinite dimensional transfer function matrix $\mathcal{H}(s)$ which describes the input-output relation for an LTP system in frequency domain

$$\begin{bmatrix} \vdots \\ Y(s-j\omega_0) \\ Y(s) \\ Y(s+j\omega_0) \\ \vdots \end{bmatrix} = \begin{bmatrix} & \vdots & \vdots & \vdots & \\ \cdots & H_{-1,-1}(s) & H_{-1,0}(s) & H_{-1,1}(s) & \cdots \\ \cdots & H_{0,-1}(s) & H_{0,0}(s) & H_{0,1}(s) & \cdots \\ \cdots & H_{1,-1}(s) & H_{1,0}(s) & H_{1,1}(s) & \cdots \\ & \vdots & \vdots & \vdots & \ddots \end{bmatrix} \begin{bmatrix} \vdots \\ U(s-j\omega_0) \\ U(s) \\ U(s+j\omega_0) \\ \vdots \end{bmatrix}.$$

With the HTF, analysis of LTP systems can be performed with methods developed for multi-input multi-output LTI systems.

The HTF approach is shown to be closely related to methods for LTP systems analysis of digital control systems. This means that many strong results developed for the analysis of the inter-sample behavior of sampled-data system also can be applied to power system analysis.

The HTF is an infinite dimensional operator, which for computations has to be approximated by a finite dimensional operator. This may lead to convergence problems. The concept of roll-off for LTP systems is defined and can be used to justify the use of truncated HTFs. Relations to power system modeling and the concept of computational causality are discussed.

The thesis contains four papers with different power system applications. Below, the contents of the papers is briefly summarized. References to related publications are also given. The work in Papers II, II, and IV, has been done in collaboration with people from the industry.

Paper I

Möllerstedt, E. and B. Bernhardsson: "Harmonic analysis of distribution networks." *Submitted Nov. 1999 to IEEE Trans. on Power Systems*.

Contributions

The paper presents a method to analyze the periodic steady-state solution of power distribution networks. Components with nonlinear and switching dynamics are replaced by Harmonic Norton Equivalents which describe the steady-state coupling between different harmonics. It is a harmonic balance approach, which utilize that the harmonic level in power system is low. This means that if the components are linearized at sinusoidal network conditions, the steady state solution of the total network can be obtained without iterative methods. The Harmonic Norton Equivalent is the steady state gain of the HTF, $\mathcal{H}(0)$. Hence, using the HTF, harmonic balance methods can be generalized to non-periodic conditions. A procedure for obtaining the models from measurements is also presented.

The paper is based on the licentiate thesis [Möllerstedt, 1998], the conference papers [Möllerstedt *et al.*, 1997a] and [Möllerstedt *et al.*, 1997b], and the technical reports [Möllerstedt *et al.*, 1997c], [Möllerstedt *et al.*, 1997d].

Paper II

Möllerstedt, E. and B. Bernhardsson (2000): "A harmonic transfer function model for a diode converter train." In *Proceedings of IEEE Power Engineering Society Winter Meeting 2000*, Singapore.

Contributions

This paper presents the analysis of a diode converter locomotive. Linearization around the nominal solution results in an LTP model which is used to derive the HTF of the locomotive. The nominal solution is obtained via time domain simulation. With this approach, a frequency domain model of the locomotive is obtained, avoiding complicated nonlinear frequency domain modeling. The model captures the dynamic coupling between the ac side and the dc side of the converter, taking into account the non-ideal commutation of the converter. The resulting frequency domain model is validated with simulations.

The model of the diode converter locomotive was derived in collaboration with Adtranz, Switzerland.

Paper III

Möllerstedt, E. and B. Bernhardsson (2000): "Out of control because of harmonics - an analysis of the harmonic response of an inverter locomotive." *IEEE Control Systems Magazine*, **20:4**, pp. 70–81.

Contributions

An LTP model of an inverter locomotive with force commuted high frequency converter is derived. By connecting the HTFs of the sub-models, the HTF of the complete locomotive, including the converter controller, is obtained. Since railway systems are single phase, the dynamic coupling between the ac side and the dc side of a converter is not captured by LTI models. Using the HTF, the system can be analyzed in frequency domain, which facilitates ways to assure stable operation of the locomotive. The amplitude margin for the controlled system is obtained from the generalized Nyquist theorem. The model of the inverter locomotive was derived in collaboration with Daimler-Chrysler, Germany, and Adtranz, Switzerland.

Paper IV

Möllerstedt, E., A. Stothert, and H. Sandberg: "Robust control of power converters." *To be submitted*.

Contributions

This paper presents a systematic approach to power converter modeling, applied to a micro-turbine line side converter. For a three-phase system, transformation to rotating coordinates results under ideal conditions in a time invariant model. Hence, linearization of the system results in an LTI model. A controller structure is proposed, which simplified converter control design and analysis. It is shown that the common objectives for converter control make linear quadratic optimal (LQ) control design suitable, and an LQ controller is derived from the nominal LTI model. The control design is evaluated with time domain simulation.

Harmonics, unbalanced ac systems, and switching dynamics of the converter implies that transformation to rotating coordinates results in a time-varying model. This means that stability cannot be guaranteed using LTI analysis only. Such non-ideal conditions are easily incorporated in the derived model, and the result is an LTP model. The model structure makes it straightforward to get the system on the so called standard form for robustness analysis. Integral Quadratic Constraints (IQCs) are used to evaluate the control design under non-ideal conditions. The paper is an extension of the work in [Möllerstedt and Stothert, 2000].

The model of the micro-turbine unit was derived in collaboration with ABB Corporate Research, Switzerland.

1.3 How to read the Thesis

The thesis consists of two parts:

Part I

In Part I the LTP system theory is developed. Chapter 2 describes concisely the concept of power system stability. In Chapter 3 background materials on LTP analysis is presented. The harmonic transfer function (HTF) is defined in Chapter 4, and it is related to the lifting approach to LTP system analysis. Using the HTF, a number of results from LTI theory are generalized to LTP systems. The HTF is an infinite dimensional operator, which for computations has to be approximated by a finite dimensional operator. This may lead to convergence problems, which is the focus of Chapter 5.

Part II

Part II consists of the four papers with power system applications for the developed LTP system theory.

Since each paper starts with a short introduction to the LTP theory, there is a considerable overlap. The theory sections in the papers show how the theory has evolved during the project. The material presented in Part I is written last, and is more complete and up-to-date. If the reader has done a good job on Part I of the thesis, he or she has the authors permission to skip the theory parts of the papers, or perhaps glance through them for the notation.

However, the reader may also start by reading the papers, and then, motivated by the applications, go back to selected sections of Part 1.

2

Power System Stability

A power system consists of a number of synchronous generators, which rotate synchronously and generate the power consumed by the loads. The generators are interconnected by the meshed transmission system. A number of distribution systems are also connected to the transmission system, via transformers that transform the high voltage of the transmission system to lower voltage levels. The distribution systems are in general radial and distribute the power to the loads.

The power transfer between two synchronously rotating machines depends on the rotor angle difference. Power is transfered from the leading machine, and the amount of transfered power is increased if the angular difference is increased. The angle-dependent torque is called the synchronizing torque: If a machine speeds up, it will automatically take a larger part of the total load and decelerate back to synchronous speed. This implies that power systems are self stabilizing.

As the load demand and the generation change continuously, the system must automatically adjust to the new conditions. Power system stability is the ability to keep the generators in synchronism, and to keep a desired voltage and frequency in the presence of load and generation variations and disturbances.

2.1 Power System Stability Analysis

Power systems are large, complex and highly nonlinear systems. Stability analysis has to be performed with simplified models. Depending on the nature of the potential instability, the size of the disturbance, and the time scale, different approaches to modeling and system analysis are used. This leads to a classification of power system stability. This classification is well known to power engineers, and can be found in any book on power system stability. A good reference is [Kundur, 1994].

Based on the nature of the potential instability the following classification is made:

Angle stability is the ability to keep the generators in synchronism. This is a problem of balancing active power, as imbalance in mechanical torque and electrical torque makes a generator accelerate or decelerate. If a generator speeds up, the load angle is increased, and the machine automatically takes a larger part of the load. This increases the electric torque and decelerates the machine. If this increase in electric torque is enough to stop the acceleration, the system remains in synchronism.

Voltage stability is the ability to supply the load with a high enough voltage. This is a problem of balancing reactive power. An inductive load supplied via a weak line leads to a large voltage drop across the line. The load voltage will then be low. Since many loads aim to draw constant power, a low voltage implies an increased current, which further increases the voltage drop. If the voltage drop cannot be compensated for by reactive power injection, the result may be a voltage collapse.

Frequency stability is the ability to keep the frequency steady at the reference frequency (for instance 50 or 60 Hz) under continuous load variations.

Stability analysis can also be classified depending on the size of the disturbance and the method used to analyze the problem. This leads to transient, or large signal, stability and steady state, or small signal, stability.

Transient stability The system must be able to withstand large disturbances like a line fault, or the loss of a generator. To keep the system stable and to return to a new steady state operating point, the system is dependent on fast operation of protection devices like breakers to clear the fault, and protection schemes for disconnecting and reconnecting components. Transients in power systems are fast phenomena, and include a mix of continuous dynamics and discrete events. The most common approach to transient analysis is time domain simulation, using Electro-Magnetic Transients Programs, like EMTP [EPRI, 1989]. Some work has also been done using energy functions and Lyapunov methods [Hiskens and Hill, 1989]. Correct transient stability analysis is dependent on accurate models, reflecting the relevant dynamics of the components and the network. This is a well established and mature area.

Small signal stability Power systems are stable but very oscillatory systems. Attempts to improve the transient stability often reduce the damping further. Damping is also reduced when power systems in separate regions are interconnected. If neighboring power systems are connected, reliability is improved and back up power can be shared between the systems. However, the interconnecting lines have limited transfer capabilities, which leads to weak couplings between the regions. The result is poorly damped swing modes, with strong regions swinging against each other. Under extreme conditions, the system becomes unstable. Stable operation is dependent on proper design and dimensioning of the transmission system.

In small signal analysis, the normal operation of the system is analyzed. Therefore protection devices do not have to be considered. Without the switching dynamics of the protection devices, the network can be analyzed with linear methods. The dominating dynamics come from the rotating machines, whose large masses result in time constants in the range of seconds. This implies that the rotational speed of the generators is kept close to the fundamental frequency (50 or 60 Hz), generating sinusoidal phase voltages.

Because of nonlinearities in the network, currents and voltages will always have a certain level of harmonics. Harmonics and unsymmetrical three phase signals result in a periodically pulsating torque on the generators, but the large masses of the synchronous machines make the influence of this negligible, and the system is well approximated by considering only the slow variations in the fundamental frequency component. Hence, normally only the fundamental frequency component of voltages and currents is considered, and the dynamics of the power lines are replaced by the fundamental frequency impedance, that is, a static gain. To fit in the linear framework, loads are normally modeled as constant current sinks, constant impedances, or constant power sinks.

2.2 Harmonic Analysis

The harmonics are traditionally seen as high frequency distortions that do not contribute to the dynamics of the system, and thus do not have to be considered in stability analysis. Harmonics are normally treated as a steady state problem, leading to increased losses, overheating, reduced life lengths of components, and malfunction of sensitive loads [Key and Lai, 1995]. As harmonics do not affect the stability of the system, a stable steady state operating point is always assumed in harmonic analysis.

A popular method for harmonic analysis is harmonic balance. This

is a frequency domain method which can be used iteratively to find the steady-state solution of a nonlinear network [Kundert and Sangiovanni-Vincentelli, 1986]. Nonlinear loads are modeled as harmonic current sources into a linear network. In each iteration the node voltages are calculated by solving a linear equation system, and then the nonlinear current sources are updated according to the improved node voltages. The convergence of the method can be improved by using Newton iterations. The Jacobian matrices used in such iterations are linear models of electric systems at non-sinusoidal conditions, and can be seen as the first linear time periodic models for power systems. The matrices describe the coupling between the Fourier coefficients of the currents and voltages. However, as only the steady state is concerned, these are static models and are not sufficient for stability analysis.

Modern Power Systems and Harmonic Instability

The introduction of power electronics in power systems has resulted in new possibilities for generation, transmission and protection. High-power electronic converters facilitate the connection systems of different frequencies. High voltage dc transmission has become a competitive alternative to ac transmission over large distances. Small flexible generation units have become an important complement to traditional large scale generation. These small units are often connected to the grid via power electronics. Fast switching power converters result in improved performance and reduced losses in electric drives. Power electronics is also used for improved reactive power compensation, where fast acting components like static var compensators or thyristor controlled series capacitors are used to maintain stable operation under a high degree of compensation.

The picture of power systems as slowly varying systems, whose stability can be determined by studying only the fundamental frequency, is changing. Power electronic devices tend to produce harmonics that may provide coupling between dynamic processes in different frequency ranges [Hauer and Taylor, 1998]. The harmonic coupling and the high complexity of the system, in combination with more stressed systems due to optimized operation, make proper analysis more and more important if stability and secure operation is to be guaranteed. The dynamic coupling between the component and the network, and between several of these components must be considered. This motivates the concept of *harmonic instability*, that is, stability problems that cannot be detected if only the fundamental frequency dynamics is considered.

The situation is particularly problematic in single phase systems, like railway networks. By considering sinusoidal conditions only, there is no way to describe the dynamic coupling between the AC dynamics and the DC dynamics of a modern locomotive. Hence, converter controllers have

to be tuned using ad hoc tuning rules verified by simulations. The regional railway system in Zürich suffered from harmonic instability twice in 1995. The traffic was operated by modern locomotives with high frequency power electronic converters. Due to improper controller software of the converters, the system became unstable and locomotives were shut down by protective equipment due to too high levels of the 6th harmonic (100 Hz) in the current. At the same time, a 165 Hz component of more that 2 kV could be observed in the voltage[Meyer, 1999].

The problem becomes emphasized in a deregulated power market. Much effort is made to get norms and standards that guarantee a safe operation of modern networks. Norms on harmonics only consider steady state harmonic interaction: How high harmonic levels must a component withstand, and how much harmonics may be injected into the grid, in steady state? This is not sufficient if stability is to be guaranteed. It is necessary to have some limits on the dynamic coupling. Forcing all components to be passive would, for instance, guarantee safe operation, but that is a too conservative demand.

A Sampled-Data System Analogy

The assumption that only the dynamics of the fundamental frequency is relevant is common in computer-controlled systems. The control is based on a sampled measurement of the process output, and the common approach is to consider the system only at the sampling instants. An anti-aliasing filter is used to make sure that no high frequencies are folded down to the sampled measurements. The control signal is applied to the process by means of a hold circuit, which keeps the control signal constant over each sampling period. This implies that high frequency harmonics are injected into the system. As the process is low pass, these high frequencies will be damped out, and no important information is lost during the sampling, as long as the sampling frequency is chosen high enough.

For a power system, this is equivalent to the assumption that only the fundamental frequency is relevant. The only difference is that the fast dynamics of the power electronic devices cannot be compensated for by choosing a higher sampling frequency. Unless the dynamics of the power electronic devices are controlled to be slow, the analysis methods must be changed, so that the frequency coupling is considered. There has been a lot of research on the inter-sample behavior of sample data systems. The system is then modeled as a linear time periodic (LTP) system. Because of the strong analogy, it is natural to try to adopt these methods to power system analysis. An LTP system is the result of linearization around a periodic solution. LTP systems capture the coupling between frequencies and can thus be used to analyze the local stability of the periodic solution, and what happens when that system is changed and new components are

added. The problem with LTP analysis is that it is somewhat more complicated than LTI analysis. However, if LTI analysis does not do the job, and simulation alone is not enough, LTP analysis might prove a valuable tool, despite the more complicated analysis.

3

Linear Time Periodic Systems

Because of the well-developed linear system theory, a common approach to system analysis is to linearize the system, and use the linearized models to analyze the local behavior of the system in the neighborhood of the linearization point.

Consider the nonlinear system

$$\begin{aligned} \frac{dx}{dt} &= f(x,u), \\ y &= g(x,u), \end{aligned}$$

where $x \in R^n$ are the state vector of the system, $u \in R^m$ is the input, and $y \in R^p$ is the output. If the system is linearized around the equilibrium point $\{x_0, u_0\}$, the result is a linear time invariant (LTI) system

$$\frac{dx}{dt} = Ax + Bu \tag{3.1}$$

$$y = Cx + Du, \tag{3.2}$$

with constant matrices

$$A = \frac{\partial f}{\partial x}(x_0,u_0), \qquad B = \frac{\partial f}{\partial u}(x_0,u_0),$$

$$C = \frac{\partial g}{\partial x}(x_0,u_0), \qquad D = \frac{\partial g}{\partial u}(x_0,u_0).$$

Linear time invariant systems have a number of properties that simplify the analysis. Stability is determined by the eigenvalues of the system matrix, A. The solution of the state equations (3.1) can be obtained analytically for given input $u(t)$ and initial state $x(t_0)$. A sinusoidal input

leads, in steady state, to a sinusoidal output of the same frequency. This frequency separation property, in combination with the linearity, makes the frequency domain attractive for input-output analysis of LTI systems.

If the system does not have an equilibrium point, the system can instead be linearized around a trajectory. The resulting linear model may then be time varying and describes the local behavior in the neighborhood of the trajectory. For general linear time varying systems, many of the nice properties of LTI systems fail to hold. For instance, even if the eigenvalues of the system matrix always remain in the left half plane, stability is not be guaranteed. The state equations do not have an analytical solution, and the frequency separation property is lost.

If the nominal trajectory, or solution, is periodic

$$\begin{aligned} u_0(t+T) &= u_0(t), \\ x_0(t+T) &= x_0(t), \end{aligned}$$

the result of the linearization is a linear time periodic (LTP) system

$$\begin{aligned} \frac{dx}{dt} &= A(t)x + B(t)u \\ y &= C(t)x + D(t)u, \end{aligned} \tag{3.3}$$

where

$$\begin{aligned} A(t) &= \frac{\partial f}{\partial x}(x_0(t), u_0(t)), & B(t) &= \frac{\partial f}{\partial u}(x_0(t), u_0(t)), \\ C(t) &= \frac{\partial g}{\partial x}(x_0(t), u_0(t)), & D(t) &= \frac{\partial g}{\partial u}(x_0(t), u_0(t)), \end{aligned}$$

are T-periodic matrices, that is, $A(t+T) = A(t)$ and similarly for $B(t)$, $C(t)$, and $D(t)$.

Periodic solutions typically arise in rotating mechanical systems. LTP systems have, for instance, for a long time been used to analyze helicopter dynamics, see for example [Wereley, 1991], [Hwang, 1997] and references therein. Periodic variations arise due to the rotation of the system. A good example is also a wind power plant, where there is a distortion in rotor torque when the rotor blade is in shadow of the tower. The periodic solution can also arise from the dynamics of the system, for instance self-excited oscillations, or limit cycles, of nonlinear systems, or in sample data system, where the periodicity arises from the periodic sampling of measured outputs and periodic updating of control signals. The periodicity implies that, to some extent, many properties of LTI systems can be generalized to hold also for LTP systems.

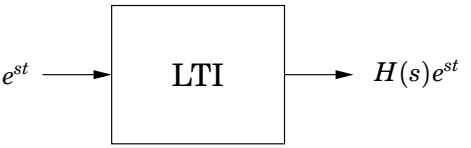

Figure 3.1 For an LTI system, the response to a complex exponential e^{st} is itself a complex exponential.

3.1 Frequency Separation of LTP Systems

A linear operator, H, is said to be time-invariant if, for every $\tau > 0$, it commutes with the shift operator, S_τ, defined by

$$S_\tau u(t) = u(t - \tau).$$

Let the input be a signal of a single complex frequency, s, that is, $u(t) = e^{st}$. This gives an output, denoted $y(t) = He^{st}$. The time invariance implies

$$y(t - \tau) = Hu(t - \tau) = He^{s(t-\tau)} = He^{st}e^{-s\tau} = e^{-s\tau}y(t),$$

where the last equality is due to the linearity of the system. This holds for any τ, in particular, $\tau = t$, and thus

$$y(t) = y(0)e^{st}.$$

The output is hence also a signal with the single frequency, s. This is the frequency separation property of LTI systems, see Fig. 3.1.

An LTP system only commutes with the shift operator when τ is a multiple of the period time T

$$HS_T = S_T H. \tag{3.4}$$

Now let the input be an exponentially modulated periodic (EMP) signal

$$u(t) = u_p(t)e^{st}, \tag{3.5}$$

where $u_p(t)$ is T-periodic. This gives an output $y(t) = Hu_p(t)e^{st}$, which due to the periodicity of the system is satisfies

$$y(t - T) = Hu(t - T) = Hu_p(t - T)e^{s(t-T)} = Hu_p(t)e^{st}e^{-sT} = y(t)e^{-sT}.$$

With $y_p(t) = y(t)e^{-st}$ this gives

$$y_p(t - T) = y(t - T)e^{-s(t-T)} = y(t)e^{-st} = y_p(t).$$

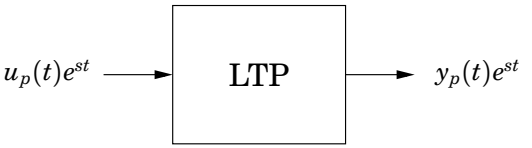

Figure 3.2 For an LTP system, the response to an EMP signal $u_p(t)e^{st}$ is itself an EMP signal.

Hence $y_p(t)$ is T-periodic. This means that the output $y(t) = y_p(t)e^{st}$ is an EMP signal. An LTP system hence maps EMP signals onto EMP signals, see Fig. 3.2. Expressing the periodic functions, u_p and y_p, with their Fourier series gives

$$u(t) = u_p(t)e^{st} = \sum u_k e^{jk\omega_0 t} e^{st} = \sum u_k e^{(s+jk\omega_0)t},$$

and similarly for $y(t)$. This means that for LTP systems there is coupling between frequencies separated by a multiple of the fundamental frequency, $\omega_0 = 2\pi/T$. This complicates the analysis of LTP systems in frequency domain.

3.2 LTP System Analysis

In this section the common approaches to analysis of LTP systems will be summarized briefly.

State Equation Solution

Consider the autonomous system

$$\frac{dx}{dt} = A(t)x(t), \qquad x(t_0) = x_0.$$

The solution of this system can be written

$$x(t) = \Phi(t, t_0)x_0,$$

where $\Phi(t, \tau)$ is the fundamental matrix, or state transition matrix of the system, satisfying

$$\frac{\partial}{\partial t}\Phi(t, \tau) = A(t)\Phi(t, \tau), \quad \Phi(\tau, \tau) = I. \tag{3.6}$$

For a system with external input $u(t)$

$$\frac{dx}{dt} = A(t)x(t) + B(t)u(t), \qquad x(t_0) = x_0,$$

the solution is given by

$$x(t) = \Phi(t, t_0)x_0 + \int_{t_0}^{t} \Phi(t, \tau)B(\tau)u(\tau)d\tau. \tag{3.7}$$

For a T-periodic linear system, the monodromy matrix

$$\Phi_T(t) = \Phi(t + T, t)$$

is a periodic matrix, describing how the states evolve over one period,

$$x(t + T) = \Phi_T(t)x(t).$$

The matrix $\Phi(t+T, t)$ is called the monodromy matrix at time t. The eigenvalues of the monodromy matrix are independent of t [Colaneri *et al.*, 1998]. These eigenvalues are the so called characteristic multipliers of $A(t)$. A T-periodic system is asymptotically stable if and only if all eigenvalues of the monodromy matrix are inside the unit disc.

For a linear time invariant system, the fundamental matrix is given by

$$\Phi(t, \tau) = e^{A(t-\tau)}.$$

For an LTP system there is no simple way to get an analytical expression for the fundamental matrix. Often one has to use time-domain simulation.

Floquet Decomposition

It was discovered by Floquet [Floquet, 1883], as early as 1883, that for any LTP system on state-space form (3.3), there is a T-periodic state transformation $x(t) = P(t)z(t)$, the so-called Floquet decomposition, that transfers the system to a similar state-space form with a constant (generally complex-valued) system matrix,

$$\begin{aligned} \frac{dz}{dt} &= \hat{A}z(t) + \hat{B}(t)u(t), \\ y(t) &= \hat{C}(t)z(t) + D(t)u(t). \end{aligned} \tag{3.8}$$

The state transformation implies that

$$\Phi(t, \tau) = P(t)\hat{\Phi}(t, \tau)P^{-1}(\tau) = P(t)e^{\hat{A}(t-\tau)}P^{-1}(\tau).$$

Inserting this into (3.6) gives that the T-periodic state transformation matrix satisfies

$$\frac{d}{dt}P(t) = A(t)P(t) - P(t)\hat{A}.$$

By choosing $P(0) = P(T) = I$, the constant matrix, $\hat{A}$, is given by

$$e^{\hat{A}T} = \Phi(T, 0),$$

that is, $\hat{A}T$ is the logarithm of the monodromy matrix of the system. Note that even if $A(t)$ is real valued, it might happen that a non-real complex matrix $\hat{A}$ is required. The eigenvalues of $\hat{A}$ are called the Lyapunov exponents of the system. The system is asymptotically stable if and only if all eigenvalues are in the open left half plane. This corresponds to the case when all eigenvalues of $\Phi(T, 0)$ are in the open unit disc.

Floquet decomposition can be used to determine stability of the system by time-invariant methods. The input-output relation is, however, still periodic.

Time Domain Analysis of Periodic Systems

Time domain methods for linear invariant systems are often straightforward to generalize to time periodic systems. Likewise, time periodic systems can be treated as a special case of linear time varying systems. The analysis often involves solving a time periodic equation. Stability, for instance, can be analyzed by means of Lyapunov theory. A periodic system is stable if the Lyapunov equation

$$\frac{d}{dt}P(t) = P(t)A^T(t) + A(t)P(t) + Q(t), \tag{3.9}$$

has a unique positive-definite solution $P(t)$, for $Q(t)$ periodic and positive-definite. The solution of (3.9) is [Kano and Nishimura, 1996]

$$P(t) = \Phi^T(0, t)P_0\Phi(0, t) - \int_0^t \Phi^T(s, t)Q(s)\Phi(s, t)ds,$$

where $P_0 = P(0)$. A T-periodic solution has $P(T) = P_0$, and thus for $t = T$ we have

$$P_0 = \Phi^T(0, T)P_0\Phi(0, T) - \int_0^T \Phi^T(s, T)Q(s)\Phi(s, T)ds.$$

This is an algebraic Lyapunov equation in discrete time. Lyapunov equations are used to determine exponential stability of periodic orbits in [Hauser and Chung, 1994].

The periodic pair $\{A(t), B(t)\}$ is said to be stabilizable if there exist a T-periodic $L(t)$ such that $A(t) - B(t)L(t)$ is stable. Likewise, the pair $\{A(t), C(t)\}$ is said to be detectable if there exist a T-periodic $K(t)$ such that $A(t) - K(t)C(t)$ is stable [Bittanti and Bolzern, 1986], [Colaneri *et al.*, 1998].

Another example where a periodic equation occurs is linear quadratic optimal (LQ) control, where the aim is to derive the state feedback gain $u(t) = -L(t)x(t)$ that minimizes a quadratic loss function

$$J = \int_0^\infty x^T M_x x + u^T M_u u dt.$$

Provided some technical conditions are fulfilled, the optimal feedback gain is given by

$$L(t) = M_u(t)^{-1} B(t)^T R(t),$$

where $R(t)$ is the unique T-periodic positive definite solution of the periodic Riccati equation

$$-\frac{d}{dt}R(t) = A(t)^T R(t) + R(t)A(t) - R(t)B(t)M_u(t)^{-1}B(t)^T R(t) + M_x(t).$$

Pole placement control design cannot be used in a straightforward way, since the eigenvalues of a periodic system are time varying. However, the characteristic multipliers of $A(t)$, that is, the eigenvalues of the monodromy matrix, $\Phi(T, 0)$, are independent of t. Hence, one possible design strategy would be to find a feedback gain $L(t)$ that gives the desired characteristic multipliers of the system [Tornambè and Valigi, 1996].

Frequency Domain Analysis of Periodic Systems

Frequency domain methods are often used for analysis and control design of linear time invariant systems. The strength of the frequency domain is the frequency domain separation of LTI systems, which implies that the systems can be analyzed frequency by frequency. Since this does not hold for periodic systems, as discussed in Section 3.1, frequency domain methods for LTI systems do not generalize to the periodic case. One way to get around this problem is to transform the periodic system to a time invariant equivalent representation. This will be explained in the next section.

3.3 Transformation to Time Invariant Representations

To be able to exploit frequency domain methods to analyze LTP systems, the systems can be transformed to equivalent time invariant representa-

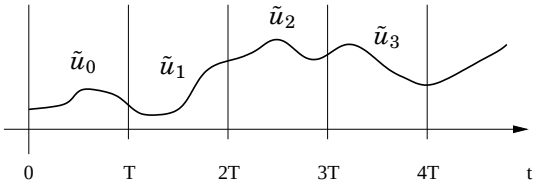

Figure 3.3 By splitting up the signals in segments $\tilde{u}_k(t)$ of length T, a T-periodic continuous time system can be transformed to a discrete time invariant system whose inputs and outputs are sequences of segments in $L_2[0,T]$.

tions. Two popular transformations are lifting and the cyclic reformulation. These are closely related; lifting leads to a more compact representation, whereas the cyclic representation [Colaneri and Kučera, 1997] is more appropriate for model reduction, as the structure of the original LTP system can be preserved.

Lifting

One way to analyze LTP systems in frequency domain is to use lifting techniques to transform a continuous time or discrete time LTP system to a discrete time LTI system, which can be analyzed with LTI methods. Lifting is a common approach to analyze the inter-sample behavior of sampled-data systems [Bamieh and Pearson, 1992], [Yamamoto and Khargonekar, 1996], [Dullerud, 1996].

For a continuous time system, lifting implies splitting the continuous input $u(t)$ into segments, $\tilde{u}_k$, of length T, as shown in Fig. 3.3, and analyzing how these segments are mapped onto similar segments of the output, $\tilde{y}_k$. If the original signal, $u(t)$, is in $L_2(-\infty,\infty)$, that is,

$$||u||^2 = \int_{-\infty}^{\infty} |u(t)|^2 dt < \infty,$$

then the lifted signal, $\tilde{u}$, is in $l_{2(L_2[0,T])}$, that is, the sum of the $L_2[0,T]$-norms of the segments is bounded.

$$||\tilde{u}||^2 = \sum_{k=-\infty}^{\infty} \int_0^T |\tilde{u}_k(t)|^2 dt = ||u||^2 < \infty.$$

As the norms are equal, lifting is an isometric mapping.

With lifted signals, a causal LTP system $H : L_2(-\infty,\infty) \to L_2(-\infty,\infty)$ is transformed to the discrete time system $\widetilde{H} : l_{2(L_2[0,T])} \to l_{2(L_2[0,T])}$. Using the fact that $h(t+T,\tau+T) = h(t,\tau)$ gives

$$\tilde{y}_n = H_{[0]}\tilde{u}_n + H_{[1]}\tilde{u}_{n-1} + H_{[2]}\tilde{u}_{n-2} + \ldots, \tag{3.10}$$

where the operator $H_{[k]} : L_2([0,T]) \to L_2([0,T])$ is defined via

$$(H_{[k]}v)(t) = \int_0^T h(kT+t,\tau)v(\tau)d\tau, \quad t \in [0,T].$$

More illustrative is to write (3.10) on vector form

$$\begin{bmatrix} \vdots \\ \tilde{y}_{n-1} \\ \tilde{y}_n \\ \tilde{y}_{n+1} \\ \vdots \end{bmatrix} = \begin{bmatrix} \ddots & \ddots & \ddots & \ddots & \ddots \\ \ddots & H_{[0]} & 0 & 0 & \ddots \\ \ddots & H_{[1]} & H_{[0]} & 0 & \ddots \\ \ddots & H_{[2]} & H_{[1]} & H_{[0]} & \ddots \\ \ddots & \ddots & \ddots & \ddots & \ddots \end{bmatrix} \begin{bmatrix} \vdots \\ \tilde{u}_{n-1} \\ \tilde{u}_n \\ \tilde{u}_{n+1} \\ \vdots \end{bmatrix}$$

The fact that lifting is isometric implies that if the original system, H, is bounded, then the lifted system $\widetilde{H}$ is also bounded and the induced L_2-norm of the original system equals the induced l_2-norm of the lifted system [Bamieh and Pearson, 1992], that is,

$$||H||_{L_2} = ||\widetilde{H}||_{l_2},$$

where

$$||H||_{L_2} = \sup_{\substack{u \in L_2 \\ u \neq 0}} \frac{||Hu||_{L_2}}{||u||_{L_2}},$$

$$||\widetilde{H}||_{l_2} = \sup_{\substack{\tilde{u} \in l_2 \\ \tilde{u} \neq 0}} \frac{||\widetilde{H}\tilde{u}||_{L_2}}{||\tilde{u}||_{L_2}}.$$

Transfer Functions for Lifted Systems

A lifted signal, $\tilde{u}$, can be transformed to frequency domain via the z-transform

$$\widehat{U}(z) = (Z\tilde{u})(z) = \sum_{k=-\infty}^{\infty} \tilde{u}_k z^{-k},$$

which is defined for those z for which the sum converges absolutely. For such z, $\widehat{U}(z) \in L_2[0,T]$. The z-transform maps an infinite sequence of

$L_2[0,T]$-functions to one $L_2[0,T]$-function that depends on the complex variable z. The infinite sequence can be recaptured with the inverse transform

$$\tilde{u}_k = \frac{1}{2\pi j}\oint \widehat{U}(z)z^{k-1}dz, \quad k = 0,1,...$$

where the integration contour encloses all singularities of $\widehat{U}(z)$. Using the z-transform, an LTP system can be analyzed by analyzing the response to an $L_2[0,T]$-valued function of z, $\widehat{U}(z)$, instead of analyzing the response to an infinite sequence of $L_2[0,T]$-functions. The input-output relation can now be written

$$\begin{aligned}\widehat{Y}(z) &= \sum_{k=-\infty}^{\infty} \tilde{y}_k z^{-k} = \sum_{k=-\infty}^{\infty}\sum_{l=0}^{\infty} H_{[l]}\tilde{u}_{k-l}z^{-k} \\ &= \left(\sum_{l=0}^{\infty} H_{[l]}z^{-l}\right)\left(\sum_{m=-\infty}^{\infty}\tilde{u}_m z^{-m}\right) = \widehat{H}(z)\widehat{U}(z),\end{aligned}$$

where the transfer function operator

$$\widehat{H}(z) = \left(\sum_{l=0}^{\infty} H_{[l]}z^{-l}\right)$$

is the z-transform of the sequence of lifted operators $\{H_{[l]}\}$. Note that the summation only involves $l \geq 0$ as H is assumed causal. An H_∞ norm of the operator $\widehat{H}$ is defined as

$$||\widehat{H}||_\infty = \sup_{|z|\geq 1}||\widehat{H}(z)||$$

As the z-transform is isometric, this norm is equal to the induced L_2-norm of the original system H [Bamieh and Pearson, 1992], that is,

$$||H||_{L_2} = ||\widehat{H}||_\infty. \tag{3.11}$$

A State-Space System

The lifted representation of a system on state-space form becomes

$$\begin{aligned}x_{k+1} &= \widetilde{A}x_k + \tilde{B}\tilde{u}_k \\ \tilde{y}_k &= \widetilde{C}x_k + \widetilde{D}\tilde{u}_k.\end{aligned} \tag{3.12}$$

Here $x_k \in R^n$ and the functions $\tilde{u}_k \in L_2^m[0,T]$ and $\tilde{y}_k \in L_2^p[0,T]$ are defined as $\tilde{u}_k = u(t+kT)$ and $\tilde{y}_k = y(t+kT)$ for $k \in Z$, and $t \in [0,T]$.

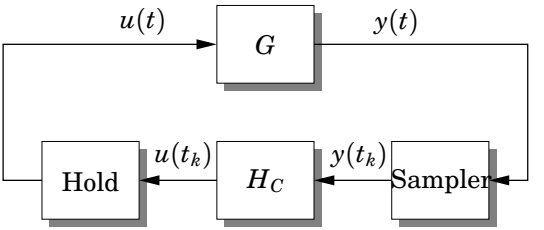

Figure 3.4 A sample data system consisting of a continuous time process controlled by a discrete time controller. A sampler (A/D converter) is used to get sampled process output data to the controller, and a hold circuit (D/A converter) converts the discrete control signal to continuous time.

The operators $\widetilde{A} : R^n \to R^n$, $\widetilde{B} : L_2^m[0,T] \to R^n$, $\widetilde{C} : R^n \to L_2^p[0,T]$, and $\widetilde{D} : L_2^m[0,T] \to L_2^p[0,T]$ are given by

$$\begin{aligned}
\widetilde{A} &= \Phi(T,0) \\
\widetilde{B}\tilde{u}_k &= \int_0^T \Phi(T,\tau)B(\tau)\tilde{u}_k(\tau)\,d\tau \\
\widetilde{C} &= C(t)\Phi(t,0) \\
\widetilde{D}\tilde{u}_k &= \int_0^t (C(t)\Phi(t,\tau)B(\tau) + D(t)\delta(t-\tau))\tilde{u}_k(\tau)\,d\tau.
\end{aligned}$$

The transfer function operator for a system on state space form becomes

$$\widehat{H}(z) = \widetilde{C}(zI - \widetilde{A})^{-1}\widetilde{B} + \widetilde{D}.$$

and is defined if z is not an eigenvalue of $\widetilde{A}$.

3.4 An LTP Model of a Sampled-Data System

For later reference, we will now show how a sampled-data system, that is, a continuous time process controlled by a discrete time controller, can be modeled as an LTP system in continuous time.

A typical sample data system is shown in Fig. 3.4. A continuous time system G is controlled by a discrete controller H. The continuous output from the system, $y(t)$, is converted to a discrete time sampled signal by the A/D-converter, or sampler. The controller use the sampled output to calculate a control signal, which is converted back to continuous time by a D/A converter, or hold circuit.

It is well known that the sampling results in aliasing, or frequency folding. For a sampled signal there is no way to separate frequencies that are separated by a multiple of the sampling frequency. The hold circuit converts the discrete control signal to a piecewise constant continuous time signal. This results in high frequency distortion into the system.

The common approach to analysis of sample data systems is to treat the combination of the hold circuit, the continuous process and the sampler as a discrete time system, which is controlled by a discrete time controller. This way, the system is only considered at the sampling instants. If the sampling frequency is high enough, the sampled output gives a good picture of the continuous time output of the process. An anti-aliasing filter is used to avoid that high frequency noise is folded down to the sampled signal. The high frequencies generated by the hold circuit do not affect the system if the dominating dynamics are of lower frequency. The choice of sampling frequency is normally done by a rule of thumb, based on the open loop or closed loop dynamics of the system [Åström and Wittenmark, 1997].

Proper process behavior cannot be guaranteed using assumptions and rules of thumb. Even though the sampled output of the system looks good, there can be hidden oscillations due to the high frequencies injected into the system. There has been a lot of research on the inter-sample behavior of sample data systems, for a good introduction and overview, see [Bamieh and Pearson, 1992].

The common approach to inter-sample analysis is to model the system as a continuous time LTP system, see for example [Åström and Wittenmark, 1997]. The discrete signal is in continuous time represented by an impulse train. This way the relation between the continuous time signal, $y(t)$, and the sampled signal, $y^*(t)$, is

$$y^*(t) = \sum_k \delta(t - kT)y(t_k) = \sum_k \delta(t - kT)y(t),$$

where T is the sampling time. Hence, the sampling can be described by a multiplication operator $y^* = my$, where

$$m(t) = \sum_k \delta(t - kT).$$

By writing $y(t_k) = \int_{-\infty}^{\infty} \delta(\tau - kT)y(\tau)d\tau$, the sampled signal can be expressed as a convolution

$$y^*(t) = \sum_k \delta(t - kT) \int_{-\infty}^{\infty} \delta(\tau - kT)y(\tau)d\tau = \int_{-\infty}^{\infty} h(t,\tau)y(\tau)d\tau,$$

where

$$h(t,\tau) = \sum_k \delta(t - kT)\delta(\tau - kT)$$

is the impulse response of the sampler.

With the sampled signal modeled as above, the input to the discrete time controller is a periodic impulse train. This means that the discrete time controller can be modeled as an LTI system. The periodicity is assured by the fact that the input is periodic. The continuous time transfer function for the controller is obtained from the discrete time transfer function $H(z)$ as

$$Y^*(s) = H_C(e^{sT})U^*(s).$$

The hold circuit keeps the signal constant over one sampling period. The impulse response should thus be a unit pulse with duration equal to the sampling time. This gives the transfer function

$$H_{hold}(s) = \frac{1 - e^{-sT}}{s}.$$

With this, instead of studying the feedback connection of a discrete time system and a discrete time controller, the system can be analyzed by studying the feedback connection of the continuous time LTI system $G(s)$ and an LTP continuous time controller.

A problem with this modeling approach is that the sampling operator is not bounded from L_2 to l_2. One way to get around this is to place a linear filter, H_f, without a direct term in front of the sampler. the operator mH_f is bounded from L_2 to l_2.

4

The Harmonic Transfer Function

In this chapter, a continuous time transfer function for linear time periodic (LTP) systems is derived based on the impulse response. The approach is closely related to the time dependent transfer function for general time.varying systems described in [Zadeh, 1950], and [Ball *et al.*, 1995], and the frequency response operator.

4.1 The Harmonic Transfer Function

The input-output relation of a linear time invariant (LTI) system is conveniently described in the frequency domain as

$$Y(s) = H(s)U(s),$$

where $U(s)$ and $Y(s)$ are Laplace transforms of the input and output respectively. The transfer function, $H(s)$ is defined as $H(s) = \mathcal{L}h$, where $h(t)$ is the impulse response of the system.

We saw in the previous chapter that for an LTP system there is coupling between frequencies separated by a multiple of the fundamental frequency, ω_0, of the system. In frequency domain, this means that there is coupling between $U(s + jm\omega_0)$ and $Y(s + jn\omega_0)$. This coupling can be described by the transfer function $H_{n,m}(s)$, Hence,

$$Y(s + jn\omega_0) = H_{n,m}(s)U(s + jm\omega_0).$$

However, there is coupling for all $m, n = 0, \pm 1, \pm 2, \ldots$. This gives

$$\begin{bmatrix} \vdots \\ Y(s-j\omega_0) \\ Y(s) \\ Y(s+j\omega_0) \\ \vdots \end{bmatrix} = \begin{bmatrix} \vdots & \vdots & \vdots & \vdots & \\ \cdots & H_{-1,-1}(s) & H_{-1,0}(s) & H_{-1,1}(s) & \cdots \\ \cdots & H_{0,-1}(s) & H_{0,0}(s) & H_{0,1}(s) & \cdots \\ \cdots & H_{1,-1}(s) & H_{1,0}(s) & H_{1,1}(s) & \cdots \\ & \vdots & \vdots & \vdots & \ddots \end{bmatrix} \begin{bmatrix} \vdots \\ U(s-j\omega_0) \\ U(s) \\ U(s+j\omega_0) \\ \vdots \end{bmatrix}, \tag{4.1}$$

or short

$$\mathcal{Y}(s) = \mathcal{H}(s)\mathcal{U}(s).$$

The doubly infinite matrix $\mathcal{H}(s)$ is called the harmonic transfer function (HTF). The HTF implies that an LTP system can be analyzed as an LTI system with infinitely many inputs and outputs. In this chapter it is shown how the elements $H_{n,m}(s)$ are obtained from time domain information of the system. It is also shown that the HTF is equivalent to the transfer function for the lifted system, with a special choice of base functions. Some basic properties and stability results are also given. The fact that the HTF is infinite dimensional implies a number of numerical difficulties. For computations, the infinite dimensional matrix has to be replaced by a finite dimensional truncated matrix. Questions about truncation errors and convergence will be treated in Chapter 5.

The HTF $\mathcal{H}(j\omega)$ is equivalent to the frequency response operator used for analysis of sampled-data systems in [Yamamoto and Khargonekar, 1996] and [Araki *et al.*, 1996].

4.2 Structure of the HTF

The response to a signal $u(t) \in L_2[0, \infty)$ is for a causal linear system given by

$$y(t) = \int_0^t h(t, \tau)u(\tau)d\tau,$$

where $h(t, \tau)$ is the impulse response, which for an LTP system satisfies

$$h(t + T, \tau + T) = h(t, \tau).$$

The function $h(t, t - r)$ is, for any fixed r, periodic in t and can, under appropriate convergence conditions, be expressed as a Fourier series

$$h(t, t - r) = \sum_{k=-\infty}^{\infty} h_k(r)e^{jk\omega_0 t},$$

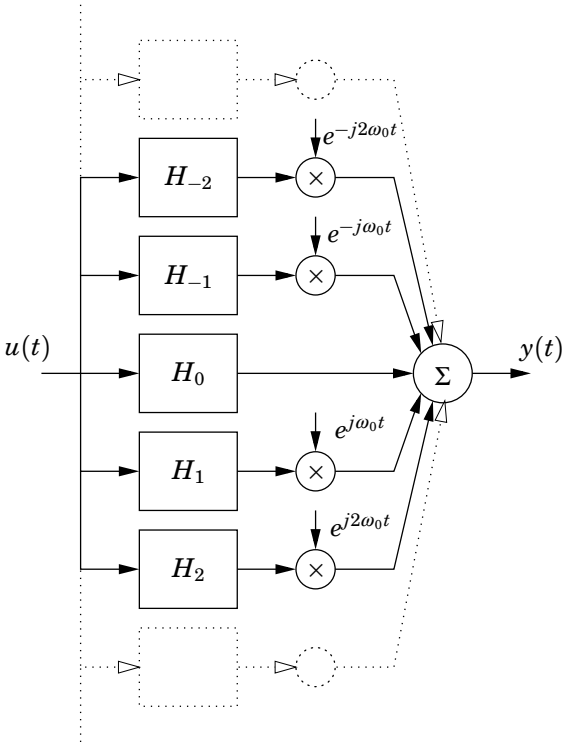

Figure 4.1 The input-output relation of an LTP system can be expressed by infinitely many LTI systems.

with

$$h_k(r) = \frac{1}{T}\int_0^T e^{-jk\omega_0 t} h(t, t-r)dt. \tag{4.2}$$

The impulse response of an LTP system can hence be written as an infinite sum of (possibly complex valued) LTI impulse responses

$$h(t,\tau) = \sum_{k=-\infty}^{\infty} h_k(t-\tau)e^{jk\omega_0 t}, \tag{4.3}$$

The input output relation corresponding to (4.3) is shown in Fig. 4.1, and

can be expressed as an infinite sum of convolutions

$$\begin{aligned} y(t) &= \int_0^t \sum_k h_k(t-\tau) e^{jk\omega_0 t} u(\tau) d\tau \\ &= \int_0^t \sum_k h_k(t-\tau) e^{jk\omega_0 (t-\tau)} u(\tau) e^{jk\omega_0 \tau} d\tau \\ &= \sum_k \int_0^t h_k(t-\tau) e^{jk\omega_0 (t-\tau)} u(\tau) e^{jk\omega_0 \tau} d\tau = \sum_k (h_k(t) e^{jk\omega_0 t} * u(t) e^{jk\omega_0 t}), \end{aligned}$$

where it is assumed that the order of integration and summation can be changed. Laplace transformation gives

$$Y(s) = \sum_k H_k(s - jk\omega_0) U(s - jk\omega_0), \tag{4.4}$$

with

$$H_k(s) = \mathcal{L} h_k = \int_0^\infty e^{-sr} h_k(r) dr.$$

Hence, $Y(s + jn\omega_0)$ is given by

$$\begin{aligned} Y(s + jn\omega_0) &= \sum_k H_k(s + j(n-k)\omega_0) U(s + j(n-k)\omega_0) \\ &= \sum_m H_{n-m}(s + jm\omega_0) U(s + jm\omega_0), \end{aligned} \tag{4.5}$$

which gives for the elements in the HTF

$$H_{n,m}(s) = H_{n-m}(s + jm\omega_0).$$

This gives the HTF a diagonal structure

$$\mathcal{H}(s) = \begin{bmatrix} \ddots & \ddots & \ddots & \ddots & \ddots \\ \ddots & H_0(s - j\omega_0) & H_{-1}(s) & H_{-2}(s + j\omega_0) & \ddots \\ \ddots & H_1(s - j\omega_0) & H_0(s) & H_{-1}(s + j\omega_0) & \ddots \\ \ddots & H_2(s - j\omega_0) & H_1(s) & H_0(s + j\omega_0) & \ddots \\ \ddots & \ddots & \ddots & \ddots & \ddots \end{bmatrix}. \tag{4.6}$$

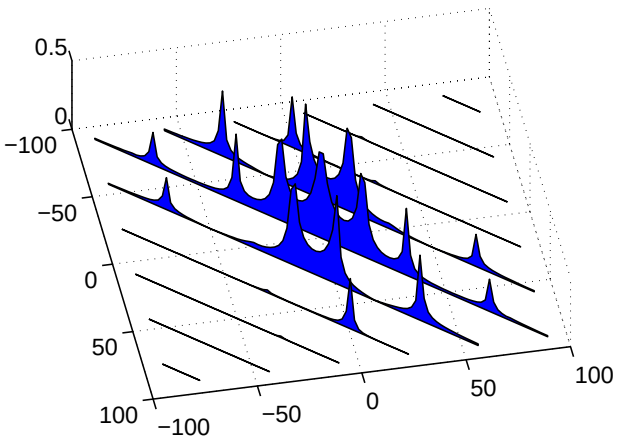

Figure 4.2 A Bode amplitude plot for an LTP system. The plot clearly shows a diagonal structure which comes from the fact that for LTP systems there is coupling between frequencies separated by the fundamental frequency of the system. The plot shows the bode amplitude of the LTI transfer function $H_k(j\omega)$ on the kth diagonal.

A Bode Amplitude Plot

The Bode plot is a popular way to graphically illustrate the frequency response of an LTI system. The Bode amplitude plot is a two dimensional plot with frequency on the x-axis, and gain on the y-axis. Because of the frequency coupling, a Bode amplitude plot for LTP system is three dimensional, with input frequency on the x-axis, output frequency on the y-axis, and gain on the z-axis. The Bode amplitude plot is obtained by plotting the absolute values of the elements of $\mathcal{H}(j\omega)$ for $-\omega_0/2 < \omega < \omega_0/2$. An example is shown in Fig. 4.2. The LTI transfer functions, $H_k(j\omega)$ are shown as diagonals.

Symmetry

For a real-valued LTI system H the transfer function satisfies the symmetry

$$H(s) = \overline{H(\overline{s})},$$

where $\overline{s}$ denotes complex conjugate of s. This means that the system only positive frequencies has to be considered, and that poles and zeros always come in conjugate pairs. The observant reader can see that $|H_k(j\omega)|$ in Fig. 4.2 is not symmetric. This is because the impulse response $h_k(t)$ (4.2) can be complex valued.

The following symmetry holds for the harmonic transfer function. It

shows that the poles and zeros of the HTF $\mathcal{H}$ come in conjugate pairs, even though this does not necessarily hold for the individual transfer functions, $H_k(s)$, since they can have complex coefficients.

THEOREM 4.1
If $h(t,\tau)$ is real-valued then

$$H_{-n,-m}(s) = \overline{H_{n,m}(\overline{s})}.$$

PROOF 4.1
As the impulse response $h(t,\tau)$ is real valued, it holds that

$$h_{-k}(r) = \overline{h_k(r)}.$$

This gives for the transfer functions

$$H_{-k}(s) = \int e^{-st} h_{-k}(t)dt = \overline{\int e^{-\overline{s}t} h_k(t)dt} = \overline{H_k(\overline{s})}.$$

Since element (n,m) in the HTF is defined as

$$H_{n,m}(s) = H_{n-m}(s + jm\omega_0),$$

a direct computation gives that

$$H_{-n,-m}(s) = H_{-(n-m)}(s - jm\omega_0) = \overline{H_{n-m}(\overline{s} + jm\omega_0)} = \overline{H_{n,m}(\overline{s})}.$$

HTF for Systems on State Space Form

In [Wereley, 1991] the harmonic transfer function matrix (HTF) for LTP systems on state space form is defined via a direct computation of the response to exponentially modulated periodic (EMP) signals (3.5). The method is based on the harmonic balance approach in [Hill, 1886]. If the input to an LTP system is EMP, then, in steady state, the state vector and output will also be EMP

$$\begin{aligned}
u(t) &= \sum_m U_m e^{s_m t}, \\
x(t) &= \sum_m X_m e^{s_m t}, \\
\frac{dx}{dt} &= \sum_m s_m X_m e^{s_m t}, \\
y(t) &= \sum_m Y_m e^{s_m t},
\end{aligned}$$

where $s_m = s + jm\omega_0$. Inserting this into (3.3) gives

$$\sum_n s_n X_n e^{s_n t} = \sum_n \left(\sum_m A_{n-m} X_m + \sum_m B_{n-m} U_m \right) e^{s_n t},$$
$$\sum_n Y_n e^{s_n t} = \sum_n \left(\sum_m C_{n-m} X_m + \sum_m D_{n-m} U_m \right) e^{s_n t},$$

where A_k, B_k, C_k, and D_k are the Fourier coefficients of the periodic system matrices. The principle of harmonic balance now implies that these equations must be fulfilled for each frequency, s_n. This can be written in a compact way

$$s\mathcal{X} = (\mathcal{A} - \mathcal{N})\mathcal{X} + \mathcal{B}\mathcal{U} \tag{4.7}$$
$$\mathcal{Y} = \mathcal{C}\mathcal{X} + \mathcal{D}\mathcal{U}, \tag{4.8}$$

where $\mathcal{U}$, $\mathcal{X}$, and $\mathcal{Y}$ are vectors of Fourier coefficients

$$\mathcal{U} = [\ldots \quad U_{-2} \quad U_{-1} \quad U_0 \quad U_1 \quad U_2 \quad \ldots]^T,$$

etc., and $\mathcal{A}$, $\mathcal{B}$, $\mathcal{C}$, and $\mathcal{D}$ are Toeplitz matrices of Fourier coefficients

$$\mathcal{A} = \begin{bmatrix} \ddots & \ddots & \ddots & \ddots & \ddots \\ \ddots & A_0 & A_{-1} & A_{-2} & \ddots \\ \ddots & A_1 & A_0 & A_{-1} & \ddots \\ \ddots & A_2 & A_1 & A_0 & \ddots \\ \ddots & \ddots & \ddots & \ddots & \ddots \end{bmatrix},$$

etc., and $\mathcal{N}$ is a block diagonal matrix

$$\mathcal{N} = \text{blkdiag}\{jn\omega_0 I\}.$$

By eliminating the state vector $\mathcal{X}$ in (4.7), the harmonic transfer function, $\mathcal{H}(s)$, is obtained as

$$\mathcal{Y} = (\mathcal{C}(sI - (\mathcal{A} - \mathcal{N}))^{-1}\mathcal{B} + \mathcal{D})\mathcal{U} = \mathcal{H}(s)\mathcal{U}. \tag{4.9}$$

4.3 Examples

The HTFs will now be derived for some simple but illustrative examples.

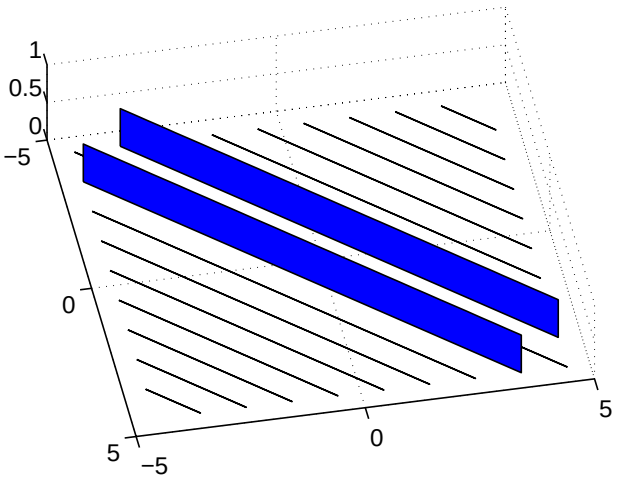

Figure 4.3 The Bode amplitude plot of a sinusoidal multiplication operator, $y(t) = \sin t \cdot u(t)$.

Example 1: Multiplication Operators A simple LTP system is multiplication with a sinusoid

$$y(t) = \sin(\omega_0 t) \cdot u(t).$$

The response to an EMP signal is

$$\begin{aligned} y(t) &= \frac{e^{j\omega_0 t} - e^{-j\omega_0 t}}{2j} \sum_m u_m e^{s_m t} \\ &= \sum_m u_m \frac{e^{s_{m+1} t} - e^{s_{m-1} t}}{2j} = \sum_m \frac{u_{m-1} - u_{m+1}}{2j} e^{s_m t} = \sum y_m e^{s_m t}. \end{aligned}$$

The HTF of the multiplication operator is thus

$$\mathcal{H}_{\sin} = \frac{1}{2j} \begin{bmatrix} \ddots & \ddots & \ddots & \ddots & \ddots & \ddots \\ \ddots & 0 & -1 & 0 & \ddots & \ddots \\ \ddots & 1 & 0 & -1 & 0 & \ddots \\ \ddots & 0 & 1 & 0 & -1 & \ddots \\ \ddots & \ddots & 0 & 1 & 0 & \ddots \\ \ddots & \ddots & \ddots & \ddots & \ddots & \ddots \end{bmatrix},$$

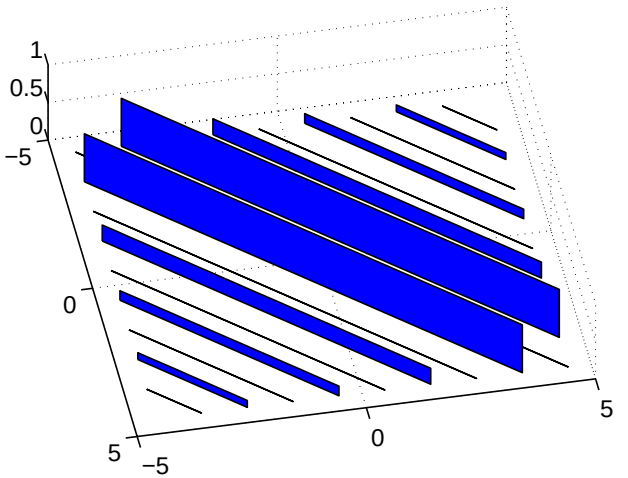

Figure 4.4 The Bode amplitude plot of a square wave multiplication operator.

that is, a constant matrix, independent of the complex frequency s, with the Fourier coefficients of $\sin \omega_0 t$ on the first off diagonals. Similar calculations give that for a general T-periodic multiplication operator

$$y(t) = D(t)u(t)$$

the HTF, $\mathcal{H}(s)$, is a Toeplitz matrix

$$\mathcal{H}(s) = \begin{bmatrix} \ddots & \ddots & \ddots & \ddots & \ddots & \ddots \\ \ddots & D_0 & D_{-1} & D_{-2} & \ddots & \ddots \\ \ddots & D_1 & D_0 & D_{-1} & D_{-2} & \ddots \\ \ddots & D_2 & D_1 & D_0 & D_{-1} & \ddots \\ \ddots & \ddots & D_2 & D_1 & D_0 & \ddots \\ \ddots & \ddots & \ddots & \ddots & \ddots & \ddots \end{bmatrix},$$

where D_k are the Fourier coefficients of $D(t)$.

Note that a multiplication operator can be seen as a state space system with only a D matrix. The result is thus covered by (4.9), with $\mathcal{H}(s) = \mathcal{D}$. It can also be obtained from the impulse response of a multiplication

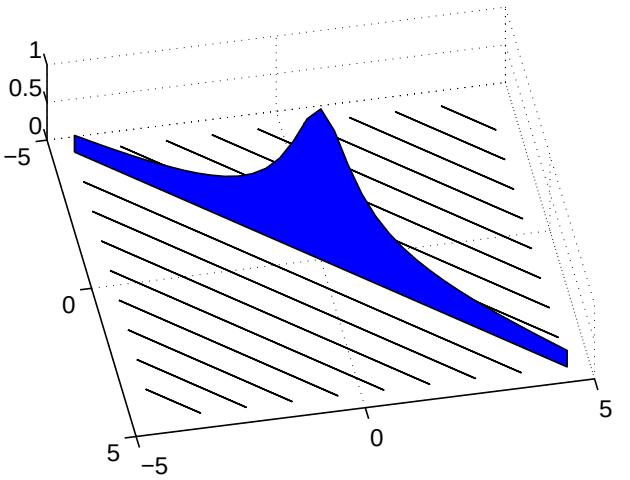

Figure 4.5 The Bode amplitude plot of an LTI system with transfer function $H_0(s) = 1/(s + 0.5)$. The diagonal structure shows that for an LTI system there is no frequency coupling.

operator

$$h(t,\tau) = D(t)\delta(t-\tau) = \sum_k D_k \delta(t-\tau)e^{jk\omega_0 t}.$$

Example 2: LTI Systems LTI systems are a special case of LTP systems, and must therefore have HTFs. For an LTI system there is no coupling between frequencies. The matrix in (4.6) has the standard transfer function $H_0(s)$ on the diagonal and all other $H_k(s)$ are zero.

Example 3: LTP Systems on State Space Form For a general LTP state space system, with time periodic $A(t)$, $B(t)$, $C(t)$, and $D(t)$, the transfer functions, $H_k(s)$, cannot be expressed as explicitly as for LTI systems, see (4.9). However, for systems with constant A-matrix, they are given by

$$H_k(s) = \sum_l \hat{C}_{k-l}((s + jl\omega_0)I - \hat{A})^{-1}\hat{B}_l + D_k. \tag{4.10}$$

where $\hat{B}_k$, $\hat{C}_k$, and D_k, are the Fourier coefficients of the periodic functions, $\hat{B}(t)$, $\hat{C}(t)$, and $D(t)$, respectively. (4.10) can be derived as the product of three matrices, the Toeplitz matrix corresponding to the periodic function, $\hat{C}(t)$, the diagonal matrix for the transfer function, $H_0(s) = (sI - \hat{A})^{-1}$, and

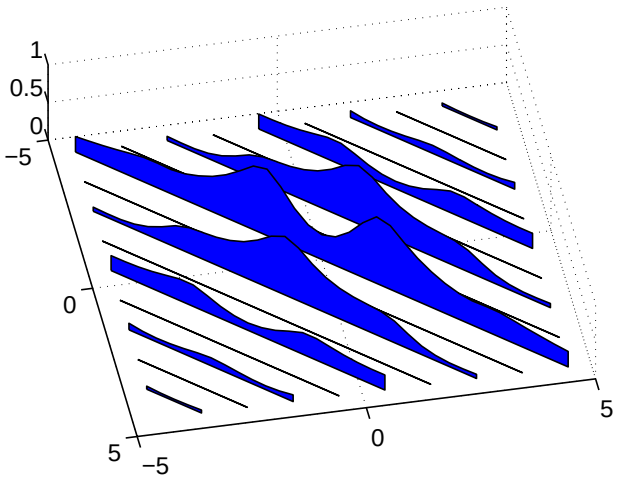

Figure 4.6 The Bode amplitude plot of an LTP system with $\hat{A} = -0.5$, and $B(t)$ and $C(t)$ as square waves. This can be seen as the LTI system in Fig. 4.5, with square wave modulation of input and output.

the Toeplitz matrix of $B(t)$. A constant A-matrix can always be obtained via Floquet decomposition.

Example 4: A Sampler The HTF of the sampler in Section 3.4 can be derived from the impulse response

$$h(t,\tau) = \sum_k \delta(t - kT)\delta(\tau - kT).$$

This gives

$$h_k(t) = \frac{1}{T}\int_0^T h(r, r-t)e^{-jk\omega_0 r}dr = \frac{1}{T}\delta(t),$$
$$H_k(s) = \int_{-\infty}^{\infty} e^{-st}h_k(t)dt = \frac{1}{T}.$$

This gives in Laplace domain

$$Y^*(s) = \sum_k \frac{1}{T}Y(s - jk\omega_0),$$

where $Y^*(s)$ is the Laplace transform of the sampled signal $y^*(t)$. The HTF of the sampler simply becomes a matrix with all elements equal

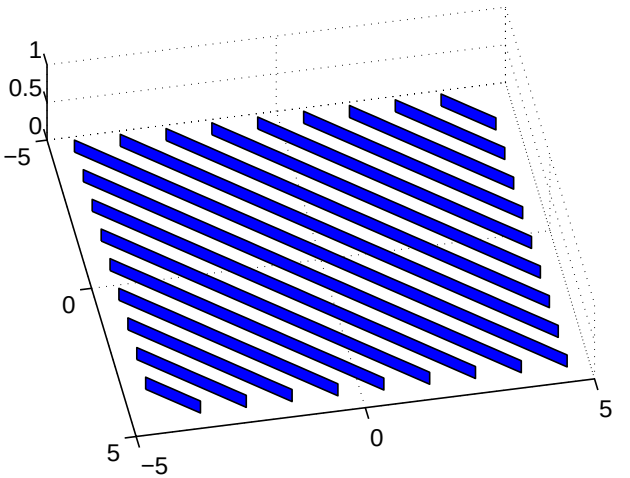

Figure 4.7 The Bode amplitude plot of a sampler. It is clear that the sampler does not distinguish between signals of frequencies separated by a multiple of the fundamental frequency. For sampled-data systems this is called aliasing.

$(= \frac{1}{T})$

$$H_{samp}(s) = \frac{1}{T}\begin{bmatrix} \ddots & \vdots & \vdots & \vdots & \ddots \\ \dots & 1 & 1 & 1 & \dots \\ \dots & 1 & 1 & 1 & \dots \\ \dots & 1 & 1 & 1 & \dots \\ \ddots & \vdots & \vdots & \vdots & \ddots \end{bmatrix}.$$

4.4 A Lifting Interpretation

LTP system analysis using the transfer function, $\widehat{H}(z)$, is complicated by the fact that it is operator valued, and thus infinite dimensional. For computations, it has to be projected on a finite dimensional basis. This can be done using several different methods. The fast sampling and lifting technique [Yamamoto *et al.*, 1997], [Lindgärde, 1999] implies that the system is sampled using a very high sampling rate. This way, the continuous signals, $\tilde{u}_k(t)$ and $\tilde{y}_k(t)$, are approximated by piecewise constant signals. This leads to a discrete time system of finite dimension.

A frequency domain approach is used in [Yamamoto and Khargonekar, 1996] to define the frequency response operator, which is equivalent to $\mathcal{H}(j\omega)$. As $\tilde{u}_k(t)$ and $\tilde{y}_k(t)$, and also $\widehat{U}(z)$ are functions in $L_2[0,T]$, they can be expressed in the base $\{e^{(j\omega+jn\omega_0)t}\}_{n=-\infty}^{\infty}$ (which for $\omega=0$ gives the classical Fourier series).

It can be shown that the HTF $\mathcal{H}(s)$ is in fact equivalent to the lifted transfer function $\widehat{H}(e^{sT})$ if instead the base $\{e^{(s+jn\omega_0)t}\}_{n=-\infty}^{\infty}$ is used. In this base, $\widetilde{U}(z)$ can be written

$$\widehat{U}(z)=\sum_{n=-\infty}^{\infty}\hat{u}_n(z,s)e^{(s+jn\omega_0)t},$$

where

$$\begin{aligned}\hat{u}_n(z,s)&=\frac{1}{2\pi j}\int_0^T\widehat{U}(z)e^{-(s+jn\omega_0)t}dt\\&=\frac{1}{2\pi j}\int_0^T\sum_{k=-\infty}^{\infty}\tilde{u}_k(t)z^{-k}e^{-(s+jn\omega_0)t}dt\\&=\frac{1}{2\pi j}\sum_{k=-\infty}^{\infty}z^{-k}\int_0^T\tilde{u}_k(t)e^{-(s+jn\omega_0)t}dt.\end{aligned}\tag{4.11}$$

The input-output relation of an LTP system can now be written

$$\widehat{\mathcal{Y}}_s(z)=\widehat{\mathcal{H}_s}(z)\widehat{\mathcal{U}}_s(z),$$

where

$$\begin{aligned}\widehat{\mathcal{U}}_s(z)&=[\ldots\quad\hat{u}_{-1}(z,s)\quad\hat{u}_0(z,s)\quad\hat{u}_1(z,s)\quad\ldots]^T,\quad\text{and}\\\widehat{\mathcal{Y}}_s(z)&=[\ldots\quad\hat{y}_{-1}(z,s)\quad\hat{y}_0(z,s)\quad\hat{y}_1(z,s)\quad\ldots]^T,\end{aligned}\tag{4.12}$$

are infinite dimensional vectors, and $\widehat{\mathcal{H}_s}(z)$ is a doubly infinite, complex valued matrix

$$\widehat{\mathcal{H}_s}(z)=\begin{bmatrix}\ddots&\cdots&\cdots&\cdots&\cdots\\\vdots&\widehat{H}_{-1,-1}(z,s)&\widehat{H}_{-1,0}(z,s)&\widehat{H}_{-1,1}(z,s)&\cdots\\\vdots&\widehat{H}_{0,-1}(z,s)&\widehat{H}_{0,0}(z,s)&\widehat{H}_{0,1}(z,s)&\cdots\\\vdots&\widehat{H}_{1,-1}(z,s)&\widehat{H}_{1,0}(z,s)&\widehat{H}_{1,1}(z,s)&\cdots\\\vdots&\vdots&\vdots&\vdots&\ddots\end{bmatrix},\tag{4.13}$$

where the elements are given by

$$\widehat{H}_{m,n}(z,s) = \frac{1}{2\pi j}\int_0^T e^{-(s+jm\omega_0)t}\left\{\widehat{H}(z)e^{(s+jn\omega_0)t}\right\}dt.$$

The matrix $\widehat{\mathcal{H}_s}(z)$ is in fact the discrete time version of the HTF. This is shown by observing that $U(s+jn\omega_0)$ can be written

$$\begin{aligned} U(s+jn\omega_0) &= \int_0^\infty e^{-(s+jn\omega_0)t}u(t)dt \\ &= \sum_{k=0}^{\infty}\int_0^T e^{-(s+jn\omega_0)(t+kT)}\widetilde{u}_k(t)dt \\ &= \sum_{k=0}^{\infty}(e^{st})^{-k}\int_0^T e^{-(s+jn\omega_0)t}\widetilde{u}_k(t)dt. \end{aligned}$$

Comparing this with the z-transform in (4.11) gives the following relation

$$U_n(s) = \hat{u}_n(e^{sT}).$$

This shows that the HTF approach is in fact equivalent to lifting, with

$$\begin{aligned} \mathcal{U}(s) &= \widehat{\mathcal{U}}_s(e^{sT}), \\ \mathcal{Y}(s) &= \widehat{\mathcal{Y}}_s(e^{sT}), \\ \mathcal{H}(s) &= \widehat{\mathcal{H}_s}(e^{sT}). \end{aligned}$$

4.5 LTP System Analysis using HTFs

The relation between the harmonic transfer function and lifting implies that many results for lifted systems can be directly applied to HTFs. Algebraic system operations, like series connection and parallel connection are preserved under lifting [Bamieh and Pearson, 1992]. The HTF for two LTP systems in series becomes

$$\mathcal{H}_{1+2} = \mathcal{H}_1 + \mathcal{H}_2,$$

and for two LTP systems in parallel

$$\mathcal{H}_{12} = \mathcal{H}_1\mathcal{H}_2.$$

LTP System Gain

For a stable LTP system, H, the H_∞ norm (3.11) can be calculated by

$$\|\mathcal{H}\|_\infty = \sup_{\substack{\text{Re } s \geq 0 \\ |\text{Im } s| < \omega_0/2}} \sigma_{max}(\mathcal{H}(s)), \tag{4.14}$$

where σ_{max} denotes the maximum singular value, which is well defined for the doubly infinite matrix $\mathcal{H}(s)$ and can be calculated as the limit of finite matrices using finite projection methods, under appropriate convergence conditions. Convergence will be dealt with in Chapter 5.

Associated with each singular value $\sigma_i(s)$ are two vectors, $\mathcal{U}_i(s)$ and $\mathcal{Y}_i(s)$, such that, if the input to the system is $\mathcal{U}(s) = \mathcal{U}_i(s)\alpha$, for some scalar α, then the resulting output is

$$\mathcal{H}(s)\mathcal{U}_i(s)\alpha = \sigma_i(s)\mathcal{Y}_i(s)\alpha.$$

This can be used to determine what combinations of frequencies are amplified the most.

Poles and Zeros

Poles and zeros of an HTF can be defined following the definitions for multi-input multi-output (MIMO) systems in [Maciejowski, 1989]. The poles of an HTF $\mathcal{H}(s)$ are those $s \in C$ for which $\mathcal{H}(s)$ is not analytic. From 4.6 it is clear that the poles correspond to the poles of the LTI transfer functions, $H_k(s)$. Furthermore, if s is a poles, so is $s + jk\omega_0$, for $k = \pm 1, \pm 2, \ldots$. Note that, as $H_k(t)$ is generally complex valued, the poles of $H_k(s)$ do not come in conjugate pairs. However, the symmetry property (Theorem 4.1) implies that the poles of $\mathcal{H}(s)$ do come in conjugate pairs. Also note that analysis of the LTI transfer functions $H_k(s)$ separately, cannot give answers to questions of multiplicity of poles.

For a system on state space form, the poles are the eigenvalues of the Floquet transformed systems matrix $\widehat{A}$. In [Wereley, 1991] the poles are obtained from the infinite dimensional eigenvalue problem

$$\{sI - (\mathcal{A} - \mathcal{N})\}\mathcal{V} = 0.$$

This results in infinitely many poles. If s solves the eigenvalue problem, so does $s + jk\omega_0$ for any $k = \pm 1, \pm 2, \ldots$. Choosing the poles in the fundamental strip of the complex plane, given by

$$\text{Im}(s) \in \left(-\frac{\omega_0}{2}, \frac{\omega_0}{2}\right],$$

gives n unique poles corresponding to the eigenvalues of $\widehat{A}$, folded into the fundamental strip. A problem with this definition is that the determinant $\det(sI-(\mathcal{A}-\mathcal{N}))$ is hard to define. Convergence is obtained for the related eigenvalue problem

$$\{I-(sI+\mathcal{N})^{-1}\mathcal{A}\}\mathcal{X}=0.$$

Following the MIMO theory in [Maciejowski, 1989], for each transmission zero z_o of $\mathcal{H}(s)$, there exist a non-zero vector $\mathcal{U}_0$ such that $\mathcal{H}(z_o)\mathcal{U}_0 = 0$. It is clear that, just as for poles, if s is a transmission zero, so is $s+jk\omega_0$. A problem with this definition is that transmission zeros of MIMO systems can in general not be solved using truncated matrices. For proper pole zero analysis, it would be convenient with a Smith-McMillan form of the harmonic transfer function.

In [Wereley, 1991] the transmission zeros of an LTP system are defined by the infinite dimensional eigenvalue problem

$$\begin{bmatrix} sI-(\widehat{\mathcal{A}}-\mathcal{N}) & -\widehat{\mathcal{B}} \\ -\widehat{\mathcal{C}} & -\mathcal{D} \end{bmatrix} \begin{bmatrix} \mathcal{V}_0 \\ \mathcal{U}_0 \end{bmatrix} = 0.$$

Also here, the convergence is problematic.

Steady State Gain and Harmonic Balance

If all signals are periodic, they can be represented by their Fourier series. The relation between the Fourier coefficients of the input and the output is then described by

$$\mathcal{Y}(0)=\mathcal{H}(0)\mathcal{U}(0).$$

The complex matrix $\mathcal{H}(0)$ can be used to obtain the steady state solution of a network, and can be seen as the steady state gain of an LTP system. The matrix is called the admittance matrix in the Harmonic Norton Equivalent described in Paper III and is the Jacobian in harmonic balancing of electrical networks, see [Arrillaga *et al.*, 1994], [Kundert and Sangiovanni-Vincentelli, 1986]. The steady-state response matrix $\mathcal{H}(0)$ has recently been developed for several electric components, for instance, transformers with nonlinear saturation curves [Acha *et al.*, 1989], [Semlyen *et al.*, 1988], [Semlyen and Rajakovic, 1989], HVDC converters [Arrillaga and Callaghan, 1991], [Song *et al.*, 1984], [Xu *et al.*, 1994], and static var compensators [Xu *et al.*, 1991]. For identification of $\mathcal{H}(0)$ from measurements, see [Thunberg, 1998] and [Möllerstedt, 1998]. However, the information in $\mathcal{H}(0)$ is not sufficient to describe stability properties of the system under aperiodic perturbations.

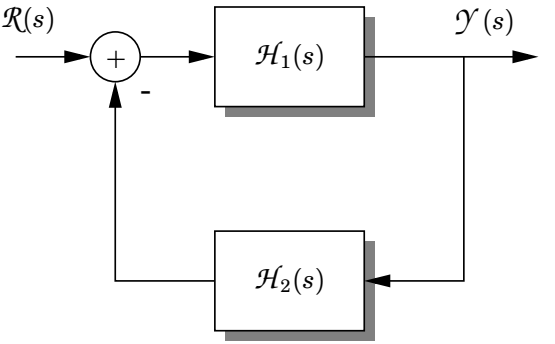

Figure 4.8 A feedback connection of two HTFs $\mathcal{H}_1$ and $\mathcal{H}_2$ results in the closed loop HTF $\mathcal{H}_{cl}(s) = (I + \mathcal{H}_1(s)\mathcal{H}_2(s))^{-1}\mathcal{H}_1(s)$.

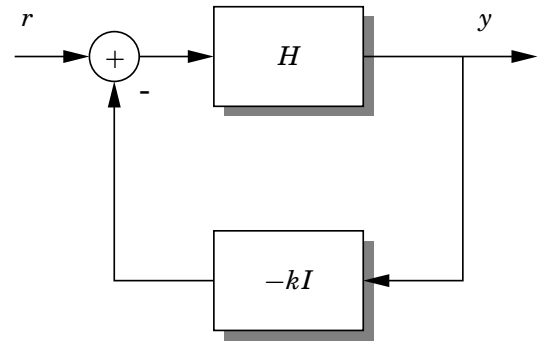

Figure 4.9 The feedback system studied in the Nyquist criterion. Here H represents a linear time periodic (LTP) system.

Analysis of Feedback Systems

Feedback stability is also preserved under lifting [Bamieh and Pearson, 1992], that is, the feedback connection of two LTP systems H_1 and H_2 is L_2-stable if and only if the feedback connection of $\widetilde{H}_1$ and $\widetilde{H}_2$ is l_2-stable. This implies that feedback connections of complex LTP systems can be analyzed using the HTFs of the subsystems. The input-output relation of the feedback system in Fig. 4.8 is given by $\mathcal{Y}(s) = \mathcal{H}_{cl}(s)\mathcal{R}(s)$, where the closed loop HTF is given by

$$\mathcal{H}_{cl}(s) = (I + \mathcal{H}_1(s)\mathcal{H}_2(s))^{-1}\mathcal{H}_1(s).$$

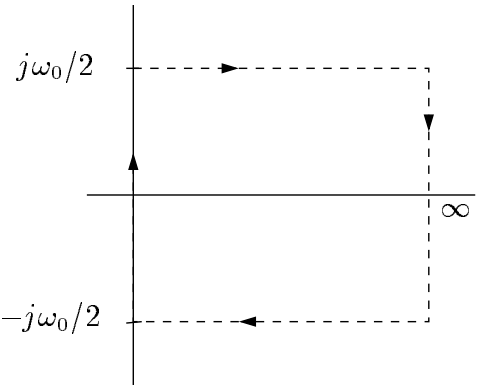

Figure 4.10 The integration contour in the Nyquist criterion for harmonic transfer functions.

The HTF Nyquist Criterion The well known Nyquist criterion can be used to analyze the stability of the closed loop system in Fig. 4.9, using information of the open loop system, H. For LTI systems, stability can be investigated by plotting the Nyquist contour $H_0(j\omega)$ for $-\infty < \omega < \infty$ and counting encirclements of the point $-1/k$. In [Wereley, 1991], the Nyquist criterion for LTP systems was stated, based on the open loop HTF, and the generalized Nyquist criterion for MIMO systems [Maciejowski, 1989].

THEOREM 4.2
Assume a linear, periodic, causal input-output relation between y and u is given by (4.4). Denote by $\{\lambda_i(s)\}_{i=-\infty}^{\infty}$ the eigenvalues of the doubly infinite matrix $\mathcal{H}(s)$ in (4.6), for s varying through the contour in Fig. 4.10. The eigenvalues produce a number of closed curves in the complex plane, called the eigen-loci of the HTF. The closed-loop system in Fig. 4.9 is L_2 stable from r to y if and only if the total number of counterclockwise encirclements of the $-1/k$ point of these curves equals the number of open-loop right half plane poles of the $\mathcal{H}(s)$ in (4.4) (hence zero if H is stable).

Passivity of LTP Systems

The concept of passivity is very important in electric networks. It is a well known fact that the feedback connection of one passive system and one strictly passive system is input-output stable. This implies that a circuit of passive elements, like resistors, inductors and capacitors is stable. The symmetry property can be used to derive a condition for passivity of LTP systems. A relation $y = Hu$ is said to be passive if for all inputs u it holds

that

$$\int_{-\infty}^{\infty} u(t)y(t)\,dt \geq 0.$$

Using Parseval's formula, this is equivalent to

$$\begin{aligned}
&\int_{-\infty}^{\infty} U^*(j\omega)Y(j\omega)\,d\omega \\
&= \int_{-\omega_0/2}^{\omega_0/2} \sum_n U^*(j\omega + jn\omega_0)Y(j\omega + jn\omega_0)\,d\omega \\
&= \int_{-\omega_0/2}^{\omega_0/2} \sum_{m,n} U_n^*(j\omega)H_{n-m}(j\omega + jm\omega_0)U_m(j\omega)\,d\omega \\
&= \int_{-\omega_0/2}^{\omega_0/2} \mathcal{U}^*(j\omega)\mathcal{H}(j\omega)\mathcal{U}(j\omega)\,d\omega \geq 0,
\end{aligned}$$

where $*$ denotes complex conjugate transposed, and $U_n(j\omega) = U(j\omega + jn\omega_0)$. The symmetry impose that

$$\begin{aligned}
&\mathcal{U}^*(-j\omega)\mathcal{H}(-j\omega)\mathcal{U}(-j\omega) \\
&\qquad = \sum_{m,n} U_n^*(-j\omega)H_{n-m}(-j\omega + jm\omega_0)U_m(-j\omega) \\
&\qquad = \sum_{m,n} U_{-n}(j\omega)^T \overline{H_{-(n-m)}(j\omega - jm\omega_0)U_{-m}(j\omega)} \\
\begin{bmatrix} -m \to n \\ -n \to m \end{bmatrix} &= \sum_{m,n} U_n^*(j\omega)H_{m-n}^*(j\omega + jn\omega_0)U_m(j\omega) \\
&\qquad = \mathcal{U}^*(j\omega)\mathcal{H}^*(j\omega)\mathcal{U}(j\omega)
\end{aligned}$$

This shows that passivity for stable LTP systems is equivalent to the condition

$$\mathcal{H}^*(j\omega) + \mathcal{H}(j\omega) \geq 0, \qquad 0 \leq \omega < \omega_0/2.$$

4.6 Conclusions

Using the harmonic transfer function, LTP system can be analyzed as a multi-input multi-output (MIMO) LTI system. The results in this chapter are just a few of the many results for LTI systems that can be generalized. So far the convergence issues of the infinite dimensional matrix $\mathcal{H}(s)$ have not been addressed. This is the topic of the next chapter.

5

Convergence and Computational Issues

When doing numerical computations with an infinite dimensional operator

$$y = Hu,$$

it has to be approximated by finite dimensional operators. For the lifting approach, functions $\tilde{u}_k(t) \in L_2[0,T]$ are approximated by finite dimensional projections $u_N = P_N u$. In [Dullerud, 1996], a truncated Fourier series is used, hence

$$u_N = P_N u = \sum_{k=-N}^{N} U_k(s) e^{(s+jk\omega_0)t},$$

whereas for the fast sampling and lifting approach [Yamamoto *et al.*, 1997], $u(t)$ is approximated by a discrete time signal

$$u_N = P_N u = \{u(kT/N)\}_{k=0}^{N-1}.$$

The mapping from u_N to y_N can be described by the finite dimensional operator $H_N = P_N H P_N$

$$y_N = P_N H P_N u = H_N u_N.$$

It is therefore of interest to study what happens with the induced L_2 norm

$$\|H - P_N H P_N\|_\infty$$

for large N when P_N is a sequence of projection operators for which $P_N \to I$. A problem is that it is not possible to find finite rank operators P_N for

which $\|P_N - I\|$ tends to zero. One therefore has to live with a weaker convergence. To get norm convergence of $P_N H P_N$ to H one has to use extra conditions on H.

Truncation of the infinite dimensional harmonic transfer matrix $\mathcal{H}(s)$ implies the use of the projection operator P_Ω that maps a signal y in L_2 to its low frequency part $y_\Omega = P_\Omega y$ given in the frequency domain by

$$\hat{y}_\Omega(j\omega) = \hat{P}_\Omega \hat{y}(j\omega) = \begin{cases} \hat{y}(j\omega) & |\omega| \le \Omega, \\ 0 & |\omega| > \Omega, \end{cases}$$

where $\hat{y}$ is the Fourier transform of y. Notice that P_Ω is not a causal operator. The triangle inequality gives

$$\|H - P_\Omega H P_\Omega\| \le \|(I - P_\Omega)H\| + \|H(I - P_\Omega)\|$$

5.1 Roll-off for LTP Systems

The finite dimensional operator, H_N, can be assumed to be a good approximation of the infinite dimensional operator, H, if the system has low gain for high frequencies. For LTI systems, such a property is denoted as roll-off. For LTP systems there is coupling between frequencies, which means that low frequency inputs can result in high frequency output. To justify the truncation, two conditions must be fulfilled; the system gain for high input frequencies must be low, and the high frequency output must be low. This leads to the following definitions.

DEFINITION 5.1
An LTP system H is said to have *input roll off k* if there exists a constant C such that

$$\|H(I - P_\Omega)\| \le C\Omega^{-k},$$

and to have *output roll off k* if there exists a constant C such that

$$\|(I - P_\Omega)H\| \le C\Omega^{-k}.$$

An LTP system is said to have *roll off k* if it has both input and output roll off k. It then follows that there exists a constant C such that

$$\|(I - P_\Omega)H(I - P_\Omega)\| \le C\Omega^{-k}.$$

It is clear that a sufficient condition for norm convergence is that the LTP system has a roll-off $k > 0$. Note that in the LTI case P_Ω and H commute, which implies that input and output roll off are equal.

Conditions for Roll-off

The goal is now to find simple conditions in the time domain, that is, on the impulse response $h(t,\tau)$ for a system to have roll off k. Before attacking the LTP case let us revisit the LTI case. For simplicity we consider only the scalar case. For an LTI system the input-output behavior is defined by the convolution

$$y(t) = \int_{-\infty}^{\infty} h(t-\tau)u(\tau)d\tau,$$

with absolute convergence if $h(\cdot) \in L_1$, and $u(\cdot) \in L_2$. The frequency response $\hat{h}(j\omega)$ is defined as

$$\hat{h}(j\omega) = \int_{-\infty}^{\infty} e^{-j\omega t}h(t)dt.$$

One then has

$$\|H\| = \sup_{\omega} |\hat{h}(j\omega)| \leq \|h\|_{L_1}$$

The Riemann-Lebesgue lemma also says that $\hat{h}(j\omega) \to 0$ as $\omega \to \infty$. By integration by parts one sees that if h is causal ($h(t) = 0$ for $t < 0$), and $h, h', \ldots, h^{(k)} \in L_1$, then

$$\begin{aligned}\hat{h}(j\omega) &= \int_0^{\infty} h(t)e^{-j\omega t}dt \\ &= \left[h(t)\frac{e^{-j\omega t}}{(-j\omega)}\right]_0^{\infty} + \frac{1}{j\omega}\int_0^{\infty} h'(t)e^{-j\omega t}dt.\end{aligned}$$

Here $h(t) \to 0$ as $t \to \infty$ since $h, h' \in L_1$. Successive integration by parts gives

$$\hat{h}(j\omega) = \frac{h(0)}{j\omega} + \ldots + \frac{h^{(k-1)}(0)}{(j\omega)^k} + \frac{1}{(j\omega)^k}\int_0^{\infty} h^{(k)}(t)e^{-j\omega t}dt.$$

If $h(0) = \ldots = h^{(k-2)}(0) = 0$ and $h, h', \ldots, h^{(k)} \in L_1$ it follows that

$$|\hat{h}(j\omega)| \leq \frac{1}{\omega^k}(|h^{(k-1)}(0)| + \|h^{(k)}\|_{L_1})$$

Using the definition of roll off for LTP systems above we can conclude that h has roll off k. For an LTI system with finite dimensional state space representation (A, B, C) with stable A matrix one sees that the condition is equivalent to $CB = \ldots = CA^{k-2}B = 0$. This shows that the definition above coincides with the standard definition of roll-off as the relative degree for LTI finite dimensional systems.

For LTP systems we would first like to obtain a similar sufficient condition in the time domain for the operator H to be a bounded operator on $L_2(-\infty,\infty)$. One condition is given by the Hilbert-Schmidt norm defined by

$$\|H\|_{HS} := \|h\| = \left(\int_{-\infty}^{\infty}\int_{-\infty}^{\infty} |h(t,\tau)|^2 dt\, d\tau\right)^{1/2} < \infty.$$

This condition is however very restrictive. The double integral is for instance infinite if $h(t,\tau)$ is a (nonzero) function of $t-\tau$, that is, for LTI systems. The condition also implies that the operator H is compact [Young, 1988], which is a severe restriction.

A less restrictive condition can be obtained by using the lifting technique described in Chapter 3. Recall that using lifting a causal LTP system H could be represented as acting on l_2-sequences of $L_2[0,T]$ signals $\widetilde{u}_k(t) = u(t+kT)$. In fact

$$\tilde{y}_n = \sum_{k=0}^{\infty} H_{[k]}\tilde{u}_{n-k},$$

where the operator $H_{[k]} : L_2([0,T]) \to L_2([0,T])$ is defined via

$$(H_{[k]}v)(t) = \int_0^T h(t+kT,\tau)v(\tau)d\tau, \quad t \in [0,T].$$

Assume now that for any $k = 0, 1, \ldots$ one has that

$$\int_0^T\int_0^T |h(t+kT,\tau)|^2 dt\, d\tau < \infty$$

(true automatically for LTI systems with $h(\cdot) \in L_\infty$. From this it follows that $H_{[k]}$ is bounded on $L_2[0,T]$, compact, and

$$\|H_{[k]}\| \le \left(\int_0^T\int_0^T |h(t+kT,\tau)|^2 dt\, d\tau\right)^{1/2}.$$

Assume furthermore that

$$\|h\|_B := \sum_{k=0}^{\infty}\left(\int_0^T\int_0^T |h(t+kT,\tau)|^2 dt\, d\tau\right)^{1/2} < \infty$$

That h satisfies this inequality will be denoted with $h \in B$. For such systems we have $\sum_{k=0}^{\infty}\|H_{[k]}\| < \infty$. Then, for a fixed $z \in C$ with $|z| \ge 1$, the

z-transform operator $\widehat{H}(z) = \sum_{k=-\infty}^{\infty} z^{-k} H_{[k]}$, is an operator on $L_2([0,T])$ with norm bounded by

$$\begin{aligned}\|\widehat{H}\| &= \sup_{|z|>1} \left\| \sum_{k=0}^{\infty} z^{-k} H_{[k]} \right\| \leq \sum_{k=0}^{\infty} \|H_{[k]}\| \\ &\leq \sum_{k=0}^{\infty} \left(\int_0^T \int_0^T |h(kT+t,\tau)|^2 dt\, d\tau \right)^{1/2} < \infty.\end{aligned}$$

This condition is much less restrictive than the Hilbert-Schmidt condition mentioned earlier. It is for instance satisfied for impulse responses of the form $h(t,\tau) = Ce^{A(t-\tau)}B$ with A Hurwitz.

Let us now study the roll-off by studying the behavior of an LTP system H on high-frequency signals. Let $h_\tau^{(i)}(t,\tau)$ denote the ith derivative of $h(t,\tau)$ with respect to the second variable, that is,

$$h_\tau^{(i)}(t,\tau) = \frac{\partial^i}{\partial \tau^i} h(t,\tau).$$

We then have the following result

THEOREM 5.1
Assume that $h_\tau^{(i)}(t,\tau) \in B$ for $i = 0, 1, \ldots, k$ and that

$$\begin{aligned}&h_\tau^{(i)}(t,t) = 0, \quad i = 0, \ldots, k-2, \\ &\operatorname*{ess.\,sup}_{0\leq t\leq T} |h_\tau^{(k-1)}(t,t)| < \infty\end{aligned}$$

then H has input roll-off k, in fact

$$\|H(I-P_\Omega)\| \leq \left(\operatorname*{ess.\,sup}_{0\leq t\leq T} |h_\tau^{(k-1)}(t,t)| + \|h_\tau^{(k)}(t,\tau)\|_B \right) / \Omega^k, \;\; \Omega > 0.$$

PROOF 5.1

$$\|H(I-P_\Omega)\| = \sup_{\|u\|_{L_2(-\infty,\infty)}=1} \|H(I-P_\Omega)u\|_{L_2} = \sup_{\|v\|_{L_2(-\infty,\infty)}=1,\;\; P_\Omega v = 0} \|Hv\|_{L_2}$$

so we should study the behavior of H on high-frequency signals v. Integration by parts gives

$$\begin{aligned}y(t) &= \int_{-\infty}^{t} h(t,\tau) v(\tau) d\tau \\ &= \left[h(t,\tau) v^{(-1)}(\tau) \right]_{-\infty}^{t} - \int_{-\infty}^{t} h_\tau(t,\tau) v^{(-1)}(\tau) d\tau,\end{aligned}$$

where $v^{(-1)}(t) = \int_{-\infty}^{t} v(r)dr$ denotes integration. Since $h_\tau^{(m)}(t,-\infty) = 0, \quad m = 0,\ldots,k-1$, Successive integration by parts gives

$$y(t) \quad = (-1)^{k-1} h_\tau^{(k-1)}(t,t)v^{(-k)}(t) + (-1)^k \int_{-\infty}^{t} h_\tau^{(k)}(t,\tau)v^{(-k)}(\tau)d\tau$$

From the fact that $v \in L_2$ and $P_\Omega v = 0$ it follows that the function $v^{(-k)}$ belongs to L_2, and has Fourier transform $\hat{v}(j\omega)/(j\omega)^k$. It follows that

$$\|y\|_{L_2} \leq \left(\operatorname*{ess.\,sup}_{0\leq t\leq T} |h_\tau^{(k-1)}(t,t)| + \|h_\tau^{(k)}(t,\tau)\|_B \right) \|v^{(-k)}\|_{L_2}$$

The result now follows from Parseval's formula and the fact that $\hat{v}(j\omega) = 0$ for $|\omega| < \Omega$.

For output roll off we have the following similar result. The difference is that the direction of derivatives changes from τ to t.

THEOREM 5.2
Assume that $h_t^{(i)}(t,\tau) \in B$ for $i = 0,1,\ldots,k$, where $h_t^{(i)}(t,\tau)$ denotes the ith derivative of $h(t,\tau)$ with respect to the first variable, and that

$$\begin{aligned} &h_t^{(i)}(t,t) = 0, \quad i = 0,\ldots,k-2, \\ &\operatorname*{ess.\,sup}_{0\leq t\leq T} |h_t^{(k-1)}(t,t)| < \infty \end{aligned}$$

then

$$\|(I - P_\Omega)H\| \leq \left(\operatorname*{ess.\,sup}_{0\leq t\leq T} |h_t^{(k-1)}(t,t)| + \|h_t^{(k)}(t,\tau)\|_B \right) / \Omega^k, \;\; \Omega > 0,$$

and hence H has output roll-off k.

PROOF 5.2
The result follows from successive differentiation of the relation $y(t) = \int_{-\infty}^{t} h(t,\tau)u(\tau)d\tau$ with respect to t and a similar technique as before. The details are left to the reader.

Roll-off for LTP systems on State Space Form

Consider the system with input and output modulation

$$\begin{aligned} \frac{dx(t)}{dt} &= Ax(t) + B(t)u(t), \\ y(t) &= C(t)x(t), \end{aligned} \tag{5.1}$$

with $B(t)$, $C(t) \in L_\infty$ and T-periodic. This means that

$$|B(t)| \leq B_{max} < \infty,$$
$$|C(t)| \leq C_{max} < \infty.$$

for almost all t. The impulse response is $h(t,\tau) = C(t)e^{A(t-\tau)}B(\tau)$, which gives for almost all t and τ

$$|h(t,\tau)| \leq |C_{max}| \cdot |e^{A(t-\tau)}| \cdot |B_{max}|.$$

As $C_{max}e^{A(t-\tau)}B_{max}$ is LTI with no direct term, it has a roll off of at least one. As the theorems for input and output roll-off only have conditions on absolute values on the impulse response and its derivatives, it is clear that any system on the form (5.1) has roll off of at least 1. In fact, using the Floquet decomposition, any LTP system on state space form with finite valued $A(t)$, $B(t)$, and $C(t)$, and $D(t) = 0$, has roll off 1.

To show higher roll off, the impulse response needs to be differentiated. For input roll off differentiation should be with respect to τ. This gives

$$h_\tau(t,t) = C(B'(t) - AB(t)).$$

If $B(t)$ is not continuous, for instance a square wave, then $B'(t)$ will be unlimited, and Theorem 5.1 cannot be used to show higher input roll off.

For output roll off differentiation should be with respect to t. This gives

$$h_t(t,t) = (C'(t) + C(t)A)B(t).$$

The same line of reasoning shows that for a discontinuous $C(t)$, Theorem 5.2 cannot be used to show higher output roll off.

Example

Consider the linear system $H = G_0B$ where $G_0(s) = 1/(s+10)^3$, that is, has roll-off 3, and $B(t)$ is a square wave with period $T = 2\pi$. Since $B(t)$ is discontinuous, we expect the system to have input roll-off 1, Since there is no output roll-off, the system will have output roll-off 3, just like G_0. In Fig. 5.1 the norms $||H(I - P_\Omega)||$ and $|(I - P_\Omega)H||$ are plotted against Ω. The plot indicates that our assumptions were correct.

5.2 Roll-off and Power System Modeling

A problem when analyzing electric systems using transfer function models is the direction of flows. Should the voltage be chosen as input and the

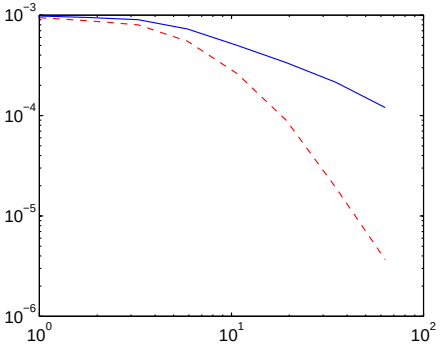

Figure 5.1 The norms $||H(I - P_\Omega)||$ (solid) and $|(I - P_\Omega)H||$ (dashed) plotted against Ω. The plot shows that the system has input roll-off 1 and output roll-off 3.

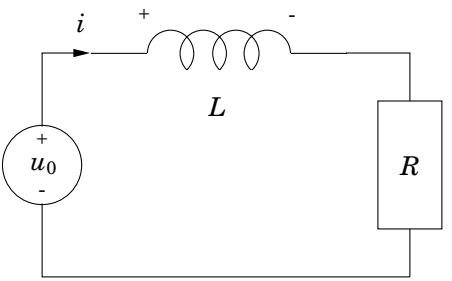

Figure 5.2 A simple electric circuit with a voltage source, an inductor, and a resistor.

current as output or should it be the other way around? This does not depend on the sub-model alone, but on the network to which it is connected. This makes an object oriented approach to modeling difficult.

Consider a simple resistor with resistance R. This can be modeled in two ways

$$u(t) = Ri(t), \quad \text{or} \quad i(t) = \frac{1}{R}u(t).$$

Which one should be chosen? A simple circuit with a voltage source, an inductor, and a resistor, is shown in Fig. 5.2. The circuit can be described by

$$u_0(t) = L\frac{d}{dt}i(t) + Ri(t).$$

The circuit can also be written as a feedback connection of the inductor and the resistor, as in Fig. 5.3(a). The closed loop transfer function from

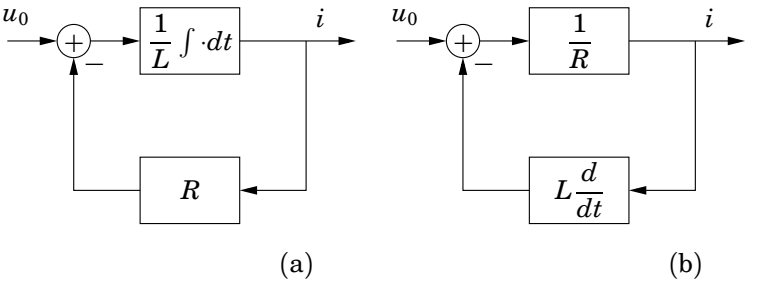

Figure 5.3 The electric network in Fig. 5.2 seen as a feedback connection.

U_0 to I becomes

$$G_{cl}(s) = \frac{\frac{1}{sL}}{1 + \frac{1}{sL}R} = \frac{1}{sL + R}.$$

However, the feedback connection is not unique. Another possible feedback connection is shown in Fig. 5.3(b), which gives the same closed loop system

$$G_{cl}(s) = \frac{\frac{1}{R}}{1 + sL\frac{1}{R}} = \frac{1}{sL + R}.$$

To limit the errors when analyzing the system using truncated HTFs for the resistor and the inductor, the representation which gives the highest roll-off should be chosen. The problem is related to numerical problems in simulations. As integration is more numerically stable than differentiation, the inductor should be modeled as an integrator, which gives the resistor model $u = Ri$. However, in another application, it might be better to model the resistor in the opposite way. This makes an object oriented approach to modeling of electric networks hard. The direction of flows is not clear, but depends on the topology of the network, that is, how the components are connected. This is called the causality assignment problem [Cellier and Elmqvist, 1993]

Most simulation tools for electric networks, like EMTP and Spice, have a fixed causality. In EMTP all dynamic components are modeled as voltage dependent current sources, that is, with voltage as input and current as output. The models are thus independent of network topology. This makes it possible to make models of subcomponents for reuse in other applications. As a drawback, the integration routine might require extremely small time steps, leading to inefficient simulation.

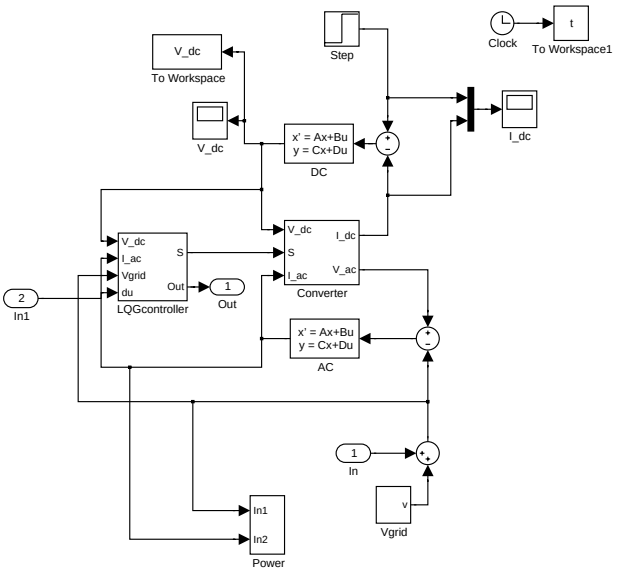

Figure 5.4 A Simulink block diagram of a micro-turbine unit, compare with Fig. 5.5.

For signal based tools like Simulink, the causality has to be determined when designing the sub-models. Component modeling requires a lot of insight in the dynamics of the complete system. This leads to application specific models, which complicates the reuse of the models. As the inputs and the outputs of the sub-models have to be connected, model diagrams tend to be messy, and will not mirror the physical model. A Simulink model of the micro-turbine unit in Paper IV is shown in Fig. 5.4.

Clearly, it would be desirable to be able to model the system without thinking of causality. A resistor should be described by the equation $u = Ri$, without specifying what is input and output. These ideas where introduced in the so called behavioral framework of system theory by Willems [Willems, 1971]. This approach is also taken in the equation-based modeling language Modelica[Elmqvist *et al.*, 1999]. In Modelica, the equations describing the physics of a system are written down as they are, thus not as assignments. The models just give relations between voltages and currents. Sub-models are connected via so called cuts. For electric components the cuts contain current and voltage, and connecting two cuts implies that the voltages are the same in the two cuts, whereas the current out of the first cut equals the current into the other cut. When

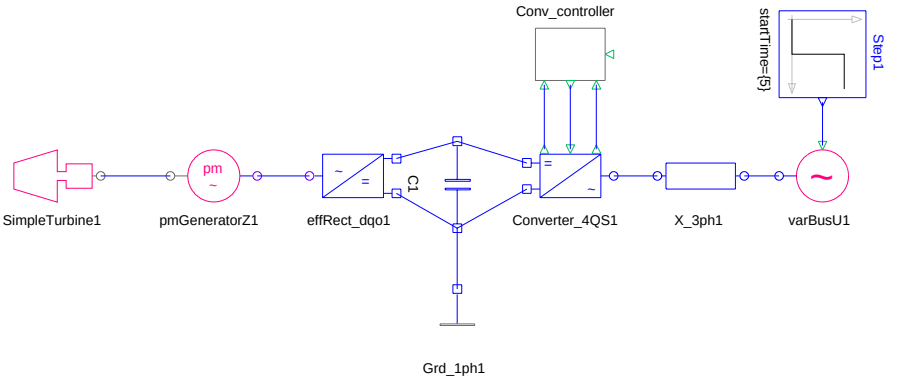

Figure 5.5 A block diagram of the micro-turbine unit in Modelica. The diagram clearly images the physical system, compare with Fig. 5.4.

the Modelica code is translated to simulation code, the causality is checked using sophisticated algorithms.

A Modelica model of the micro-turbine unit is shown in Fig 5.5. The advantage compared to Simulink is clear. The diagram resembles the physical system. Sub-models are connected via cuts, electrical (with voltage and current) and mechanical (with speed and torque).

6

Concluding Remarks

Stable operation of networks with power electronic devices is highly dependent on good control. The Harmonic Transfer Function (HTF) has been presented as a means to analyze modern power systems with switching power electronics. The HTF transforms a linear time periodic system to a time invariant equivalent, and makes it possible to take advantage of the many frequency domain tools, which are developed for analysis of and control design for linear time invariant systems.

Four different power system applications, where the HTF has been used to analyze the system, are presented in the four papers, which are included in the thesis.

Future Work

The work in this thesis opens new possibilities for a lot of interesting research problems in power system analysis. The presented framework gives valuable insight in system dynamics. These include modeling aspects to facilitate improved analysis, robust model reduction, which is essential for analysis of complex power systems, and efficient simulation. This is a great help when formulating control objectives for, for instance, converter controllers, and when developing norms and standard for the connection of power electronic components to the grid.

The framework opens possibilities to use the well-developed theory for linear time invariant systems to achieve robust control design and harmonic filtering. It also facilities a way to dynamically analyze the performance of, for example, solutions for pulse width modulation, and phase locked loops.

7

References

Acha, E., J. Arrillaga, A. Medina, and A. Semlyen (1989): "General frame of reference for analysis of harmonic distortion in systems with multiple transformer nonlinearities." *IEE Proceedings*, **136C:5**, pp. 271–278.

Araki, M., Y. Ito, and T. Hagiwara (1996): "Frequency response of sampled-data systems." *Automatica*, **32:4**, pp. 483–497.

Arrillaga, J. and C. Callaghan (1991): "Three phase AC-DC load and harmonic flows." *IEEE Trans. on Power Delivery*, **6:1**, pp. 238–244.

Arrillaga, J., A. Medina, M. Lisboa, M. A. Cavia, and P. Sánchez (1994): "The harmonic domain. A frame of reference for power system harmonic analysis." *IEEE Trans. on Power Systems*, **10:1**, pp. 433–440.

Åström, K. J. and B. Wittenmark (1997): *Computer-Controlled Systems*, third edition. Prentice Hall.

Ball, J., I. Gohberg, and M. Kaashoek (1995): "A frequency response function for linear time-varying systems." *Math. Control Signals Systems*, **8:4**, pp. 334–351.

Bamieh, B. and J. Pearson (1992): "A general framework for linear periodic systems with applications to H_∞ sampled-data control." *IEEE Transactions on Automatic Control*, **37**, pp. 418–435.

Bittanti, S. and P. Bolzern (1986): "Stabilizability and detectability of linear periodic systems." *Systems & Control Letters*, **No 6**, pp. 141–145.

Cellier, F. and H. Elmqvist (1993): "Automated formula manipulation supports object-oriented modelling." *IEEE Control Systems Magazine*, **13:2**, pp. 28–38.

Colaneri, P., C. de Souza, and V. Kučera (1998): "Output stabilizability of periodic systems: necessary and sufficient conditions." In *Proceedings of the American Control Conference*. IEEE, Philadelphia, Pennsylvania, USA.

Colaneri, P. and V. Kučera (1997): "Model matching for periodic systems." In *Proceedings of the American Control Conference*. IEEE, Albuquerque, New Mexico, USA.

Dullerud, G. E. (1996): *Control of Uncertain Sampled-Data Systems*. Birkhäuser Boston, Cambridge, MA, USA.

Electric Power Research Institute, Inc. (EPRI), 3412 Hillview Avenue, Palo Alto, California 94304, USA (1989): *Electromagnetic Transients Program (EMTP) Revised Rule Book Version 2.0*.

Elmqvist, H., S. E. Mattsson, and M. Otter (1999): "Modelica – a language for physical system modeling, visualization and interaction." In *Proceedings of the 1999 IEEE Symposium on Computer-Aided Control System Design*. Hawaii, USA.

Floquet, G. (1883): "Sur les équations différentielles linéaires a coefficients périodiques." *Annales de L'Ecole Normale Supérieure*, **12**, pp. 47–89.

Hauer, J. and C. Taylor (1998): "Information, reliability, and control in the new power system." In *Proceedings of the American Control Conference*. Philadelphia, Pennsylvania.

Hauser, J. and C. C. Chung (1994): "Converse lyapunov functions for exponentially stable periodic orbits." *Systems & Control Letters*, **No 23**, pp. 27–34.

Hill, G. (1886): "On the part of the lunar perigee which is a function of the mean motions of the sun and the moon." *Acta Mathematica*, **8**, pp. 1–36.

Hiskens, I. A. and D. Hill (1989): "Energy functions, transient stability and voltage behaviour in power systems with nonlinear loads." *IEEE Trans. on Power Systems*, **4:4**, pp. 1525–1533.

Hwang, S. (1997): *Frequency Domain System Identification of Helicopter Rotor Dynamics incorporationg Models with Time Periodic Coefficients*. PhD thesis, Dept. of Aerospace Engineering, University of Maryland.

Kano, H. and T. Nishimura (1996): "A note on periodic lyapunov equations." In *Proceedings of the 35th Conference on Decision and Control*. IEEE, Kobe, Japan.

Key, T. and J. S. Lai (1995): "Costs and benefits of harmonic current reduction for switch-mode power supplies in a commercial office building." In *Conference Records of IEEE IAS Annual Meeting*. Orlando, Florida, USA.

Kundert, K. and A. Sangiovanni-Vincentelli (1986): "Simulation of nonlinear circuits in the frequency domain." *IEEE Trans. on Computer-Aided Design*, **5:4**, pp. 521–535.

Kundur, P. (1994): *Power System Stability and Control*. McGraw-Hill Inc., USA.

Lindgärde, O. (1999): *Frequency Analysis of Sampled-Data Systems Applied to a Lime Slaking Process*. PhD thesis, Chalmers University of Technology, Göteborg, Sweden.

Maciejowski, J. M. (1989): *Multivariable Feedback Design*. Addison-Wesley, Reading, Massachusetts.

Meyer, M. (1999): "Netzstabilität in grossen Bahnnetzen." *Eisenbahn-Revue*, **No 7-8**, pp. 312–317.

Möllerstedt, E., S. E. Mattsson, and B. Bernhardsson (1997a): "A new approach to steady-state analysis of power distribution networks." In Sydow, Ed., *15th IMACS World Congress*, vol. 5, pp. 677–682. W& T Verlag, Berlin, Germany.

Möllerstedt, E., B. Bernhardsson, and S. E. Mattsson (1997b): "A simple model for harmonics in electrical distribution networks." In *Proceedings of the 36th IEEE Conference on Decision and Control*. San Diego, California, USA.

Möllerstedt, E. and A. Stothert (2000): "A model of a micro-turbine line side converter." *To appear in Proceedings of IEEE PowerCon 2000*. Perth, Australia.

Möllerstedt, E. (1998): *An Aggregated Approach to Harmonic Modelling of Loads in Power Distribution Networks*. Lic Tech thesis ISRN LUTFD2/TFRT--3221--SE, Department of Automatic Control, Lund Institute of Technology, Lund, Sweden.

Möllerstedt, E., S. E. Mattsson, and B. Bernhardsson (1997c): "Modeling of electricity distribution networks and components. Status report for Elforsk project 3153." Report ISRN LUTFD2/TFRT--7557--SE. Department of Automatic Control, Lund Institute of Technology, Lund, Sweden.

Möllerstedt, E., S. E. Mattsson, and B. Bernhardsson (1997d): "Modeling of electricity distribution networks and components. Status report 1997-11-30 for Elforsk project 3153." Report ISRN LUTFD2/TFRT--7570--SE. Department of Automatic Control, Lund Institute of Technology, Lund, Sweden.

Semlyen, A., E. Acha, and J. Arrillaga (1988): "Newton-type algorithms for the harmonic phasor analysis of non-linear power circuits in periodical steady state with special reference to magnetic non-linearities." *IEEE Trans. on Power Delivery*, **3:3**, pp. 1090–1098.

Semlyen, A. and N. Rajakovic (1989): "Harmonic domain modeling of laminated iron core." *IEEE Trans. on Power Delivery*, **4:1**, pp. 382–390.

Song, W., G. Heydt, and W. Grady (1984): "The integration of HVDC subsystems into the harmonic power flow algorithm." *IEEE Trans. on Power Apparatus and Systems*, **PAS-103:8**, pp. 1953–1961.

Thunberg, E. (1998): *Measurement Based Harmonic Models of Distribution Systems*. Lic Tech thesis, Electric Power Systems, Royal Institute of Technology, Stockholm, Sweden.

Tornambè, A. and P. Valigi (1996): "Asymptotic stabilization of a class of continuous-time linear periodic systems." *Systems & Control Letters*, **No 30**, pp. 189–196.

Wereley, N. (1991): *Analysis and Control of Linear Periodically Time Varying Systems*. PhD thesis, Dept. of Aeronautics and Astronautics, MIT.

Willems, J. C. (1971): *The Analysis of Feedback Systems*. MIT Press, Cambridge, MA, USA.

Xu, W., J. Drakos, Y. Mansour, and A. Chang (1994): "A three-phase converter model for harmonic analysis of HVDC systems." *IEEE Trans. on Power Delivery*, **9:3**, pp. 1724–1731.

Xu, W., J. Marti, and H. Dommel (1991): "A multiphase harmonic load flow solution technique." *IEEE Trans. on Power Systems*, **6:1**, pp. 174–182.

Yamamoto, Y. and P. P. Khargonekar (1996): "Frequency response of sampled-data systems." *IEEE Transactions on Automatic Control*, **41:2**, pp. 166–176.

Yamamoto, Y., A. G. Madievski, and B. D. O. Anderson (1997): "Computation and convergence of frequency response via fast sampling for

sampled-data control systems." In *Proceedings of the 36th Conference on Decisions & Control*, pp. 2157–2162. San Diego, California, USA.

Young, N. (1988): *An introduction to Hilbert space*. Cambridge University Press, Cambridge, UK.

Zadeh, L. (1950): "Frequency analysis of variable networks." *Proceedings of the Institute of Radio Engineers*, **38**, pp. 291–299.

Paper I

Harmonic Analysis of Distribution Networks

Erik Möllerstedt and Bo Bernhardsson

Abstract

Harmonic analysis of power systems is often performed in frequency domain. Iterative methods are used to find the steady state solution. For components with nonlinear and switching dynamics, the current spectrum is derived from the node voltages, and used to update the node voltages in the next iteration. Newton iterations can be used to improve convergence. The local behavior of a component is then characterized by the Jacobian. The current spectrum and the Jacobian represent the component and are often referred to as the Harmonic Norton Equivalent.

For distribution networks, the approximate voltage is known in advance. As only small distortions are allowed, models that are derived for the nominal voltage are valid for any network under normal operation. The result is a model that is linear in the Fourier coefficients. The linear structure is validated for a dimmer, and shown to be accurate for distortions within the prescribed limits for total harmonic distortion.

The models can be precalculated, which supports an object oriented approach to network modeling and the use of model libraries for reuse of models. Network solving is done using linear algebra, avoiding iterative methods. A procedure for obtaining the Harmonic Norton Equivalents from measurements or time domain simulation is presented and shows good agreement with the validation data.

1. Introduction

When analyzing and simulating networks that include power electronic devices, a mix of time domain and frequency domain methods are often required[Mohan *et al.*, 1994]. For proper handling of the switchings of the power electronics, time domain simulation is most appropriate. Stability analysis and control design, on the other hand, is conveniently performed in frequency domain, by means of the transfer function of the linearized system. Linear analysis does not take the effects of the switchings into account, and the performance of the resulting system must therefore be validated in time domain.

The primary goal of the analysis is often to derive a steady state solution. This is desired for harmonic distortion analysis, but is also used to get proper initial values for time domain simulations and as the operating point around which a linearization should be performed.

To obtain the steady state solution via time domain simulation is very time consuming. If the system has slowly varying states, it has to be simulated for a long time before steady state is reached. The switchings also require a very small time step. For this reason, many frequency domain methods for steady state analysis of this class of systems has been developed. Most of these are based on the method of harmonic balance, [Kundert and Sangiovanni-Vincentelli, 1986; Gilmore and Steer, 1991]. This is an iterative method, and depending on the numerical method used in the iterations, it has been given many various names; Newton's method of harmonic balance is called *Harmonic Power Flow Study* in [Xia and Heydt, 1982], *Unified Solution of Newton Type* in [Acha *et al.*, 1989], and *Harmonic Domain Algorithm* in [Arrillaga *et al.*, 1994]. Harmonic balance with relaxation is called *Iterative Harmonic Analysis* in [Arrillaga *et al.*, 1987], and Newton's method with a diagonal Jacobian is called *A Multiphase Harmonic Load Flow Solution Technique* in [Xu *et al.*, 1991].

A problem with these frequency domain methods is that proper modeling of the switching dynamics is cumbersome in frequency domain. Numerous papers have been written on frequency domain modeling of various components, for instance, transformers with nonlinear saturation curves [Semlyen *et al.*, 1988; Semlyen and Rajakovic, 1989; Acha *et al.*, 1989], HVDC converters [Song *et al.*, 1984; Arrillaga and Callaghan, 1991; Xu *et al.*, 1994] and static var compensators [Xu *et al.*, 1991].

For a distribution network, the approximate operating point for all components is well known in advance. In Europe we have 230 V RMS and 50 Hz. Furthermore, there are standards and regulations that limit the amount of distortion. This means that a model that is linearized around the nominal operating point is valid under normal operation of a network, that is, when the distortions are within the limits.

The model structure described in this paper is based on linearization around the nominal voltage of the system. The linearization implies that aggregation of models and network solving is a non-iterative procedure, using linear algebra. The models, called Harmonic Norton Equivalents, can be interpreted as an extension of the Norton equivalent for linear subnetworks. It facilitates a compact way to represent the behavior of a large nonlinear and switching networks and it can be obtained through simple experiments avoiding detailed modeling.

The structure of the Harmonic Norton Equivalents has been developed for the purpose of analyzing nonlinear and switching networks, with respect to harmonic contents, periodic stability, and robustness. They can also be used for improved load representation in time domain simulation programs. Furthermore, existing model libraries from time domain simulation programs can be used to obtain the equivalents, which means that frequency domain modeling of nonlinear and switching loads is not necessary.

2. A Linearized Approach

Power networks with nonlinear and switching components are time varying systems, with a periodic excitation due to the applied sinusoidal voltage. Linearizing around the nominal 50 or 60 Hz voltage results in linear time periodic models:

$$\begin{aligned} \frac{dx(t)}{dt} &= A(t)x(t) + B(t)u(t) \\ y(t) &= C(t)x(t) + D(t)u(t), \end{aligned}$$

where $A(t)$, $B(t)$, $C(t)$, and $D(t)$ are T-periodic matrices.

A linear model approximates the system well at limited voltage distortions. In steady state, signals are periodic and can be represented approximately by truncated Fourier series

$$\begin{aligned} i(t) &= \sum_{k=-N}^{N} C_k e^{jk\omega_0 t}, \\ v(t) &= \sum_{k=-N}^{N} c_k e^{jk\omega_0 t}, \end{aligned}$$

with spectra

$$I = [\, C_{-N} \quad C_{-N+1} \quad \dots \quad C_{N-1} \quad C_N \,]^T,$$
$$V = [\, c_{-N} \quad c_{-N+1} \quad \dots \quad c_{N-1} \quad c_N \,]^T.$$

The linearization implies that there is a linear relationship between the voltage distortion and the current distortion

$$I = I_0 + Y(V - V_0). \tag{1}$$

The model is thus defined by an admittance matrix, Y, and a nominal current spectrum, I_0, which describes the current at nominal voltage, with spectrum V_0.

The admittance matrix Y describes how the current spectrum is affected by deviations from the nominal voltage. Each column in Y describes the change in the current spectrum when a small cosine or sine component of a certain harmonic frequency is added to the nominal voltage,

$$Y = \frac{\partial I}{\partial V} = \begin{bmatrix} \frac{\partial C_{-N}}{\partial c_{-N}} & \frac{\partial C_{-N}}{\partial c_{-N+1}} & \cdots & \frac{\partial C_{-N}}{\partial c_N} \\ \frac{\partial C_{-N+1}}{\partial c_{-N}} & \frac{\partial C_{-N+1}}{\partial c_{-N+1}} & \cdots & \frac{\partial C_{-N+1}}{\partial c_N} \\ \vdots & \vdots & \ddots & \vdots \\ \frac{\partial C_N}{\partial c_{-N}} & \frac{\partial C_N}{\partial c_{-N+1}} & \cdots & \frac{\partial C_N}{\partial c_N} \end{bmatrix}.$$

A Harmonic Balance Interpretation

Solving a network using these linearized models can be seen as one iteration of Newton's method of Harmonic Balance [Kundert and Sangiovanni-Vincentelli, 1986; Gilmore and Steer, 1991], with a natural choice of initial values. The Jacobian is built up by admittance matrices, like Y in Equation 1. The admittance matrices are fixed and do not, for reasonable harmonic levels, depend on the network configuration. They can thus be precalculated or measured. This results in fast solving without convergence problems. The network is solved by successively aggregating the components. This supports an object oriented approach to network analysis, where model libraries can be composed for reuse of aggregated load models.

A Norton Equivalent Interpretation

In Figure 1 it is shown how the models can be interpreted as Norton Equivalents, that is, an admittance in parallel with a current source. The admittance is replaced by an admittance matrix, Y, and the harmonic current source, I_E, is defined as

$$I_E = YV_0 - I_0.$$

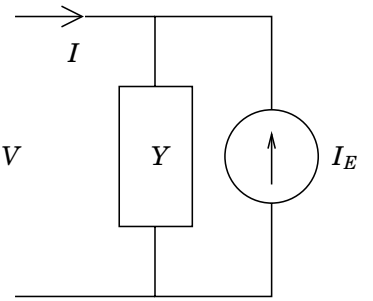

Figure 1 The model can be interpreted as a Norton equivalent, with an admittance matrix, Y, and a current source, I_E.

The current I through the component is given as an affine function of the voltage

$$I = YV - I_E.$$

Representing nonlinear and switching loads with their Harmonic Norton Equivalent, all calculations from traditional linear network theory still apply. As the models are linear, aggregation of loads and network solving are non-iterative procedures using linear algebra.

Because of the structure, frequency domain models used with Newton's method of harmonic balance have often been referred to as Harmonic Norton Equivalents, [Xu *et al.*, 1991; Acha *et al.*, 1989].

The powerful property of the traditional Norton equivalent, however, is not its structure, but the fact that a simple model can equivalently describe the performance of a large linear network. The proposed model structure facilitates a simple way to aggregate components for model reduction, which allows large networks at steady state to be equivalently described by simple models, that is, an admittance matrix, Y, and a harmonic current source, I_E. The models can be estimated by means of simple experiments with measurements or by time domain simulation. This way, detailed modeling of large networks is avoided. The name Harmonic Norton Equivalent is thus motivated.

3. Validation of the Model Structure

For the Harmonic Norton Equivalent, modeling errors occur both due to the linearization and the truncation of the Fourier series. Here, a dimmer is investigated to get an indication of the accuracy of the model structure.

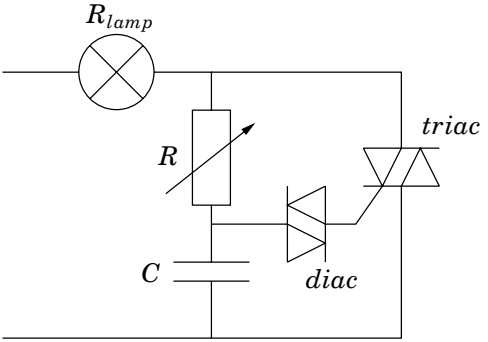

Figure 2 A circuit diagram of a dimmer.

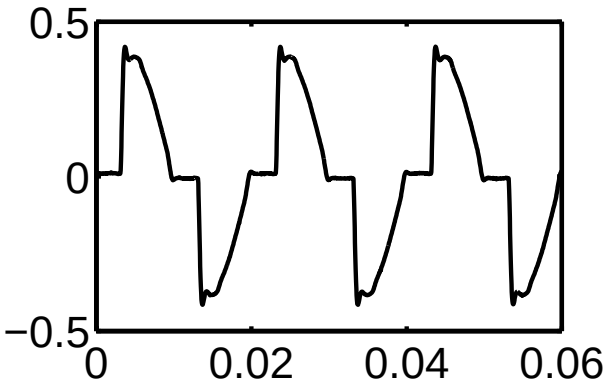

Figure 3 Measured current through a dimmer.

A Model for a Dimmer

The dimmer is a power electronic device used to limit the power and thus dim the light from a light bulb. A circuit diagram of a dimmer is shown in Figure 2. The dimmer works as an open circuit for a part of each period, and thus blocks the current through the lamp. The rest of the period, it works as a short circuit. The turn on delay depends on the value of the variable resistor, R.

The current through the dimmer is shown in Figure 3. The switching nature of the dimmer implies that there is a sharp discontinuity in the current, which results in high distortion also at high frequencies. The dimmer constitutes a good test device. It is simple, but still has the problems associated with modeling and simulation of power electronics. The Harmonic Norton Equivalent for the dimmer is derived in [Möllerstedt, 1998].

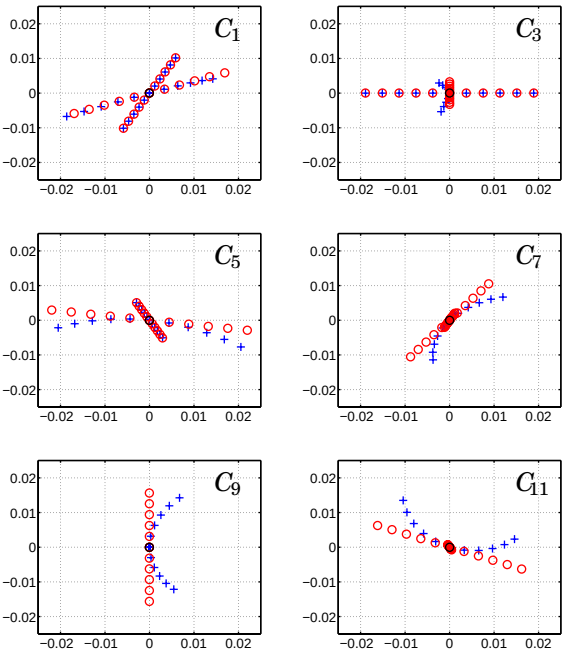

Figure 4 The plots show the deviation of the first six complex Fourier coefficients, $C_1, ..., C_{11}$, of the current through the dimmer, due to a third harmonic voltage disturbance. Each plot shows the result of a cosine disturbance and a sine disturbance. As the dimmer is linear with respect to a cosine disturbance, there is a perfect fit between the linear model ($\circ$), and the nonlinear time domain model ($+$). For a sine disturbance, however, the result of the linearization is obvious. The larger the disturbance, the larger the misfit of the model.

To validate the Harmonic Norton Equivalent for the dimmer, it is investigated how a distortion in the voltage affects the current. For the dimmer model only odd harmonics up to order 11 are considered. The turn on delay, d, for the dimmer is set to $d = T/6$, where T is the cycle time. This means that the dimmer is off for one sixth of a period, every half period. The lamp resistance is $R_{lamp} = 600\,\Omega$. For comparison, a nonlinear time-domain model for an ideal dimmer is simulated to steady state.

In Figure 4, a voltage distortion of the third harmonic frequency is added to the fundamental frequency voltage. The plots show how the Fourier coefficients of the current are affected when a cosine or sine dis-

turbance is applied to the voltage, that is

$$v(t) = a_1^0 \cos \omega_0 t + \widehat{a}_3 \cos 3\omega_0 t, \text{ or}$$
$$v(t) = a_1^0 \cos \omega_0 t + \widehat{b}_3 \sin 3\omega_0 t.$$

The Fourier coefficients of the current distortion is plotted in the complex plane, for the first six odd harmonics. This way, both phase and amplitude of the distortion is shown in one plot. The voltage distortion amplitude, $\widehat{a}_3$ and $\widehat{b}_3$, range in steps of 2% from –10% to +10% of the nominal voltage, $a_1^0 = 230 \cdot \sqrt{2}\,\text{V}$. The fundamental frequency is $\omega_0 = 2\pi \cdot 50\,\text{rad/s}$.

For the linear model, that is, the Harmonic Norton Equivalent, the plots show equally spaced points on straight lines. A doubled voltage distortion amplitude results in a doubled amplitude for the current deviation, whereas the phase is the same. The dimmer is exactly linear with respect to a cosine disturbance. The reason for this is that a cosine disturbance does not affect the zero-crossing of the current, which determines the turn off time for the dimmer. This linear behavior is shown in the plots, where there is a perfect fit for the linear model compared with a nonlinear model. For a sine disturbance, however, the result of the linearization is clearly seen. The larger the amplitude of the disturbance, the larger the deviations from the linear model.

A disturbance with arbitrary phase can be seen as a superposition of a cosine disturbance and a sine disturbance. Thus for a dimmer, the worst case is a pure sine disturbance. It is shown that the linear model is a reasonably good approximation for amplitudes of the distortion limited to 6 % of the fundamental amplitude regardless of the phase of the disturbance.

Harmonic Norton Equivalents in Distribution Networks

The increasing use of power electronics has led to an increase in voltage distortion. The result of this is a need for standards on allowed distortion levels, to guarantee a good power quality and also to determine how the responsibility for keeping the quality should be shared. In a typical standard, the maximum allowed distortion in a distribution networks is 4% for each harmonic component, and 6% total harmonic distortion (THD), for the voltage. The fact that only small deviations from the nominal voltage are allowed, justifies the use of a linear relation, and indicates that the Harmonic Norton Equivalents are valid for analysis of networks under normal conditions.

4. Solving a Small Network

The steady state solution of a network is conveniently derived using Harmonic Norton Equivalents. The method is used to calculate the total current, I_1, in the small network in Figure 5, with two dimmers in parallel, and small net impedances.

The two dimmers, with resistive loads of $20\,\Omega$, are represented by Harmonic Norton Equivalents, $(Y_1,\ I_{1\,E})$ and $(Y_2,\ I_{2\,E})$. The reason for chosing $R_{lamp} = 20\,\Omega$ instead of a $R_{lamp} = 600\,\Omega$ as in Section 3 is to get high enough currents, so that the voltage too gets distorted. The chosen R_{lamp} can be interpreted as 30 normal dimmed light bulbs at the same place in the network.

The net impedances, modelled as a resistor and an inductor in series, are represented by matrices, $Y_{net\,1}$ and $Y_{net\,2}$. The net resistances are $R_{net\,1} = 0.75\,\Omega$ and $R_{net\,2} = 0.25\,\Omega$, and the inductances are $L_{net\,1} = 0.0024\,H$ and $L_{net\,2} = 0.0008\,H$, respectively. The voltage source is purely sinusoidal, with RMS value 230 V and frequency 50 Hz.

The amount of distortion of the current through the dimmer depends on the turn on delay, d, for the dimmer. If $d = 0$, the dimmer is always on, and it is thus linear and there is no current distortion. The longer the turn on time, the larger is the relative distortion. When the delay is half a period, the dimmer is always off. To see if the accuracy depends on the level of distortion, the dimmer was simulated with the turn on time varying from zero to half a period. In Figure 6, Fourier coefficients of the resulting current vector, I_1, is compared with the current obtained in a time domain simulation. The plots show that the method works well for all delays, d.

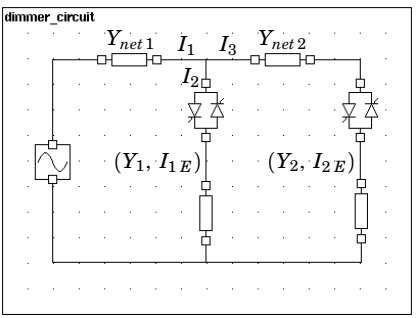

Figure 5 A small circuit with two dimmers, $(Y_1,\ I_{1\,E})$ and $(Y_2,\ ,\ I_{2\,E})$, and line losses, $Y_{net\,1}$ and $Y_{net\,2}$

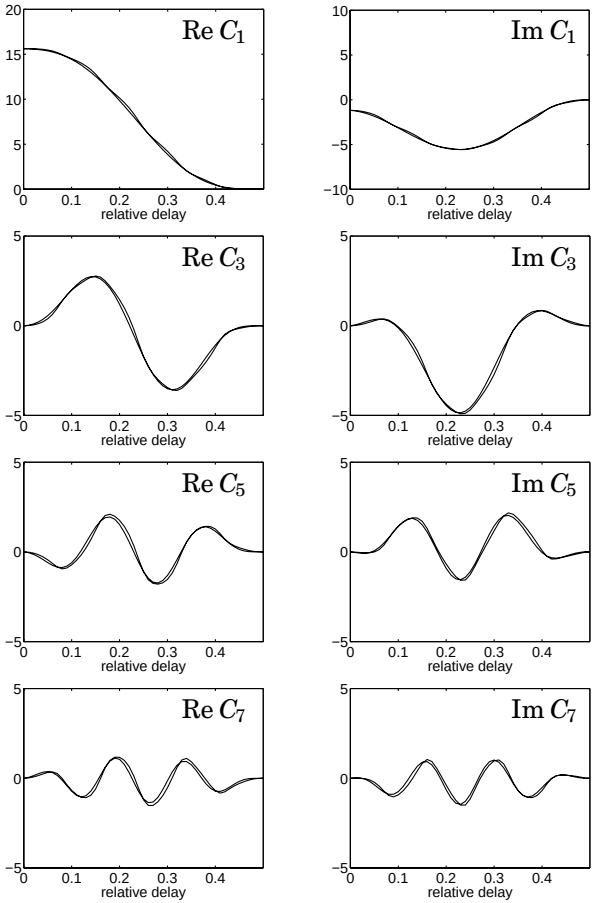

Figure 6 Plots showing the real and imaginary parts of the linearized and simulated Fourier coefficients, $C_1, ..., C_7$, for the current, I_1, in the circuit in Figure 5 as a function of the turn on delay for the dimmers. When the relative delay is 0.5 the dimmer is permanently turned off.

5. A Procedure for Parameter Estimation

For complex systems, it would be desirable to use different tools to analyze different parts of the network. For example use EMTP for the linear network and the generators, SPICE for protective power electronic devices, and some general purpose simulation tool to simulate the control algorithms. To avoid impossible, detailed modelling of aggregated loads, like office buildings, residential areas or even whole suburbs, it would be

desirable to be able to obtain the models through real measurements.

Real measurements and time domain simulation generate sampled time domain data. Harmonic Norton Equivalents for a subsystem can be obtained from sampled time domain data by applying distorted signals to the system. A procedure for this is presented in four steps:

1. Determine the nominal current, $i_0(t)$, by applying the nominal voltage, $v_0(t) = a_0 \cos \omega_0 t$, where a_0 is the nominal amplitude, and ω_0 is the fundamental frequency.
2. Measure current and voltage for, at least, $2N$ different small periodic distortions from the nominal wave shape of the voltage. For example

$$\begin{aligned} v(t) &= v_0(t) + \widehat{a}_k \cos k\omega_0 t \\ v(t) &= v_0(t) + \widehat{b}_k \sin k\omega_0 t \end{aligned} \qquad k = 1, 2, \ldots, N. \tag{2}$$

3. Use the Discrete Fourier Transform to calculate current and voltage spectra from the sampled time domain signals. The nominal spectra are called I_0, and V_0, respectively, and let I_k and V_k represent the spectra from the kth distorted measurement.
4. The admittance matrix Y is obtained through the linear equation system

$$Y\widehat{V} = \widehat{I}, \tag{3}$$

where

$$\begin{aligned} \widehat{V} &= [\, V_1 - V_0 \quad V_2 - V_0 \quad \ldots \quad V_{2N} - V_0 \,], \\ \widehat{I} &= [\, I_1 - I_0 \quad I_2 - I_0 \quad \ldots \quad I_{2N} - I_0 \,]. \end{aligned}$$

Finally, the harmonic current source, I_E, is derived

$$I_E = YV_0 - I_0.$$

Estimating the Parameters of a Dimmer Model

The procedure was applied with good result on a dimmer. The experiment setup is shown in Figure 7. The desired distorted voltage shape, see (2), is obtained in the following way. A switched voltage converter is used to produce a PWM waveform. The pulse width is proportional to a reference signal, which is calculated and output from a PC. The converter switching frequency is 4 kHz. To get rid of the high frequencies generated by the

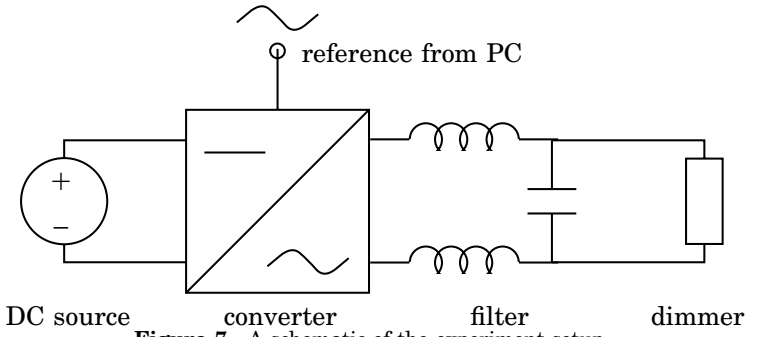

Figure 7 A schematic of the experiment setup.

switching, a low pass LCL-filter with a bandwidth of 3 kHz is used to smooth the voltage.

In order to check whether the procedure gives accurate models, the estimated dimmer model was validated by comparing predicted current spectra with measured spectra for arbitrary voltage distortions. For the voltage distortion in Figure 8 the harmonic distortion in the first 13 harmonics is 9% of the nominal voltage, which is much higher than what is allowed in distribution networks. There is also a considerable amount of distortion at higher frequencies. Still, the model predicts the resulting current distortion really good. Predicted and measured current distortions are shown in Figure 9.

At higher power levels it is, however, unrealistic to generate all power internally, which is needed for the experiments. In [Thunberg, 1998] it is

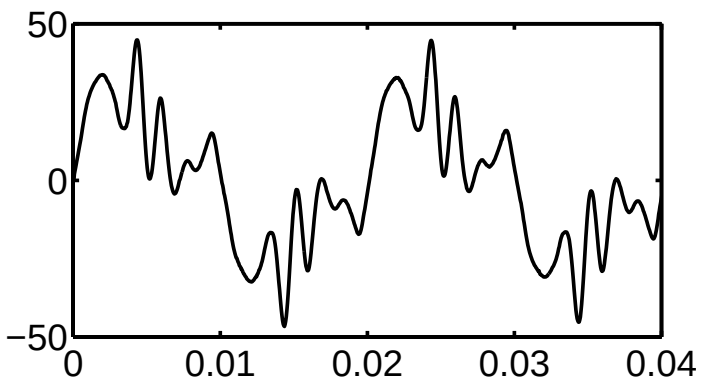

Figure 8 The voltage distortion used for validation. The total harmonic distortion is over 9%.

shown how a diagonal Y-matrix for a distribution network can be obtained by switching in and out large capacitor banks, and thus changing the supplied voltage. It is possible that the full Y-matrix can be obtained by switching in and out other components than capacitors. In some cases, it may be enough to use the natural variations in the supplying network.

Comparison with Estimation of Linear Loads

For linear systems, a single frequency input results at steady state in an output of the same frequency. Different frequencies can be treated separately, and the resulting output is a superposition of all frequencies in the input. For nonlinear systems, this is not the case. A sinusoidal input will at steady state give an output with not only the same frequency, but harmonic frequencies, and possibly sub-harmonic frequencies, too. When

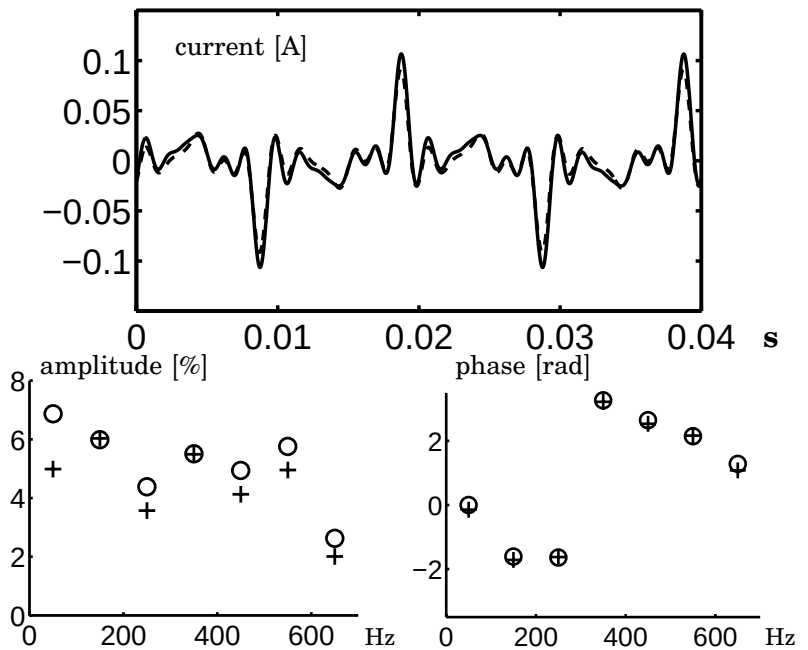

Figure 9 Validation of the model using the voltage in Figure 8. The upper plot shows the deviation from the current due to the voltage distortion. The estimated current is solid, whereas the measured current is dashed. The lower plots show amplitude and phase of the Fourier coefficients of the current. Estimated values are marked with circles, (o), and measured values with a plus, (+).

linearizing the system around the nominal voltage, it is measured how a small voltage superimposed to the nominal one affects the nominal current spectrum. A small voltage distortion of a harmonic frequency affects all current harmonics and not just the current component with the same frequency as the added voltage. Furthermore, the current variations depend on both frequency and phase of the superimposed voltage.

When sampling a continuous time signal, an anti-aliasing filter must be used to avoid aliasing problems. The sensors used for the measurements may also be low pass filtering. The filters affect the amplitude and the phase of the signals. When estimating linear systems, this does not cause any problems, because both inputs and outputs are affected in the same way, as the different frequencies are considered separately. With nonlinear loads, however, the signals contain many frequencies at the same time. As the filter effects are different for different frequencies, the dynamics of the filter must be known and compensated for.

6. Stability of the Periodic Solution

Linear time periodic (LTP) systems occur in many different applications, where there is a periodic excitation, and a lot of work has been done on stability and robustness analysis on this class of systems, see [Wereley, 1991] and the references therein. With the method described in this paper, the existence of a periodic solution is presumed. However, the approach can be used also for stability and robustness analysis, that is, to analyze whether a periodic solution exists.

7. Conclusions

The proposed Harmonic Norton Equivalent is a linearized description of the relation between the current and voltage spectra of nonlinear and switching electrical components. The linearization implies that aggregation of loads and network solving is performed using linear algebra. Common iterative frequency domain methods are avoided, and thus any convergence problems associated with the iteration. Representing nonlinear and switching loads by HNEs, network solving can be performed using traditional linear network methods.

A procedure for experimental estimation of models has been presented. It can be used either for real measurements or for obtaining models using time domain simulation.

To show the usefulness of the model structure, the light dimmer has been used as an example. It is shown that, for the dimmer, the accuracy

of the model structure is satisfying under voltage distortions within the allowed limits. The model for a real dimmer was estimated using the proposed procedure. The obtained model shows a good agreement with the validation data.

8. Acknowledgments

This work was performed under financial support from Elforsk AB, within the Elektra program.

9. References

Acha, E., J. Arrillaga, A. Medina, and A. Semlyen (1989): "General frame of reference for analysis of harmonic distortion in systems with multiple transformer nonlinearities." *IEE Procedings*, **136C:5**, pp. 271–278.

Arrillaga, J. and C. D. Callaghan (1991): "Three phase AC-DC load and harmonic flows." *IEEE Trans. on Power Delivery*, **6:1**, pp. 238–244.

Arrillaga, J., A. Medina, M. L. V. Lisboa, M. A. Cavia, and P. Sánchez (1994): "The harmonic domain. A frame of reference for power system harmonic analysis." *IEEE Trans. on Power Systems*, **10:1**, pp. 433–440.

Arrillaga, J., N. R. Watson, J. F. Eggleston, and C. D. Callaghan (1987): "Comparison of steady-state and dynamic models for the calculation of AC/DC system harmonics." *IEE Proceedings*, **134C:1**, pp. 31–37.

Gilmore, R. J. and M. B. Steer (1991): "Nonlinear circuit analysis using the method of harmonic balance – A review of the art. Part I. Introductory concepts." *Int J. Microwave and Millimeter-Wave Computer-Aided Eng.*, **1:1**, pp. 22–37.

Kundert, K. S. and A. Sangiovanni-Vincentelli (1986): "Simulation of nonlinear circuits in the frequency domain." *IEEE Trans. on Computer-Aided Design*, **5:4**, pp. 521–535.

Mohan, N., W. P. Robbins, T. M. Undeland, R. Nilssen, and O. Mo (1994): "Simulation of power electronic and motion control systems – an overview." *Proc. of the IEEE*, **82:8**, pp. 1287–1302.

Möllerstedt, E. (1998): *An Aggregated Approach to Harmonic Modelling of Loads in Power Distribution Networks*. Lic Tech thesis, Department of Automatic Control, Lund Institute of Technology, Lund, Sweden.

Semlyen, A., E. Acha, and J. Arrillaga (1988): "Newton-type algorithms for the harmonic phasor analysis of non-linear power circuits in periodical steady state with special reference to magnetic non-linearities." *IEEE Trans. on Power Delivery*, **3:3**, pp. 1090–1098.

Semlyen, A. and N. Rajaković (1989): "Harmonic domain modeling of laminated iron core." *IEEE Trans. on Power Delivery*, **4:1**, pp. 382–390.

Song, W., G. T. Heydt, and W. M. Grady (1984): "The integration of HVDC subsystems into the harmonic power flow algorithm." *IEEE Trans. on Power Apparatus and Systems*, **PAS-103:8**, pp. 1953–1961.

Thunberg, E. (1998): *Measurement Based Harmonic Models of Distribution Systems*. Lic Tech thesis, Electric Power Systems, Royal Institute of Technology, Stockholm, Sweden.

Wereley, N. M. (1991): *Analysis and Control of Linear Periodically Time Varying Systems*. PhD thesis, Dept. of Aeronautics and Astronautics, MIT.

Xia, D. and G. T. Heydt (1982): "Harmonic power flow studies, Part I – Formulation and solution, Part II – Implementation and practical aspects." *IEEE Trans. on Power Apparatus and Systems*, **101:6**, pp. 1257–1270.

Xu, W., J. E. Drakos, Y. Mansour, and A. Chang (1994): "A three-phase converter model for harmonic analysis of HVDC systems." *IEEE Trans. on Power Delivery*, **9:3**, pp. 1724–1731.

Xu, W., J. R. Marti, and H. W. Dommel (1991): "A multiphase harmonic load flow solution technique." *IEEE Trans. on Power Systems*, **6:1**, pp. 174–182.

Paper II

A Harmonic Transfer Function Model for a Diode Converter Train

Erik Möllerstedt and Bo Bernhardsson

Abstract

A method for analysis of electric networks with nonlinear and switching components is presented. The method is based on linearization around the nominal AC voltage, which results in linear time periodic (LTP) models. For nonlinear and switching components, there is coupling between different frequencies, which may cause stability and resonance problems. The models capture this coupling and can thus be used for small signal stability and robustness analysis. A short introduction to transfer functions for LTP systems is given.

To illustrate the method, an LTP model for the Adtranz locomotive Re 4/4 is derived. The system consists of an AC-side with a transformer, and a DC-side with a DC-motor and a smoothing choke. The AC-side and the DC-side are connected by a diode bridge rectifier. The model clearly shows the coupling between frequencies.

1. Introduction

Modern trains use power electronic converters to shape the supplying AC-voltage. These switching converters introduce harmonics in the supplying network. Under unfortunate operating conditions, the introduced harmonics may interact with other trains. This may trigger resonances and cause instability. Known incidents have occurred in:

- Italy: Electrical line disturbances in 1993–95.
- Denmark: Several protective shutdowns of the net in 1994.
- Great Britain: Problem with the signaling system in 1994–95.
- Switzerland: Several modern converter locomotives shut down due to network resonance in 1995.
- Germany: S-bahn in Berlin exceeded the limits for harmonic perturbations in 1995.

This is not a problem for train networks alone, but for all power networks with components that modulate the frequency, for instance HVDC systems [Hauer and Taylor, 1998].

When analyzing electric networks, one is often restricted to time domain simulation. Very accurate and thoroughly validated models have been developed for use with, for instance, EMTP and EMTDC. However, no matter how accurate the models are, there is no way that simulations alone can guarantee that all critical parameter values and operating conditions are found so that new incidents can be avoided in the future. Simulations can only give a yes or no answer to stability, and do not say anything about robustness to a set of uncertainties. Thus, no uncertainty in model parameters is allowed, no unmodeled dynamics, and all possible operating conditions must be analyzed.

In control design, robustness has been a main concern for a long time. There now exist powerful tools for robustness analysis such as μ-analysis, H_∞-design and also nice methods for model aggregation, which make modularized modeling and analysis easier. Most of these methods are only available for linear systems. The use of power electronics, however, implies that traditional linear analysis does not apply. The switching introduces coupling between different frequencies. For proper analysis, the models have to consider this coupling.

The supplied AC-voltage leads to a periodic excitation of the system. A natural approach is to linearize around the nominal voltage. This results in a linear model, however not time invariant but time periodic. These linear time periodic (LTP) models capture the coupling between frequencies and can thus be used for analysis of networks including nonlinear and switching components.

For periodic signals, an LTP model gives a linear relation between the Fourier coefficients of the inputs and the outputs. This is the reason why frequency domain methods are popular for steady state analysis of power networks. LTP models for steady state analysis have been developed for numerous electric components, for instance transformers with nonlinear saturation curves [Semlyen *et al.*, 1988; Semlyen and Rajakovic, 1989; Acha *et al.*, 1989], HVDC converters [Song *et al.*, 1984; Arrillaga and Callaghan, 1991; Xu *et al.*, 1994] and static var compensators [Xu *et al.*, 1991].

When the harmonic balance solution for a network is obtained via Newton iterations [Kundert and Sangiovanni-Vincentelli, 1986], and [Gilmore and Steer, 1991], the Jacobians are LTP models that improve the convergence of the solution. Newton's method of harmonic balance has been used for analysis of power networks under various names, *Harmonic Power Flow Study* in [Xia and Heydt, 1982], it is called *Unified Solution of Newton Type* in [Acha *et al.*, 1989], and *Harmonic Domain Algorithm* in [Arrillaga *et al.*, 1994]. Harmonic balance with relaxation is called *Iterative Harmonic Analysis* in [Arrillaga *et al.*, 1987], and Newton's method with a diagonal Jacobian is called *A Multiphase Harmonic Load Flow Solution Technique* in [Xu *et al.*, 1991].

In [Wereley, 1991] and [Hwang, 1997] a transfer function for LTP systems is derived and used to analyze vibrations in helicopter rotors. Via this transfer function many stability and robustness results for linear time invariant systems can be generalized to hold also for LTP systems. These references also give a nice historical background and relates the method to Floquet theory, Lyapunov exponents and to so called lifting methods.

In this paper, a transfer function for a diode converter locomotive is derived, and it is shown how the Nyquist criterion can be used to guarantee stability when the locomotive is connected to the power system. For related work see also [Sandberg, 1999] where the harmonic transfer function method is used to study harmonic interaction for a four-quadrant converter locomotive.

2. Analysis of LTP Systems

For linear time invariant systems, many stability and robustness results are based on the transfer function operator. To generalize these results to LTP systems, we need a corresponding transfer function.

Let the input, $u(t)$, be an exponentially modulated periodic (EMP)

signal with period T

$$u(t) = e^{st} \sum_m U_m e^{jm\omega_0 t} = \sum_m U_m e^{(s+jm\omega_0)t}, \tag{1}$$

where $\omega_0 T = 2\pi$. In Appendix A it is shown that an LTP system maps an EMP input to an EMP output, that is, the output too is an EMP signal

$$y(t) = e^{st} \sum_n Y_n e^{jn\omega_0 t} = \sum_n Y_n e^{(s+jn\omega_0)t}.$$

If the EMP input signal U and output signal Y are written on vector form

$$\begin{aligned} U(s) &= [\ldots \quad U_{-1} \quad U_0 \quad U_1 \quad \ldots]^T e^{st}, \\ Y(s) &= [\ldots \quad Y_{-1} \quad Y_0 \quad Y_1 \quad \ldots]^T e^{st}, \end{aligned}$$

then their relation is described by a linear equation

$$Y(s) = H(s)U(s).$$

The transfer function matrix $H(s)$ defines the coupling between different frequencies and is called the harmonic transfer function (HTF) and can, formally, be represented as a doubly-infinite matrix, see Appendix A.

$$H(s) = \begin{bmatrix} \ddots & \cdots & \cdots & \cdots & \cdots \\ \vdots & H_{-1,-1}(s) & H_{-1,0}(s) & H_{-1,1}(s) & \cdots \\ \vdots & H_{0,-1}(s) & H_{0,0}(s) & H_{0,1}(s) & \cdots \\ \vdots & H_{1,-1}(s) & H_{1,0}(s) & H_{1,1}(s) & \cdots \\ \vdots & \vdots & \vdots & \vdots & \ddots \end{bmatrix}.$$

3. A Diode Converter Train

An LTP model for the Adtranz locomotive Re 4/4 is derived. A Simulink model for the locomotive, which consists of a transformer, a diode bridge rectifier, a smoothing choke and a DC motor, is shown in Fig. 1.

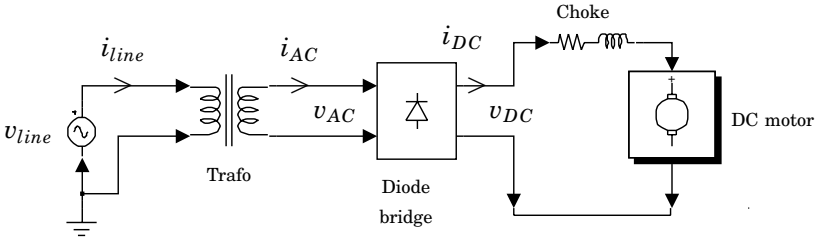

Figure 1 A Simulink model for the diode converter locomotive. The harmonic transfer function derived in Section III describes the harmonic interaction between the variable i_{AC}, v_{AC}, i_{DC} and v_{DC}, see Fig. 7

A Diode Bridge Rectifier Model

The diode bridge rectifier ensures that the AC-side and the DC-side are related by a time varying modulation

$$\begin{aligned} v_{DC}(t) &= B(t)v_{AC}(t), \\ i_{AC}(t) &= C(t)i_{DC}(t). \end{aligned} \tag{2}$$

The current and voltage on both sides of the rectifier are shown in Fig. 2.

The diodes in the diode bridge are not ideal, which means that it takes some time for the AC-current to change sign. During this period current flows through all diodes. This is called commutation. The result is that the commutation functions, $B(t)$ and $C(t)$, are not square waves. Typical shapes are shown in Fig. 3. To avoid detailed modeling of the converter, these modulation functions can be obtained via simulation or measurement. We have used data from time domain simulation using Simulink's Power System Blockset toolbox. For a diode bridge rectifier, the switching instants are determined by the zero-crossings of the AC-voltage. A voltage distortion will hence affect the switching instants and thus the periodicity.

Linearizing (2) around the periodic functions, $B_0(t)$ and $C_0(t)$ and the nominal signals, $v^0_{AC}(t)$ and $i^0_{DC}(t)$, gives

$$\Delta v_{DC}(t) = B_0(t)\Delta v_{AC}(t) + \Delta B(t)v^0_{AC}(t), \tag{3}$$

$$\Delta i_{AC}(t) = C_0(t)\Delta i_{DC}(t) + \Delta C(t)i^0_{DC}(t). \tag{4}$$

The deviations from the periodicity, $\Delta B(t)$ and $\Delta C(t)$, are due to distortion of v_{AC}. The effect of $\Delta B(t)$ is neglectable since $v^0_{AC}(t)$ is small around the zero crossing. The effect of $\Delta C(t)$ is analyzed in the next section, see (9). The analysis will show that an HTF for the diode bridge has the following

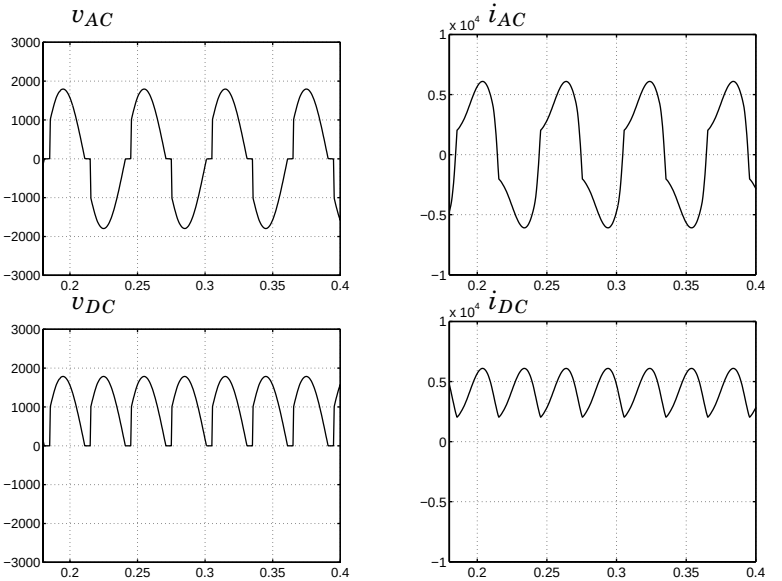

Figure 2 Simulation of AC- and DC-voltages and currents for the diode converter locomotive, see also (2). Small-signal linearization around these nominal trajectories leads to the model in Fig. 7.

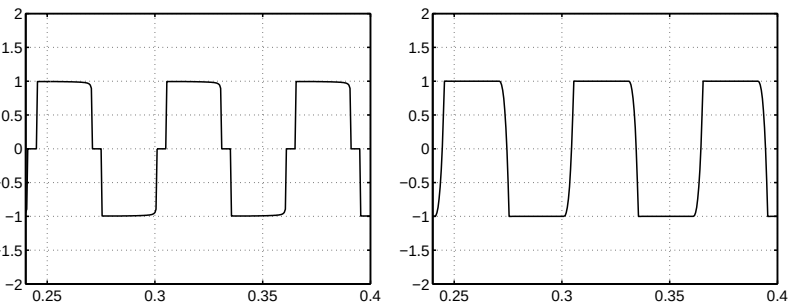

Figure 3 Modulation functions, $B_0(t)$ and $C_0(t)$. Changes in v_{AC} change the switch instances but not the form of the modulation functions.

structure

$$\Delta V_{DC}(s) = B_0(s)\Delta V_{AC}(s), \tag{5}$$

$$\Delta I_{AC}(s) = C_0(s)\Delta I_{DC}(s) + D(s)\Delta V_{AC}(s), \tag{6}$$

where $D(s)$ is due to non-periodic switching. The rectifier can hence be described by the block diagram in Fig. 7.

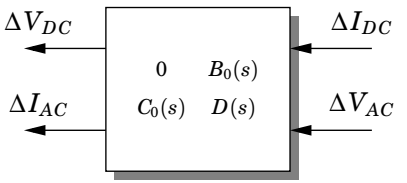

Figure 4 A block diagram of the linearized diode rectifier. The HTF models $B_0(s)$, $C_0(s)$ and $D(s)$ are derived in the text and have been verified by time domain simulations. The diode rectifier model is connected with the DC dynamics in Fig. 5.

Deriving the HTF for the Rectifier

The periodic functions $B_0(t)$ and $C_0(t)$ can be expressed by their Fourier series $B_0(t) = \sum_{k=-\infty}^{\infty} B_k e^{jk\omega_0 t}$. With $\Delta v_{AC}(t)$ being an EMP signal we get

$$\begin{aligned}\Delta v_{DC}(t) = B_0(t)\Delta v_{AC}(t) &= e^{st}\sum_m \sum_k B_k V_{AC,m} e^{j(m+k)\omega_0 t} \\ &= e^{st}\sum_n \sum_m B_{n-m} V_{AC,m} e^{jn\omega_0 t}.\end{aligned}$$

Thus, the HTF is a static Toeplitz matrix

$$B_0(s) = \begin{bmatrix} \ddots & \ddots & \ddots & \ddots & \ddots & \ddots \\ \ddots & B_0 & B_{-1} & B_{-2} & \ddots & \ddots \\ \ddots & B_1 & B_0 & B_{-1} & B_{-2} & \ddots \\ \ddots & B_2 & B_1 & B_0 & B_{-1} & \ddots \\ \ddots & \ddots & B_2 & B_1 & B_0 & \ddots \\ \ddots & \ddots & \ddots & \ddots & \ddots & \ddots \end{bmatrix},$$

and similarly for $C_0(s)$.

We will now analyze the part of i_{AC} that is due to changes in switching instants, $\Delta C(t) i^0_{DC}(t)$. A good approximation is that a change in switching instant does not affect the shape of the modulation function, but only shifts it in time.

$$C(t) = C_0(t - \Delta t) \approx C_0(t) - \frac{dC_0(t)}{dt}\Delta t,$$

The change in switching at time t_k only affects the current until the next switch occurs around $t_{k+1} = t_k + T/2$. A switch change Δt_k at time t_k gives

$$\Delta C(t) = -\Pi(t - t_k)\frac{dC_0(t)}{dt}\Delta t_k = \begin{cases} -\dfrac{dC_0(t)}{dt}\Delta t_k & t \in [t_k, t_{k+1}), \\ 0 & \text{otherwise}, \end{cases} \tag{7}$$

where $\Pi(t)$ is a unit pulse with width $T/2$.

We must now relate the zero crossing change, Δt, with the voltage distortion. Let the nominal voltage be

$$v_{AC}^0(t) = V_0 \sin \omega_0 t,$$

with zero-crossings at $t_k = kT/2 = k\pi/\omega_0$. A distortion $\Delta v_{AC}(t)$ gives a change in switching time, Δt. This change is approximately given by the voltage distortion at the nominal switching time, t_k

$$\Delta v_{AC}(t_k) \approx -\frac{dv_{AC}^0(t_k)}{dt}\Delta t_k = -(-1)^k V_0 \omega_0 \tag{8}$$

Using (7) and (8) and assuming a constant $i_{DC}^0(t) = i_{DC}^0(t_0)$ now gives

$$\begin{aligned} \Delta C(t) i_{DC}^0(t) &= -\Pi(t - t_k)\frac{dC_0(t)}{dt}\Delta t_k i_{DC}^0(t_0) \\ &= (-1)^k \frac{i_{dc}^0(t_0)}{V_0\omega_0}\frac{dC_0(t)}{dt}\Pi(t - t_k)\Delta v_{AC}(t_k) \\ &= \int h(t,\tau)\Delta v_{AC}(\tau)d\tau, \end{aligned} \tag{9}$$

where $h(t,\tau)$ is the impulse response. If all zero-crossings are considered, the impulse response is hence given by

$$h(t,\tau) = \frac{i_{dc}^0(t_0)}{V_0\omega_0}\frac{dC_0(t)}{dt}\sum_k (-1)^k \Pi(t - t_k)\delta(\tau - t_k). \tag{10}$$

The time periodic transfer function becomes

$$\begin{aligned} H(s,t) &= e^{-st}\int h(t,\tau)e^{s\tau}d\tau \\ &= e^{-st}\frac{i_{dc}^0(t_0)}{V_0\omega_0}\frac{dC_0(t)}{dt}\sum_k (-1)^k \Pi(t - t_k)e^{st_k}, \end{aligned}$$

which gives

$$\begin{aligned}\hat{H}_k(s) &= \frac{1}{T}\int_0^T H(s,t)e^{-jk\omega_0 t}dt \\ &= \frac{i_{dc}^0(t_0)}{V_0 2\pi}\left(\int_0^{T/2}\frac{dC_0(t)}{dt}e^{-(s+jk\omega_0)t}dt \right. \\ &\qquad \left. - \int_{T/2}^{T}\frac{dC_0(t)}{dt}e^{sT/2}e^{-(s+jk\omega_0)t}dt\right) \\ &= \frac{i_{dc}^0(t)}{V_0 2\pi}\int_0^{T/2}\sum_l (1-e^{j(l-k)\omega_0 T/2})jl\omega_0 c_l e^{-(s+j(k-l)\omega_0)t}dt \\ &= -\frac{i_{dc}^0(t)}{V_0 2\pi}\sum_l (1-(-1)^{k-l})jl\omega_0 c_l \frac{e^{-(s+j(k-l)\omega_0)T/2}-1}{s+j(k-l)\omega_0}.\end{aligned}$$

The HTF $D(s)$ is then obtained as in Appendix A.

The DC-Side

A DC motor consists of two windings, the rotating armature winding and the field winding. Due to the rotation an electro-magnetic force, e_a, is induced in the armature winding, $e_a = k_1\Phi_s(i_s)\omega$, the flux Φ_s is a function of the stator current and ω is the rotor speed.

For a series excited DC-motor $i_s = i_a$. Assuming the speed of the train to be constant, a linearized model for the DC motor can be seen as a resistor, $\Delta e_a = R_{ind}\Delta i_a$, where R_{ind} depends on i_s^0 and ω^0. The transfer function from DC-voltage to DC-current is hence given by

$$\Delta I_{DC}(s) = \frac{1}{R+sL}\Delta V_{DC}(s) = G(s)\Delta V_{DC}(s),$$

where, $L = L_c + L_a + L_e$ is the sum of the choke inductance and the inductances in the armature and field windings, and similarly $R = R_c + R_a + R_e + R_{ind}$.

Assemblying the Locomotive

The model for the diode converter including the DC side dynamics is shown in Fig. 5. The HTF, $H_{db}(s)$, for the diode bridge rectifier and the DC side dynamics is hence given by

$$\begin{aligned}\Delta I_{AC}(s) &= H_{db}(s)\Delta V_{AC}(s) \\ &= (C_0(s)\widetilde{G}(s)B_0(s) + D(s))\Delta V_{AC}(s),\end{aligned}$$

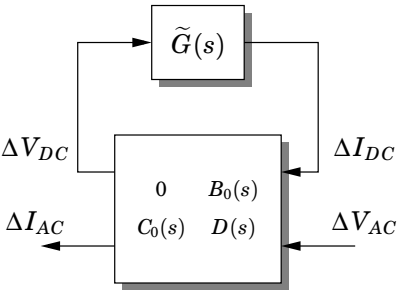

Figure 5 The diode converter with the DC dynamics $\tilde{G}(s)$ connected. The resulting HTF, $H_{db}(s)$, is then connected with a model of the transformer $\tilde{Z}_{traf}(s)$, see Fig. 6.

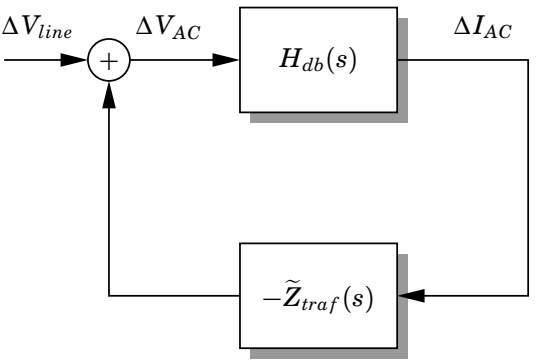

Figure 6 The electrical network described by a feedback connection. The relation between harmonic disturbances on the line and in the AC-current is given by $H_{loco}(s)$, see 12.

where

$$\widetilde{G}(s) = \operatorname{diag}(\ldots \quad G(s-j\omega_0) \quad G(s) \quad G(s+j\omega_0) \quad \ldots). \tag{11}$$

The transformer is modeled as an ideal transformer plus an equivalent impedance on the low voltage side. The effect of the impedance is shown in Fig. 6 and gives $\Delta I_{AC}(s) = H_{loco}(s)\Delta V_{line}(s)$, where

$$H_{loco}(s) = (I + H_{db}(s)\widetilde{Z}_{traf}(s))^{-1} H_{db}(s). \tag{12}$$

The amplitude of H_{loco} is plotted in Fig. 7. The diagonal structure shows that there is only coupling between frequencies separated by $33\frac{1}{3}$ Hz.

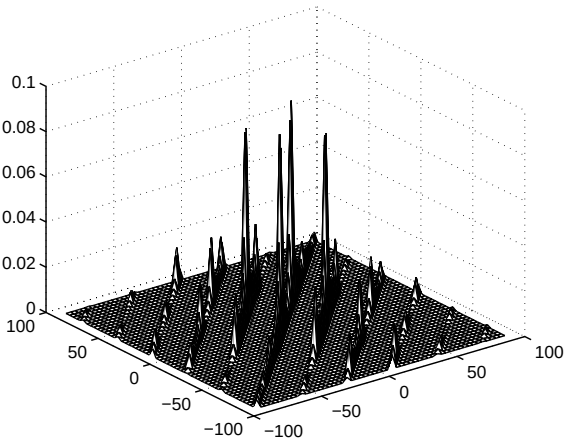

Figure 7 The amplitude plot of the HTF H_{loco}. Notice the large out-diagonal bands, illustrating the nonlinear coupling between different frequencies in V_{line} and I_{AC}.

4. A Nyquist Criterion for LTP Systems

On matrix form it is clear that an LTP system formally can be treated as a LTI system with infinitely many inputs and outputs. Transmission zeros and poles can thus be derived from theory for multi-input multi-output (MIMO) systems, see for instance [Maciejowski, 1989]. These poles determine the stability of the system.

A Nyquist criterion for LTP systems based on HTFs was presented in [Wereley, 1991]. It is based on the generalized Nyquist criterion for MIMO systems. It states that stability of the closed loop system can be determined by plotting the eigenvalue curves of the open loop HTF, $H(j\omega)$ for $-\omega_0/2 < \omega < \omega_0/2$. If the open loop system is stable, and the Nyquist curve does not enclose the point -1, then the closed loop system is stable.

Consider the locomotive connected to a fictive (non-passive) line environment, modeled as an impedance given by $Z_{grid}(s) = 5000K/(s^2 + 5s + 5000)$. The open loop system is given by $\widetilde{Z}_{grid}(s)H_{loco}(s)$ where $\widetilde{Z}_{grid}(s)$ is defined as in (11).

In Fig. 8, the Nyquist plot for the HTF of the locomotive and the grid is plotted for $K = 1$. The curve crosses the negative real axis at $s \approx -0.2$. The Nyquist criterion states that the system is stable for $K < A_m = 1/0.2 = 5$. A time domain simulation shows that the system is stable for $K = 4$ but not for $K = 6$. This indicates that the Nyquist criterion does a good job in

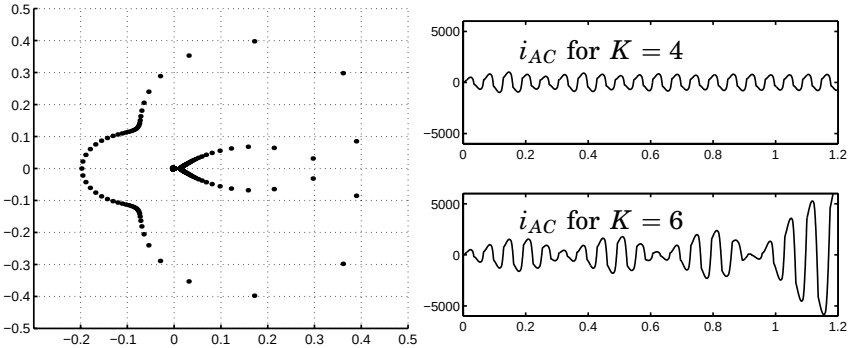

Figure 8 The Harmonic Nyquist plot, i.e. the eigenvalues of $\tilde{Z}_{grid} H_{loco}(j\omega)$ for $-\omega_0/2 \leq \omega \leq \omega/2$, for the locomotive attached to the line. Notice that the curve indicates a harmonic amplitude margin of $A_m = 5$. This corresponds well with the results from time domain simulations.

predicting harmonic stability of the full nonlinear locomotive. The derived model can now be used for analysis, such as harmonic interaction with other trains on the same line.

5. Conclusions

The Harmonic transfer function method of modeling linear time periodic systems has been described. A HTF model has been derived for a diode converter locomotive. The model has been verified with time domain simulations and is a good starting point for further analysis of resonance risks and harmonic interaction.

6. Acknowledgment

The model of the diode converter locomotive was kindly provided by Markus Meyer at Adtranz, Zürich. The work was financially supported by Elforsk AB under Elektra project 3320.

Appendix A. Analysis of LTP Systems

The transfer function plays a central role in stability and robustness analysis as well as control design. For LTI-systems, the transfer function is a

linear operator on the class of exponentially modulated sinusoids

$$u(t) = U_0 e^{st}, \qquad y(t) = H_0(s)U_0 e^{st} = Y_0 e^{st}.$$

To get a transfer function for LTP systems, we need a corresponding class of test signals. For an LTP system on state space form, Floquet decomposition reveals that a suitable test signal is the class of exponentially modulated periodic (EMP) signals, see [Wereley, 1991]

$$u(t) = e^{st} \sum_m U_m e^{jm\omega_0 t} = \sum_m U_m e^{(s+jm\omega_0)t}. \tag{13}$$

Not all systems have a state space representation. A general LTP system can be defined by its impulse response, $h(t,\tau)$. The periodicity of the system implies that

$$h(t+T, \tau+T) = h(t,\tau), \tag{14}$$

where T is the period time. Assume the input, $U(s)$, is given in Laplace domain. The corresponding time domain signal is

$$u(t) = \mathcal{L}^{-1}(U)(t) = \frac{1}{2\pi j} \int_{\sigma-j\infty}^{\sigma+j\infty} e^{st} U(s) ds.$$

This gives the following output

$$\begin{aligned} y(t) &= \int_{-\infty}^{\infty} h(t,\tau) u(\tau) d\tau \\ &= \int_{-\infty}^{\infty} h(t,\tau) \frac{1}{2\pi j} \int_{\sigma-j\infty}^{\sigma+j\infty} e^{s\tau} U(s) ds d\tau \\ &= \frac{1}{2\pi j} \int_{\sigma-j\infty}^{\sigma+j\infty} e^{st} H(s,t) U(s) ds. \end{aligned}$$

Here, $H(s,t)$ is a time periodic transfer function

$$H(s,t) = e^{-st} \int_{-\infty}^{\infty} e^{s\tau} h(t,\tau) d\tau$$

which is periodic in t. The periodicity implies that $H(s,t)$ can be written as a Fourier series with the fundamental frequency $\omega_0 = 2\pi/T$

$$\begin{aligned} H(s,t) &= \sum_k \hat{H}_k(s) e^{jk\omega_0 t}, \\ \hat{H}_k(s) &= \frac{1}{T} \int_0^T H(s,t) e^{-jk\omega_0 t} dt. \end{aligned}$$

The output can now be written

$$y(t) = \frac{1}{2\pi j}\int_{\sigma-j\infty}^{\sigma+j\infty}\sum_k \hat{H}_k(s)e^{(s+jk\omega_0)t}U(s)ds$$
$$= \frac{1}{2\pi j}\int_{\sigma-j\infty}^{\sigma+j\infty}\sum_k \hat{H}_k(s-jk\omega_0)e^{st}U(s-jk\omega_0)ds.$$

Here, we recognize the definition of the inverse Laplace transform. In Laplace domain, the output is hence

$$Y(s) = \sum_k \hat{H}_k(s-jk\omega_0)U(s-jk\omega_0). \tag{15}$$

From this we conclude that for LTP-systems there is coupling between frequencies that are separated by a multiple of the fundamental frequency of the system, ω_0. Laplace transformation of the EMP signal defined by (13) gives

$$U = 2\pi\sum_m U_m\delta_{s+jm\omega_0}$$

Equation (15) gives that the output too is an EMP signal

$$Y = 2\pi\sum_n Y_n\delta_{s+jn\omega_0},$$

where

$$Y_n = \sum_m \hat{H}_{n-m}(s_0+jm\omega_0)U_m.$$

The doubly-infinite matrix in Section II is hence given by

$$H_{n,m}(s) = \hat{H}_{n-m}(s+jm\omega_0). \tag{16}$$

7. References

Acha, E., J. Arrillaga, A. Medina, and A. Semlyen (1989): "General frame of reference for analysis of harmonic distortion in systems with multiple transformer nonlinearities." *IEE Procedings*, **136C:5**, pp. 271–278.

Arrillaga, J. and C. D. Callaghan (1991): "Three phase AC-DC load and harmonic flows." *IEEE Trans. on Power Delivery*, **6:1**, pp. 238–244.

Arrillaga, J., A. Medina, M. L. V. Lisboa, M. A. Cavia, and P. Sánchez (1994): "The harmonic domain. A frame of reference for power system harmonic analysis." *IEEE Trans. on Power Systems*, **10:1**, pp. 433–440.

Arrillaga, J., N. R. Watson, J. F. Eggleston, and C. D. Callaghan (1987): "Comparison of steady-state and dynamic models for the calculation of AC/DC system harmonics." *IEE Proceedings*, **134C:1**, pp. 31–37.

Gilmore, R. J. and M. B. Steer (1991): "Nonlinear circuit analysis using the method of harmonic balance – A review of the art. Part I. Introductory concepts." *Int J. Microwave and Millimeter-Wave Computer-Aided Eng.*, **1:1**, pp. 22–37.

Hauer, J. F. and C. W. Taylor (1998): "Information, reliability, and control in the new power system." In *Proceedings of the American Control Conference*. Philadelphia, Pennsylvania.

Hwang, S. (1997): *Frequency Domain System Identification of Helicopter Rotor Dynamics incorporationg Models with Time Periodic Coefficients*. PhD thesis, Dept. of Aerospace Engineering, University of Maryland.

Kundert, K. S. and A. Sangiovanni-Vincentelli (1986): "Simulation of nonlinear circuits in the frequency domain." *IEEE Trans. on Computer-Aided Design*, **5:4**, pp. 521–535.

Maciejowski, J. M. (1989): *Multivariable Feedback Design*. Addison-Wesley, Reading, Massachusetts.

Sandberg, H. (1999): "Nonlinear modeling of locomotive propulsion system and control." Master Thesis TFRT-5625. Department of Automatic Control, Lund.

Semlyen, A., E. Acha, and J. Arrillaga (1988): "Newton-type algorithms for the harmonic phasor analysis of non-linear power circuits in periodical steady state with special reference to magnetic non-linearities." *IEEE Trans. on Power Delivery*, **3:3**, pp. 1090–1098.

Semlyen, A. and N. Rajaković (1989): "Harmonic domain modeling of laminated iron core." *IEEE Trans. on Power Delivery*, **4:1**, pp. 382–390.

Song, W., G. T. Heydt, and W. M. Grady (1984): "The integration of HVDC subsystems into the harmonic power flow algorithm." *IEEE Trans. on Power Apparatus and Systems*, **PAS-103:8**, pp. 1953–1961.

Werely, N. M. (1991): *Analysis and Control of Linear Periodically Time Varying Systems*. PhD thesis, Dept. of Aeronautics and Astronautics, MIT.

Xia, D. and G. T. Heydt (1982): "Harmonic power flow studies, Part I – Formulation and solution, Part II – Implementation and practical aspects." *IEEE Trans. on Power Apparatus and Systems*, **101:6**, pp. 1257–1270.

Xu, W., J. E. Drakos, Y. Mansour, and A. Chang (1994): "A three-phase converter model for harmonic analysis of HVDC systems." *IEEE Trans. on Power Delivery*, **9:3**, pp. 1724–1731.

Xu, W., J. R. Marti, and H. W. Dommel (1991): "A multiphase harmonic load flow solution technique." *IEEE Trans. on Power Systems*, **6:1**, pp. 174–182.

Paper III

Out of Control Because of Harmonics – An Analysis of the Harmonic Response of an Inverter Locomotive

Erik Möllerstedt and Bo Bernhardsson

Introduction

On Sunday April 9, 1995, a large number of the regional trains stopped in Zürich, Switzerland.[1] The locomotives were automatically shut down by protective equipment because of excessively high harmonic currents. The Swiss railway had recently replaced many of their old locomotives with the new generation of locomotives, which use high-frequency converters to improve performance and reduce losses. Such converters inherently generate harmonics, but by proper design and control, the level of harmonics was believed to be kept low. However, these converters can interact with each other via the supplying network, causing unpredicted instability problems.

Evidence supporting this explanation was that the incident occurred on a Sunday, during low traffic, when only modern locomotives were used. With a few of the old trains running on the system, the losses in these old trains were enough to damp the oscillations. By adjusting the algorithm for zero-crossing detection of the grid voltage, the problem was believed to be solved, but a new incident occurred in September of the same year, also on a weekend (i.e. at low-load conditions with mainly new locomotives running). After adjustments to the software for converter control, the Swiss network now seems to be stable, but as other countries begin replacing old locomotives with new ones, the problems are likely to occur elsewhere.

The result of the Swiss incidents is that very high demands are placed on locomotive manufacturers. To sell a locomotive, you must be able to guarantee that it is compatible with the rest of the system. If an incident occurs, the manufacturer of the last locomotives added to the system is likely to come under scrutiny. The United Kingdom has imposed especially tough constraints, making it hard to sell new locomotives there. The ability to guarantee performance of converter trains and to formulate reasonable performance requirements, will require methods for proper analysis of these systems.

Modern converters serve as very powerful actuators. Directions of power flows can be changed in fractions of a second. The time-varying components introduce couplings between different frequencies. Energy can be moved between different frequency regions, creating instability loops that involve many different frequencies. If the dominating loads are fed by such converters, this harmonic interaction must be taken into account. In traditional analysis, however, electric networks are treated as linear, and nonlinear loads are modelled as current sources, possibly behind a

[1]The Swiss incidents and more technical background are described in detail in [Meyer, 1999].

linear impedance to increase the validity region of the model. Stability analysis is performed with linear time-invariant methods, frequency by frequency, supported by extensive time domain simulations. With the new generation of high-frequency converters, such analysis is not sufficient.

Analysis of the complete railway system is, of course, difficult (see [Meyer, 1999] for a discussion). Several locomotives can be moving along the power distribution line at the same time, and depending on the distance between the locomotives, the interaction changes. The power consumption also changes, depending on operating modes. During normal operation, energy is consumed from the net, but as modern locomotives use electrical breaking, the power flow changes direction during deceleration, and energy is delivered back to the grid. The inverter trains are no passive elements. The converters are controlled with only limited system knowledge (local measurements of currents and voltages), making analysis and control design an even bigger challenge.

Linear Time Periodic (LTP) Control Systems

Since the locomotive system is driven by a periodic electrical signal, we want to study local stability around a periodic system trajectory. Denote the system states in the locomotive by $x(t)$ and the nominal trajectory by $x_0(t)$, where $x_0(t+T) = x_0(t)$ with $\omega_0 T = 2\pi$. In Switzerland, $\omega_0 = 100\pi/3$, since the line frequency is 16-2/3 Hz.

For a nonlinear system of the form $\dot{x} = f(x,u)$, where u is the input signals and x the states, the linearization near the trajectory $x_0(t)$ is given by

$$\frac{d}{dt}\Delta x(t) = A(t)\Delta x(t) + B(t)\Delta u(t),$$

where $A(t) = f_x(x_0(t))$ and $B(t) = f_u(x_0(t))$. (Here, and in the rest of the article, Δ denotes deviation from the nominal trajectory, so $\Delta x = x - x_0$.) Since much of the design engineer's intuition is in the frequency domain, we turn to analysis of linear time periodic (LTP) systems in the frequency domain.

An LTP system H, with period $T > 0$, is a relation $y = Hu$ that commutes with the time shift operator S_T (i.e., $HS_T = S_T H$, where $S_T(f)(t) = f(t+T)$). Analysis of this class of systems has a long history, going back to the work of Floquet and Hill (see [Floquet, 1883], [Hill, 1886]). Periodic control systems have been widely studied since the 1950s when computer-controlled systems were introduced. The motivation comes from the use of periodic sample and hold circuits (see [Bamieh and Pearson, 1992], [Chen and Francis, 1995]). In other areas, the periodicity

arises because of the controlled process; one example is in helicopter vibration control (see [Hwang, 1997], [Wereley, 1991]). Many system theory questions, such as controllability, observability, and linear quadratic control, have been studied for LTP systems (see, for example, [Kamen and Sills, 1993], [Kano and Nishimura, 1985], [Richards, 1983], and [Wereley and Hall, 1991]). Very little of this powerful control theory seems to have been used for analysis of electrical power systems and networks. Two well established techniques for analysis of LTP systems are Floquet analysis and lifting.

Floquet Analysis

Causal, finite-dimensional, proper LTP systems also have state-space representations

$$\begin{aligned} \frac{dx}{dt} &= A(t)x + B(t)u \\ y &= C(t)x + D(t)u, \end{aligned} \tag{1}$$

where $A(t) \in R^{n\times n}, B(t) \in R^{n\times m}, C(t) \in R^{p\times n}$, and $D(t) \in R^{p,m}$ are T-periodic matrix functions of appropriate dimensions. The stability of such systems can be determined via Floquet decomposition, which is a T-periodic state transformation $z(t) = P(t)x(t)$ that transfers the system to a similar state-space form with a constant (generally complex-valued) system matrix, $\hat{A} = \log \Phi(T, 0)$, where $\Phi(T, 0)$ denotes the so-called monodromy matrix of the system and $\Phi(t, \tau)$ is the fundamental matrix of the system defined via the differential equation

$$\frac{d}{dt}\Phi(t, \tau) = A(t)\Phi(t, \tau), \quad \Phi(t, t) = I.$$

The transformed system

$$\begin{aligned} \frac{dz}{dt} &= \hat{A}z(t) + \hat{B}(t)u(t) \\ y(t) &= \hat{C}(t)z(t) + D(t)u(t) \end{aligned} \tag{2}$$

is asymptotically stable if the eigenvalues of $\hat{A}$ are in the open left half plane. The complex-valued state transformation $P(t) \in C^{n\times n}$ can be determined by solving the matrix differential equation $\dot{P}(t) = A(t)P(t) - P(t)\hat{A}$, $P(0) = I$.

Lifting Techniques

Another way of analyzing periodic linear systems using theory for the time-invariant case is to rewrite (1) into the integral operator state-space

model

$$\begin{aligned} \tilde{x}_{k+1} &= \tilde{A}\tilde{x}_k + \tilde{B}\tilde{u}_k \\ \tilde{y}_k &= \tilde{C}_k\tilde{x}_k + \tilde{D}_k u_k. \end{aligned} \tag{3}$$

Here $\tilde{x}_k \in R^n$, the functions $\tilde{u}_k \in L_2^m[0,T]$ and $\tilde{y}_k \in L_2^p[0,T]$ are defined as $\tilde{u}_k = u(t+kT)$ and $\tilde{y}_k = y(t+kT)$ for $k \in Z$, and $t \in [0,T]$. The operators $\tilde{A} : C^n \to C^n$, $\tilde{B} : L_2^m[0,T] \to C^n$, $\tilde{C} : C^n \to L_2^p[0,T]$, and $\tilde{D} : L_2^m[0,T] \to L_2^p[0,T]$ are given by

$$\begin{aligned} \tilde{A} &= \Phi(0,T) \\ \tilde{B}\tilde{u}_k &= \int_0^T \Phi(T,\tau)B(\tau)\tilde{u}_k\, d\tau \\ \tilde{C} &= C(t)\Phi(t,0) \\ \tilde{D}\tilde{u}_k &= \int_0^t (C(t)\Phi(t,\tau)B(\tau) + D(t)\delta(t-\tau))\tilde{u}_k\, d\tau. \end{aligned}$$

The time-invariant system (3), which maps sequences of $L_2^m(0,T)$ functions into sequences of $L_2^p(0,T)$ functions, can now be analyzed using time-invariants techniques.

Harmonic Analysis by Harmonic Transfer Functions (HTFs)

In this article, we will pursue a third direction for analysis, which can also be used for systems lacking a state-space representation. Assume the input-output relation is given by

$$y(t) = \int_{-\infty}^{\infty} h(t,\tau)u(\tau)\, d\tau,$$

where $h(t,\tau)$ is the so-called impulse response of the system. This represents a T-periodic input-output relation if $h(t+T,\tau+T) = h(t,\tau)$.

The Laplace transform of a signal $u(t)$ is defined as

$$U(s) = \int_{-\infty}^{\infty} e^{-st}u(t)dt$$

with absolute convergence for s belonging to a strip in the complex plane. For linear T-periodic systems with impulse response $h(t,\tau)$, a direct computation shows that

$$Y(s) = \sum_{k=-\infty}^{\infty} H_k(s - jk\omega_0)U(s - jk\omega_0), \tag{4}$$

where the transfer functions H_k are defined by

$$\begin{aligned} H_k(s) &= \mathcal{L}(h_k(t)) = \int_{-\infty}^{\infty} e^{-st} h_k(t) dt, \quad \text{with} \\ h_k(t) &= \frac{1}{T} \int_0^T h(r, r-t) e^{-jk\omega_o r}\, dr. \end{aligned}$$

The impulse responses, $h_k(t)$, are the Fourier coefficients of $h(r, r-t)$, which is periodic in r. The mapping in (4) shows that there is coupling between frequencies separated by a multiple of the system frequency ω_0.

By restricting ourself to a strip in the complex plane, given by $-\omega_0/2 < \mathrm{Im}(s) \leq \omega_0/2$, and defining

$$\begin{aligned} \mathcal{U}(s) &= [\ldots \quad U(s-j\omega_0) \quad U(s) \quad U(s+j\omega_0) \quad \ldots]^T \\ &= [\ldots \quad U_{-1}(s) \quad U_0(s) \quad U_1(s) \quad \ldots]^T, \end{aligned} \tag{5}$$

and $\mathcal{Y}(s)$ analogously, (4) can be written in a more compact way:

$$\mathcal{Y}(s) = \mathcal{H}(s)\mathcal{U}(s),$$

where $\mathcal{H}(s)$ is a doubly infinite matrix defined as

$$\mathcal{H}(s) = \begin{bmatrix} \ddots & \cdots & \cdots & \cdots & \cdots \\ \vdots & H_{-1,-1}(s) & H_{-1,0}(s) & H_{-1,1}(s) & \cdots \\ \vdots & H_{0,-1}(s) & H_{0,0}(s) & H_{0,1}(s) & \cdots \\ \vdots & H_{1,-1}(s) & H_{1,0}(s) & H_{1,1}(s) & \cdots \\ \vdots & \vdots & \vdots & \vdots & \ddots \end{bmatrix}, \tag{6}$$

with $H_{n,m}(s) = H_{n-m}(s + jm\omega_0)$.

Using (5), a signal with Laplace transform $U(s)$ can be written

$$u(t) = \int_{\sigma-j\infty}^{\sigma+j\infty} e^{st} U(s) ds = \int_{\sigma-j\omega_0/2}^{\sigma+j\omega_0/2} e^{st} u_s(t) ds, \tag{7}$$

where for each s, $u_s(t) = \sum_m e^{jm\omega_0 t} U_m(s)$ is a periodic function.

From (4) and (7) it can be concluded that, just as linear time-invariant (LTI) systems can be studied by analyzing the response to signals of the form e^{st}, so-called characters, and then using superposition, one can study

LTP systems by superposition of characters called exponentially modulated periodic (EMP) signals with period T. These have the form

$$u(t) = e^{st} \sum_m U_m e^{jm\omega_0 t}, \quad -\omega_0/2 < \mathrm{s} \leq \omega_0/2, \quad U_m \in C.$$

EMP signals with base frequency s are mapped to EMP signals with the same base frequency:

$$y(t) = e^{st} \sum_n Y_n e^{jn\omega_0 t} = \sum_n Y_n e^{(s+jn\omega_0)t}.$$

The transfer function matrix $\mathcal{H}(s)$ defines the coupling between different frequencies and is called the harmonic transfer function (HTF) (see [Wereley, 1991]). An LTP system can thus be treated as an LTI system with infinitely many inputs and outputs. Transmission zeros and poles can be derived from multi-variable time-invariant theory.

If all signals are periodic, they can be represented by their Fourier series. The relation between the Fourier coefficients of the input and the output is then described by

$$\mathcal{Y}(0) = \mathcal{H}(0)\mathcal{U}(0).$$

The complex matrix $\mathcal{H}(0)$ can be used to obtain the steady state solution of a network. The matrix is called the admittance matrix in the Harmonic Norton Equivalent described in [Möllerstedt, 1998] and is the Jacobian in harmonic balancing of electrical networks (see [Arrillaga *et al.*, 1994], [Kundert and Sangiovanni-Vincentelli, 1986]). The steady-state response matrix $\mathcal{H}(0)$ has recently been developed for several electric components, for instance, transformers with nonlinear saturation curves [Acha *et al.*, 1989], [Semlyen *et al.*, 1988], [Semlyen and Rajakovic, 1989], HVDC converters [Arrillaga and Callaghan, 1991], [Song *et al.*, 1984], [Xu *et al.*, 1994], and static var compensators [Xu *et al.*, 1991]. For identification of $\mathcal{H}(0)$ from experimental data, see [Möllerstedt, 1998]. However, the information in $\mathcal{H}(0)$ is not sufficient to describe stability properties of the system under aperiodic perturbations. This information is contained in $\mathcal{H}(j\omega)$, $-\omega_0/2 \leq \omega < \omega_0/2$.

Example 1: LTI Systems For an LTI system, the matrix in (4) has the standard transfer function $H_0(s)$ on the diagonal and all other $H_k(s)$ are zero.

Example 2: Multiplication Operators If the relation between inputs and outputs is given by the static time-varying map

$$y(t) = h(t)u(t)$$

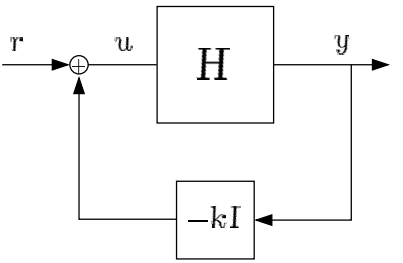

Figure 1 The feedback system studied in the Nyquist criterion. Here H represents a linear time periodic (LTP) system.

with a T-periodic function $h(t)$, for instance a sinusoid or a periodic switch signal, then $\mathcal{H}(s)$ is a Toeplitz matrix independent of the complex frequency s

$$\mathcal{H}(s) = \begin{bmatrix} \ddots & \ddots & \ddots & \ddots & \ddots & \ddots \\ \ddots & H_0 & H_{-1} & H_{-2} & \ddots & \ddots \\ \ddots & H_1 & H_0 & H_{-1} & H_{-2} & \ddots \\ \ddots & H_2 & H_1 & H_0 & H_{-1} & \ddots \\ \ddots & \ddots & H_2 & H_1 & H_0 & \ddots \\ \ddots & \ddots & \ddots & \ddots & \ddots & \ddots \end{bmatrix},$$

where H_k are the Fourier coefficients of $h(t)$.

Example 3: LTP Systems on State Space Form The harmonic transfer function of an LTP system on state space form (2) is, neglecting the direct term, the product of three matrices, the Toeplitz matrix corresponding to the periodic function, $\hat{C}(t)$, the diagonal matrix for the transfer function, $H_0(s) = (sI - \hat{A})^{-1}$, and the Toeplitz matrix of $B(t)$. Explicitly, this gives

$$H_k(s) = \sum_l \hat{C}_{k-l}((s + jl\omega_0)I - \hat{A})^{-1}\hat{B}_l + D_k,$$

where $\hat{B}_k$, $\hat{C}_k$, and D_k, are the Fourier coefficients of the periodic functions, $\hat{B}(t)$, $\hat{C}(t)$, and $D(t)$, respectively.

The Nyquist Criterion for Harmonic Transfer Functions

It is often interesting to analyze the stability properties of the feedback system in Fig. 1, where H represents the mapping in (4). For LTI systems,

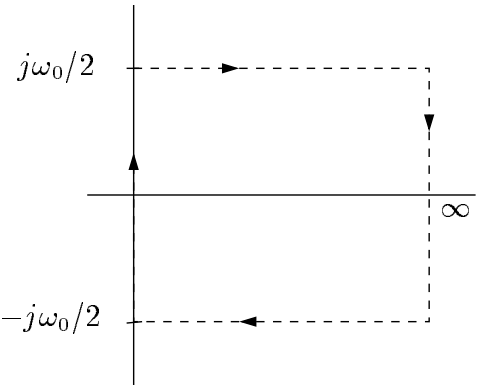

Figure 2 The integration contour in the Nyquist criterion for harmonic transfer functions.

stability can be investigated by plotting the Nyquist contour $H_0(j\omega)$ for $-\infty < \omega < \infty$ and counting encirclements of the point $-1/k$. For LTP systems of the form (4), the following generalized Nyquist criterion holds.
Theorem [Wereley, 1991] *Assume a linear, periodic, causal input-output relation between y and u is given by (4). Denote by* $\{\lambda_i(s)\}_{i=-\infty}^{\infty}$ *the eigenvalues of the doubly infinite matrix* $\mathcal{H}(s)$ *in (6), for s varying through the contour in Fig. 2. The eigenvalues produce a number of closed curves in the complex plane, called the eigen-loci of the HTF. The closed-loop system in Fig. 1 is* L_2 *stable from r to y if and only if the total number of counterclockwise encirclements of the* $-1/k$ *point of these curves equals the number of open-loop right half plane poles of the* $\mathcal{H}(s)$ *in (4) (hence zero if H is stable).*

Analysis by Finite Projection Methods

For computation, the doubly infinite matrix must be approximated by a finite truncated matrix. The best way to do this is an open issue. If we simply choose a truncation number N and a frequency grid size M and calculate the eigenvalues of the finite matrix with matrix elements

$$H_{n,m}(s_k) = H_{n-m}(s_k + jn\omega_0), \quad -N \le m, n \le N$$

for a grid $s_k = i\omega_k$ with $\omega_{k+1} - \omega_k = \omega_0/2M$, we get $2M+1$ matrices of size $(2N+1) \times (2N+1)$, hence a total of $(2N+1)(2M+1)$ eigenvalues.

Although convergence issues of the infinite matrices have not been considered,the roll off of the system normally assures correct results using

truncated matrices. To get an appropriate value for N, this is increased until the result does not change, and the additional eigenvalues end up in the origin.

Passivity

The concept of passivity is very important in electrical networks. A relation $y = Hu$ is said to be passive if for all inputs u it holds that

$$\int_{-\infty}^{\infty} u(t)y(t)\,dt \geq 0.$$

Parseval's formula and the relation

$$\begin{aligned}
&\int_{-\infty}^{\infty} U^*(j\omega)Y(j\omega)\,d\omega \\
&= \int_{-\omega_0/2}^{\omega_0/2} \sum_{m,n} U^*(j\omega + jn\omega_0)H_{n-m}(j\omega + jm\omega_0)U(j\omega + jm\omega_0)\,d\omega \\
&= \int_{-\omega_0/2}^{\omega_0/2} \mathcal{U}^*(j\omega)\mathcal{H}(j\omega)\mathcal{U}(j\omega)\,d\omega \\
&= \int_{0}^{\omega_0/2} \mathcal{U}^*(j\omega)(\mathcal{H}^*(j\omega) + \mathcal{H}(j\omega))\mathcal{U}(j\omega)\,d\omega.
\end{aligned}$$

show that passivity for stable LTP systems is equivalent to the condition

$$\mathcal{H}^*(j\omega) + \mathcal{H}(j\omega) \geq 0, \qquad 0 \leq \omega < \omega_0/2,$$

where $\mathcal{H}$ is the matrix in (6).

Robustness of LTP Systems to Model Errors

Robustness under unmodeled dynamics is an important issue for successful controller design. A large set of frequency domain analysis tools is available where an LTI system is connected in feedback with a possibly nonlinear perturbation operator Δ. Many of these tools can be used also for LTP system; for example, the small gain criterion, which can be stated in the following way.

Theorem *Given a stable LTP system H with $\|H\|_\infty = \gamma_1$, the closed-loop system in Fig. 3 is stable for all nonlinear perturbations Δ with $\|\Delta\|_\infty \leq \gamma_2$ if $\gamma_1\gamma_2 < 1$.*

The induced L_2-norm (i.e., the H_∞ norm) of a possibly nonlinear operator N is given by

$$\|N\|_\infty = \sup_{L_2 \ni u \neq 0} \frac{\|Nu\|_{L_2}}{\|u\|_{L_2}}.$$

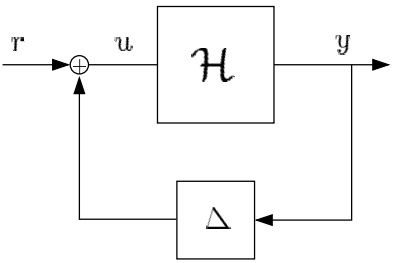

Figure 3 The feedback system in the small gain criterion. Here $\mathcal{H}$ is a stable LTP system and Δ is a general stable nonlinear operator, which can describe, for instance, unmodeled dynamics. The norm $\|\mathcal{H}\|_\infty$ of the LTP system can be calculated from (8).

For a stable LTP system $\mathcal{H}$, the H_∞ norm can be calculated by

$$\|\mathcal{H}\|_\infty = \sup_{\substack{\text{Re } s \geq 0 \\ |\text{Im } s| < \omega_0/2}} \sigma_{max}(\mathcal{H}(s)), \tag{8}$$

where σ_{max} denotes the maximum singular value (which is well defined for the doubly infinite matrix $\mathcal{H}(s)$ and can be calculated as the limit of finite matrices using finite projection methods, under appropriate convergence conditions).

For more background on frequency response analysis of time-varying systems see [Ball *et al.*, 1995] or [Wereley, 1991].

Analysis of an Inverter Locomotive Using HTFs

We will now discuss the use HTFs for analyzing an inverter locomotive in the frequency domain. Tuning the controller for the converter switching is problematic, as the effect of the converters cannot be captured well using common LTI models. Instead, one must rely on ad hoc tuning rules, and validation is done with time domain simulations. With this approach, it is impossible to guarantee controller robustness. Time domain simulation can only give a yes or no answer to stability, and it is impossible to simulate every possible operating condition. HTFs provide a way to take stability and robustness into account. Note, however, that the validity of the linearization is restricted to the neighborhood of the nominal trajectory; hence only local stability is studied. Different HTFs must be obtained for different nominal load cases.

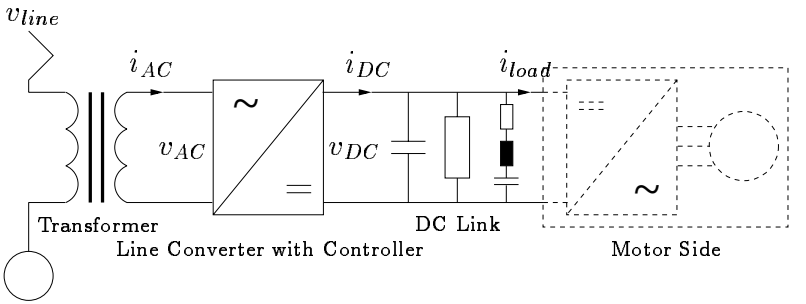

Figure 4 A schematic of an inverter locomotive. The locomotive consists of a transformer, a line converter, a DC link, and the motor side. The construction opens new possibilities for control, and for operating the same locomotive on different power grids, which simplifies border crossing.

An inverter locomotive is shown in Fig. 4. The locomotive consists of a transformer, a line converter, a DC link, and the motor side. The motor side consists of a motor converter (or possibly many), similar to the line converter but with 3 phase AC, and asynchronous motors. This topology with two controlled converters connected by a DC link, often called a back-to-back converter, is common in variable-speed drives in many different applications. It is a flexible structure that allows fast control of the power flow. By controlling the power flow from the grid, the DC link voltage can be kept constant at a high level. This facilitates that the motor power can be increased and ensures that the size of the stabilizing DC link capacitor can be reduced. This capacitor is expensive and very heavy, adding considerable weight to the locomotive. Among other advantages of the back-to-back converter are possibilities for active filtering and reactive power compensation, and to feed braking energy back into the power grid. In Europe, there are five different electrical railroad systems, both DC and AC of different amplitude and frequency. The back-to-back converter offers the possibility of operating the same locomotive in all systems, which simplifies border crossing.

The harmonic transfer functions gives a model description that facilitates reuse of sub-models. This is a key issue for handling complexity and improving system understanding. For a discussion of modern trends in continuous-time object-oriented modeling and simulation, see [Åström *et al.*, 1998].

The idea is here to derive the HTF for each subsystem. A subsystem can later be replaced by more detailed descriptions without recalculating the whole system, as long as the nominal periodic trajectory used for the

linearization is not affected. For example, the goal could be to compare different control strategies, to include saturation in the transformer, or to improve the modeling of the motor side, which in the following is simply modeled as a constant (or very slowly varying) current sink. From the HTFs of the different sub-models, the HTF for the whole locomotive is obtained by simple matrix manipulations. A common controller structure for the line converter controller is investigated, and stability margins are obtained via the generalized Nyquist criterion.

The harmonic transfer functions gives a model description that facilitates reuse of sub-models. This is a key issue for handling complexity and improving system understanding. For a discussion of modern trends in continuous-time object-oriented modeling and simulation, see [Åström *et al.*, 1998].

The idea is here to derive the HTF for each subsystem. A subsystem can later be replaced by more detailed descriptions without recalculating the whole system, as long as the nominal periodic trajectory used for the linearization is not affected. For example, the goal could be to compare different control strategies, to include saturation in the transformer, or to improve the modeling of the motor side, which in the following is simply modeled as a constant (or very slowly varying) current sink. From the HTFs of the different sub-models, the HTF for the whole locomotive is obtained by simple matrix manipulations. A common controller structure for the line converter controller is investigated, and stability margins are obtained via the generalized Nyquist criterion.

The Transformer

In this example, the transformer is simply modeled as a linear impedance on the low-voltage side. If a more accurate model is required, a steady-state frequency domain model (i.e., $\mathcal{H}(0)$) of a transformer with saturation is derived in [Semlyen *et al.*, 1987]. This can be extended to a full HTF model $\mathcal{H}(s)$.

The transformer is described by the transfer function

$$I_{tr}(s) = G_{trafo}(s)V_{tr}(s) = \frac{1}{sL_{tr} + R_{tr}}V_{tr}(s),$$

where $I_{tr} = I_{AC}$ describes the current through the transformer and $V_{tr} = V_{line} - V_{AC}$ describes the voltage.

The actual transformation is ignored, as only local analysis is considered. This means that the line voltage in the following is a low-voltage equivalent to the actual line voltage. When connecting the locomotive to a network, its transfer function must be divided by the transformer ratio

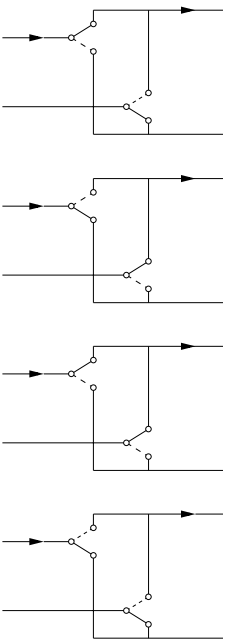

Figure 5 The four possible states for the converter. The first state gives $m = 1$, the second gives $m = -1$, and the last two states correspond to $m = 0$. For a loss-free converter, the relations (9) and (10) hold at all times.

squared; that is,

$$\mathcal{H}_{loco}^{HV} = \frac{1}{n^2}\mathcal{H}_{loco}^{LV},$$

where n is the transformer ratio (unless per-unit quantities are used).

The Line Converter

The converters complicate analysis of inverter locomotives. They describe the coupling between the AC side and the DC side, and cannot be well approximated by LTI models. A modern converter has no energy storage and is practically lossless. This means that a power balance must always be fulfilled

$$v_{AC}(t)i_{AC}(t) = v_{DC}(t)i_{DC}(t)$$

for all t. The power that flows into the converter from the AC side equals the power that flows out on the DC side. The directions of flow correspond to the definitions of voltages and current directions in Fig. 4. The converter

implies a modulation of the voltage and the current:

$$v_{AC}(t) = m(t)v_{DC}(t), \tag{9}$$
$$i_{DC}(t) = m(t)i_{AC}(t). \tag{10}$$

If the switching is considered ideal, the modulation function, $m(t)$, can take three different values: +1, -1, and 0, according to the switching schemes shown in Fig. 5. In older trains with line-commutated converters, $m(t)$ is determined by the line voltage and current. Modern converters are implemented using very fast gate turn-off (GTO) thyristors or insulated gate bipolar transistors (IGBTs), which allow switching frequencies of several kHz. Using pulse width modulation (PWM), for instance, $m(t)$ can, after low-pass filtering, approximate any function with amplitude less than, or just above, 1. As the DC voltage is kept approximately constant and the AC voltage is nearly sinusoidal, $m(t)$ is typically shaped as a sine wave of fundamental frequency.

The DC Link

The DC link is meant to provide the motor side with a constant DC voltage and thus separate the motor side from the line side. This way, the motor control can hopefully be treated without taking into account line-side variations and disturbances. The DC link has a large capacitor to stabilize the DC voltage, a resistor, and a passive filter, tuned at twice the line frequency (see Fig. 4). As the DC current is the product of two sinusoidal functions (10), it will inherently have a strong component at twice the fundamental frequency. The filter is meant to reduce the influence on the DC voltage.

Consequently, the DC link is described by a fourth-order transfer function from current to voltage

$$V_{DC}(s) = G_{link}(s)(I_{load}(s) - I_{DC}(s))$$
$$G_{DC-link}(s) = -\frac{C_f L_f s^2 + C_f R_f s + 1}{(C_f L_f s^2 + C_f R_f s + 1)(Cs + 1/R) + C_f s},$$

where C is the capacitance of the large DC link capacitor, R is the resistor, and C_f, L_f, and R_f belong to the filter.

The Motor Dynamics

A detailed model of how the load current depends on DC link voltage, mechanical torque, and torque set point is derived in [Sandberg, 1999]. To simplify the analysis here, the motor and the motor converter are replaced by a current sink, I_{load}.

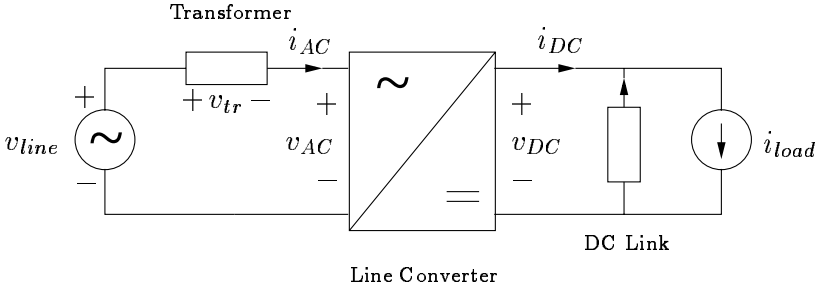

Figure 6 A circuit diagram of the inverter locomotive. The supporting line produces a driving electrical voltage v_{line}, which might contain harmonics (created by other locomotives, for instance). The voltage is transformed to the line converter, which by proper control of $m(t)$ in (9) and (10) supplies the DC link with energy. The voltage v_{DC} should be kept close to constant, since electrical ripples create mechanical ripples on the motor side. The motor side is modeled as a constant current sink i_{load}.

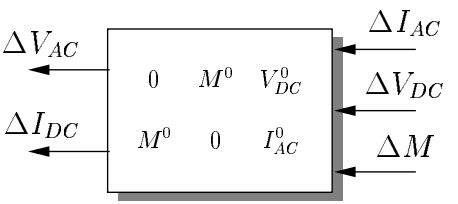

Figure 7 Block diagram of the line converter. The HTFs M^0, V^0_{DC}, and I^0_{AC} are Toeplitz matrices. The line converter is connected to the transformer and DC link in Fig. 9.

A Harmonic Transfer Function for the Inverter Locomotive

A circuit diagram of the low-voltage side of the inverter locomotive is shown in Fig. 6. To get a model for the entire locomotive, we will derive HTFs for each subsystem and connect them to form the closed-loop HTF.

Linearizing the Line Converter For small distortions around a periodic solution, the converter is approximated well by linearizing (9) and (10)

$$\Delta v_{AC}(t) = m^0(t)\Delta v_{DC}(t) + v^0_{DC}(t)\Delta m(t)$$
$$\Delta i_{DC}(t) = m^0(t)\Delta i_{AC}(t) + i^0_{AC}(t)\Delta m(t),$$

where $m^0(t)$, $v^0_{DC}(t)$, and $i^0_{AC}(t)$ are periodic signals according to the nominal periodic solution. The converter is thus modeled as an LTP model with three inputs and two outputs, as shown in Fig. 7. The nominal periodic

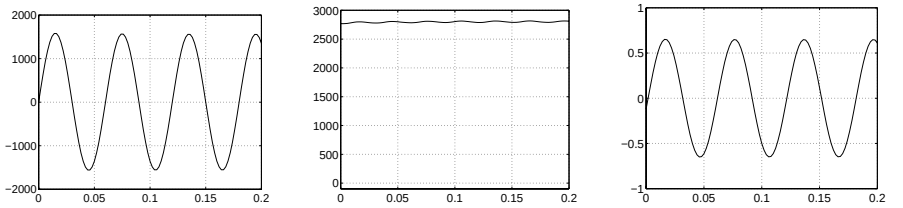

Figure 8 The periodic solution used for the linearization. $I_{load} = 500\,\mathrm{A}$. From the left: $i_{AC}(t)$, $v_{DC}(t)$, and $m(t)$. The DC link filter and proper converter control keeps the ripple in DC voltage small.

operating trajectory used for the linearization can be derived analytically, but is conveniently obtained via one time domain simulation. With more complex models, simulation is the only reasonable approach.

The nominal solution is illustrated in Fig. 8.

HTFs for the Subsystems As the converter implies only multiplication with periodic signals, its HTF is given by

$$\begin{bmatrix} \Delta V_{AC} \\ \Delta I_{DC} \end{bmatrix} = \begin{bmatrix} 0 & M^0 & V^0_{DC} \\ M^0 & 0 & I^0_{AC} \end{bmatrix} \begin{bmatrix} \Delta I_{AC} \\ \Delta V_{DC} \\ \Delta M \end{bmatrix},$$

where the matrices M_0, V^0_{DC}, and I^0_{AC} are Toeplitz matrices with the Fourier coefficients of the corresponding time domain signals as coefficients, as in the previous examples.

As the transformer and the DC link are linear, their HTFs are given by diagonal matrices, according to Example 1,

$$\mathcal{H}_{trafo}(s) = \begin{bmatrix} \ddots & & & & \\ & G_{trafo}(s - j\omega_0) & & 0 & \\ & & G_{trafo}(s) & & \\ & 0 & & G_{trafo}(s + j\omega_0) & \\ & & & & \ddots \end{bmatrix}$$

and similarly for $\mathcal{H}_{DC-link}(s)$.

The transformer and the DC link define feedback connections between the outputs and inputs of the converter (see the block diagram in Fig. 9). The transfer function of the locomotive without converter control can now be derived using the common rules for connecting LTI transfer functions.

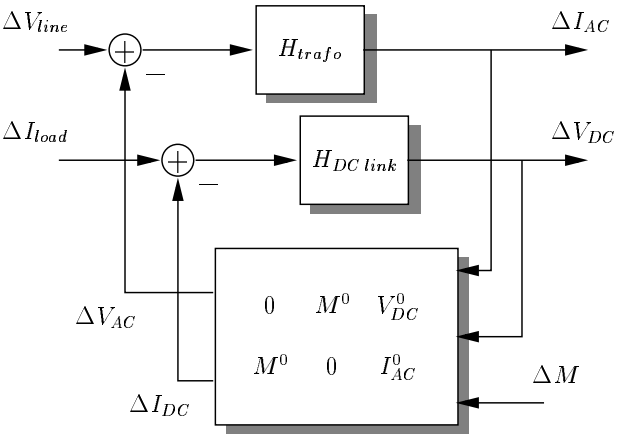

Figure 9 A block diagram of the linearized inverter locomotive without converter controller. Also see Fig. 11 for the total controlled locomotive.

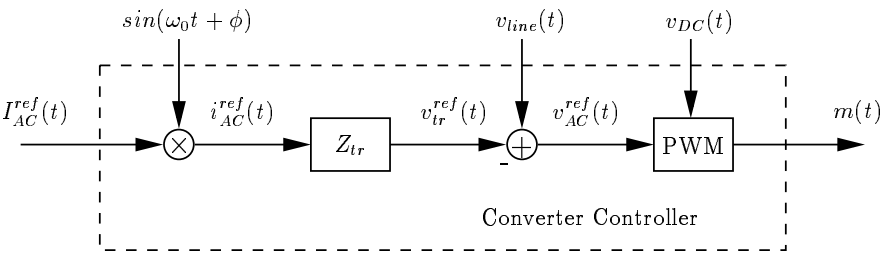

Figure 10 A converter controller that generates a modulation function, $m(t)$, which leads to a sinusoidal line current with amplitude given by the input, $I_{AC}^{ref}(t)$.

The Line Converter Controller

The basic purpose of line converter switching is to supply the motor side with its desired average power. With proper switching, the converter AC voltage is shaped so that a sinusoidal current is drawn from the line, if we neglect the influence of the pulse-width modulation (PWM). A sinusoidal current, i_{AC}, is desirable so that the locomotive does not give rise to any voltage distortion in the supplying network. If the line current is in phase with the line voltage, the locomotive will behave as a resistor. By allowing a phase shift, the locomotive can be used for reactive power compensation.

A common switching strategy shaping the AC voltage is shown in Fig. 10. The desired current amplitude, $I_{AC}^{ref}(t)$, can be slowly time vary-

ing and can be obtained, for instance, via feedforward from the measured load current. By multiplying with a sinusoid, the current is transformed to AC and given a desired phase, ϕ, relative to the line voltage

$$i_{AC}^{ref}(t) = I_{AC}^{ref}(t)\sin(\omega_0 t + \phi).$$

The frequency and phase of the sinusoid is obtained from the line voltage by means of a phase locked loop (PLL). The dynamics of this is not included in the analysis but could be done by deriving its HTF – an interesting challenge for future research.

The AC current gives rise to a voltage drop v_{tr} across the transformer. In Fig. 10, Z_{tr} is a low-pass approximation of the transformer impedance, $R_{tr} + sL_{tr}$. The desired AC voltage, $v_{AC}^{ref}(t)$, is obtained by subtracting the transformer voltage from the line voltage, as shown in Fig. 6.

Pulse Width Modulation (PWM)

From $v_{AC}^{ref}(t)$, the switching pattern is obtained by means of pulse width modulation. The HTF of a PWM is derived in [Sandberg, 1999], which shows that for frequencies below the switching frequency of the converter there is no frequency interaction, and the PWM can be approximated by a time delay of half the switching period. A switching frequency of 250 Hz thus gives a time delay of 2 ms. This has negligible influence on the stability and is therefore not included in the model. Instead, the PWM is modeled as ideal; that is, the modulation function is obtained from (9) as

$$m(t) = \frac{1}{v_{DC}(t)} v_{AC}^{ref}(t).$$

This expression is nonlinear due to the division by $v_{DC}(t)$. To carry through the analysis, it is linearized:

$$\Delta m(t) = -\frac{v_{AC}^{ref\,0}(t)}{(v_{DC}^{0}(t))^2}\Delta v_{DC}(t) + \frac{1}{v_{DC}^{0}(t)}\Delta v_{AC}^{ref}(t).$$

Here $v_{AC}^{ref\,0}(t)$ is the periodic reference AC voltage corresponding to the nominal periodic solution.

A DC Link PI Controller

If the reference current is based only on feedforward from the load current, the system will not handle disturbances. Under line voltage fluctuations, the converter controller will keep the desired line current, but there will be fluctuations in the DC voltage. As the motor control relies on a constant torque, this will lead to torque offset or torque pulsation.

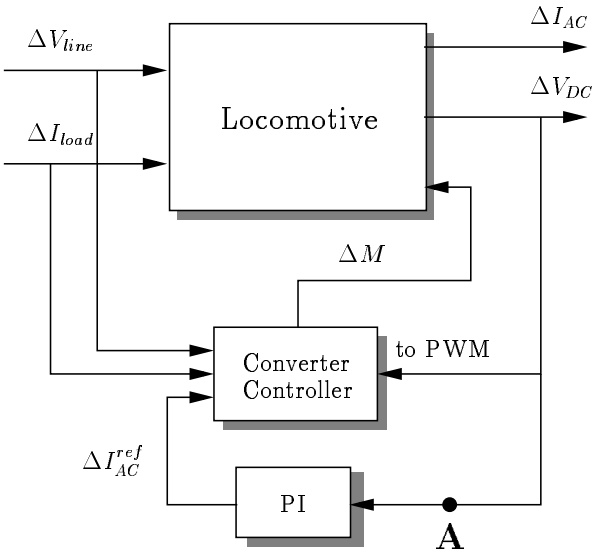

Figure 11 A block diagram of the locomotive including converter control and DC link controller. Point A is where the loop is broken to plot the open-loop Nyquist plot in Fig. 12. The admittance HTF, $\mathcal{H}_{cl}$, from ΔV_{line} to ΔI_{AC} is shown in Fig. 14. The choice of the gain in the DC link PI controller is a tradeoff between small DC ripple and small admittance $\mathcal{H}_{cl}$.

Using a DC link controller, the DC voltage is stabilized at a desired reference value. In Fig. 11, the DC link is stabilized with a PI controller

$$\Delta I_{AC}^{ref}(s) = K(1 + \frac{1}{sT_i})\Delta V_{DC}(s).$$

The output is used to adjust the AC current amplitude reference, I_{AC}^{ref}.

Results

The linear frequency domain model obtained in the previous section can be used in several ways to improve system knowledge. The main goal is not only to obtain simulation results, which can be done using standard time domain simulation, but also to understand system properties and tradeoffs.

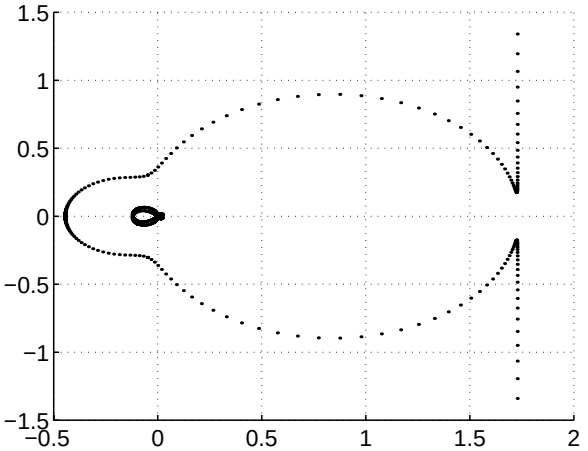

Figure 12 A Nyquist plot for the inverter locomotive at point A, for $I_{load} = 500A$. The diagram predicts a stability limit of $K = 2.23$. This agrees well with the time-domain simulations in Fig. 13. Note that the Nyquist curve for an LTP system consists of a number of disjoint curves. For stability, the total number of counter-clockwise encirclements of the point $-1/K$ of these curves must equal the number of open-loop unstable poles.

An HTF Nyquist Plot

We first verify that the HTFs we have obtained give results that agree with standard time domain simulation. If the loop is broken at point A in Fig. 11, the Nyquist plot for the locomotive, including the controller, can be plotted. Fig. 12 shows the Nyquist plot for the locomotive with load current $i^0_{load} = 500\,\mathrm{A}$ and DC voltage reference $v^0_{DC} = 2800\,\mathrm{V}$. The controller parameters are $K = 1$ and $T_i = 60$. From the Nyquist theorem, we conclude that the stability limit is $K = 2.23$. This agrees very well with simulations (see Fig. 13, which shows that the system is stable for a controller gain of $K = 2.2$ but unstable when $K = 2.3$). For the Nyquist plot, the HTF is truncated at $N = 5$, which means that frequencies up to the fifth harmonic are considered, hence the HTF is an 11x11 matrix. Increasing N only leads to additional eigenvalues in the origin, due to the roll-off of the system.

Amplitude Diagrams of HTFs

By determining the HTF-admittance $\mathcal{H}_{cl}$ of the total locomotive, (i.e., the closed-loop transfer function from disturbances in line voltage, ΔV_{line}, to disturbances in line current, $\Delta I_{line} = \Delta I_{AC}$), the model can be used as a starting point to determine the stability of a larger system consisting

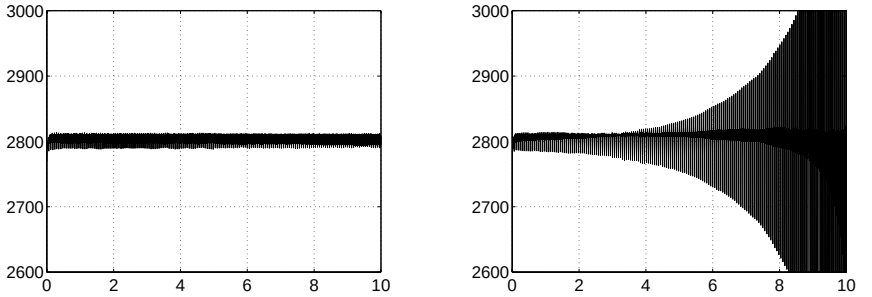

Figure 13 The DC voltage for $K = 2.2$ (left) and $K = 2.3$ (right). The amplitude margin is 2.23. The results agree well with the Nyquist plot in Fig. 12

.

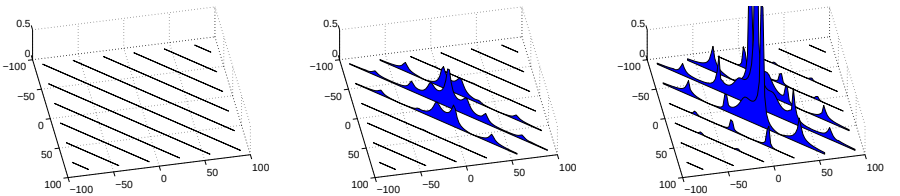

Figure 14 Plots showing the amplitude of the coupling between different frequencies for the HTF from Δv_{line} to Δi_{ac} for DC link controller gains $K = 0$, $K = 1$, and $K = 2.23$. The load current is $I_{load} = 500\,\mathrm{A}$. The diagonal structure shows that for LTP systems, there is interaction between frequencies separated by a multiple of f_0. For $K = 0$, the admittance is zero. By increasing K, it is obvious that the DC link controller leads to cross-frequency interaction with the supplying network.

of several trains and a distribution network. The amplitude of the coupling between input frequencies and output frequencies, $\mathcal{H}_{cl}$, is plotted in Fig. 14 for DC link controller gains $K = 0$, $K = 1$, and $K = 2.23$. Due to symmetry, there is only coupling between frequencies separated by a multiple of double the fundamental frequency, $2 \cdot f_0 = 33 - 1/3\,\mathrm{Hz}$. It is easy to determine that the admittance is zero when $K = 0$, so the interaction with the net arises from the DC voltage controller. There will be a tradeoff between a small DC ripple, requiring large controller gains, and small admittance, requiring small controller gains.

Fig. 15 shows the amplitude plot of the HTF-admittance for a negative load current, $I_{load} = -500\,\mathrm{A}$. A negative load current occurs when the locomotive is braking. The controller parameters are $K = 1$ and $T_i = 60$. A comparison with the middle plot of Fig. 15 shows that the HTF is considerably different.

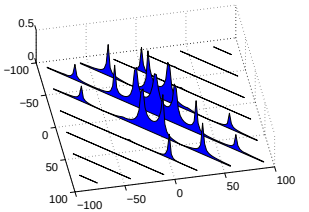

Figure 15 The amplitude plot for a negative load current, $I_{load} = -500\,\mathrm{A}$. The controller parameters are $K = 1$ and $T_i = 60$. The plot is quite different that that for a positive load current, shown in Fig. 14.

Conclusions

The Swiss incidents have shown that overall system stability is highly dependent on good converter control. The time varying nature of the converters implies that control theory for LTI systems cannot be used in a straightforward way. This paper has shown how the Harmonic Transfer Function facilitates a way to generalize many results to hold also for LTP systems. Stability and robustness analysis and controller design can be performed in a more systematic way. In this paper we have only presented a few example of the theorems and results that can be useful when analyzing modern electric networks.

The model we have derived and analyzed should only be viewed as a starting point for analysis of the complete train system. In the model, we have neglected certain dynamics that have been thought to be of minor importance, such as the dynamics introduced by the non-ideal pulse-width modulation and the phase-locked loop adjusting the phase angle ϕ. A related assumption is that we have no active control of reactive line power. In addition, the motor dynamics have been left out.

The model of the inverter locomotive is of independent value due to the object-oriented approach to modeling made possible by the method. Different subcomponents can be modeled and verified by simulations and measurements and then analyzed together, which is a significant advantage.

Acknowledgment

The model of the inverter locomotive was kindly provided by Markus Meyer at Adtranz, Zürich. The work was financially supported by Elforsk AB under Elektra project 3320.

References

Acha, E., J. Arrillaga, A. Medina, and A. Semlyen (1989): "General frame of reference for analysis of harmonic distortion in systems with multiple transformer nonlinearities." *IEE Proceedings*, **136C:5**, pp. 271–278.

Arrillaga, J. and C. Callaghan (1991): "Three phase AC-DC load and harmonic flows." *IEEE Trans. on Power Delivery*, **6:1**, pp. 238–244.

Arrillaga, J., A. Medina, M. Lisboa, M. A. Cavia, and P. Sánchez (1994): "The harmonic domain. A frame of reference for power system harmonic analysis." *IEEE Trans. on Power Systems*, **10:1**, pp. 433–440.

Åström, K., H. Elmqvist, and S. Mattsson (1998): "Evolution of continuous-time modeling and simulation." In Zobel and Moeller, Eds., *Proceedings of the 12th European Simulation Multiconference, ESM'98*, pp. 9–18. Society for Computer Simulation International, Manchester, UK.

Ball, J., I. Gohberg, and M. Kaashoek (1995): "A frequency response function for linear time-varying systems." *Math. Control Signals Systems*, **8:4**, pp. 334–351.

Bamieh, B. and J. Pearson (1992): "A general framework for linear periodic systems with applications to H_∞ sampled-data control." *IEEE Transactions on Automatic Control*, **37**, pp. 418–435.

Chen, T. and B. Francis (1995): *Optimal Sampled-Data Control Systems*. Springer-Verlag.

Floquet, G. (1883): "Sur les équations différentielles linéaires a coefficients périodiques." *Annales de L'Ecole Normale Supérieure*, **12**, pp. 47–89.

Hill, G. (1886): "On the part of the lunar perigee which is a function of the mean motions of the sun and the moon." *Acta Mathematica*, **8**, pp. 1–36.

Hwang, S. (1997): *Frequency Domain System Identification of Helicopter Rotor Dynamics incorporationg Models with Time Periodic Coefficients*. PhD thesis, Dept. of Aerospace Engineering, University of Maryland.

Kamen, E. and J. Sills (1993): "The frequency response function of a linear time varying system." In *IFAC 12th Triennal World Congress*, pp. 315–318. Sydney.

Kano, H. and T. Nishimura (1985): "Controllability, stabilizability, and matrix Riccati equations for periodic systems." *IEEE Transactions on Automatic Control*, **30:11**, pp. 1129–1131.

Kundert, K. and A. Sangiovanni-Vincentelli (1986): "Simulation of nonlinear circuits in the frequency domain." *IEEE Trans. on Computer-Aided Design*, **5:4**, pp. 521–535.

Meyer, M. (1999): "Netzstabilität in grossen Bahnnetzen." *Eisenbahn-Revue*, **No 7-8**, pp. 312–317.

Möllerstedt, E. (1998): *An Aggregated Approach to Harmonic Modelling of Loads in Power Distribution Networks*. Lic Tech thesis, Department of Automatic Control, Lund Institute of Technology, Lund, Sweden.

Richards, J. (1983): *Analysis of Periodically Time Varying Systems*. Communications and Control Engineering Series. Springer-Verlag, Berlin.

Sandberg, H. (1999): "Nonlinear Modeling of Locomotive Propulsion System and Control." Master's thesis ISRN LUTFD2/TFRT--5625--SE, Department of Automatic Control, Lund Institute of Technology, Sweden.

Semlyen, A., E. Acha, and J. Arrillaga (1987): "Harmonic Norton Equivalent for the magnetisation branch of a transformer." *Proc. IEE Pt. C*, **134:2**, pp. 162–169.

Semlyen, A., E. Acha, and J. Arrillaga (1988): "Newton-type algorithms for the harmonic phasor analysis of non-linear power circuits in periodical steady state with special reference to magnetic non-linearities." *IEEE Trans. on Power Delivery*, **3:3**, pp. 1090–1098.

Semlyen, A. and N. Rajakovic (1989): "Harmonic domain modeling of laminated iron core." *IEEE Trans. on Power Delivery*, **4:1**, pp. 382–390.

Song, W., G. Heydt, and W. Grady (1984): "The integration of HVDC subsystems into the harmonic power flow algorithm." *IEEE Trans. on Power Apparatus and Systems*, **PAS-103:8**, pp. 1953–1961.

Wereley, N. (1991): *Analysis and Control of Linear Periodically Time Varying Systems*. PhD thesis, Dept. of Aeronautics and Astronautics, MIT.

Wereley, N. and S. Hall (1991): "Linear time periodic systems: Transfer function, poles, transmission zeros and directional properties." In *Proceedings of the American Control Conference*. Boston, MA.

Xu, W., J. Drakos, Y. Mansour, and A. Chang (1994): "A three-phase converter model for harmonic analysis of HVDC systems." *IEEE Trans. on Power Delivery*, **9:3**, pp. 1724–1731.

Xu, W., J. Marti, and H. Dommel (1991): "A multiphase harmonic load flow solution technique." *IEEE Trans. on Power Systems*, **6:1**, pp. 174–182.

Paper IV

Robust Control of Power Converters

Erik Möllerstedt, Alec Stothert, and Henrik Sandberg

Abstract

The paper presents a systematic approach to power converter modeling, applied to a micro-turbine line side converter. For a three-phase system, transformation to rotating coordinates results under ideal conditions in a time invariant model. This means that linearization of the system results in a linear time invariant (LTI) model. A controller structure is proposed, which simplified converter control design and analysis of the resulting closed loop system. It is shown that the common objectives for converter control make linear quadratic optimal (LQ) control design suitable, and an LQ controller is derived from the nominal LTI model. The control design is evaluated with time domain simulation.

Harmonics, unbalanced ac systems, and switching dynamics of the converter implies that transformation to rotating coordinates results in a time-varying model. This means that stability cannot be guaranteed using LTI analysis only. Such non-ideal conditions are easily incorporated in the derived model, and the result is an LTP model. The model structure makes it straightforward to get the system on the so called standard form for robustness analysis. Integral Quadratic Constraints are then used to evaluate the control design under non-ideal conditions.

1. Introduction

Regulatory changes, increased competition, new business models, and technological advances in electrical power generation have combined to create an alternative framework for electricity generation – distributed power generation (DPG). The distributed power generation framework moves away from traditional large-scale power generation plants (several hundred MW) located near the natural resource converted to electricity, to small power generators (a few kW to 10 MW) sited at the load. Typically installation of a large power station/unit is proceeded by extensive analysis and simulations. To assure proper operation, controllers and filters are tuned manually on site. To make distributed power generation competitive, these initial investments must be reduced — cost effectiveness relies on mass production and plug and play solutions. A DPG unit has to be able to operate satisfactorily without extensive on-site analysis and with factory tuned controllers.

Typical DPG sources include micro turbines (see Fig. 1), fuel cells, wind mills, and solar cells. For physical and efficiency reasons, these

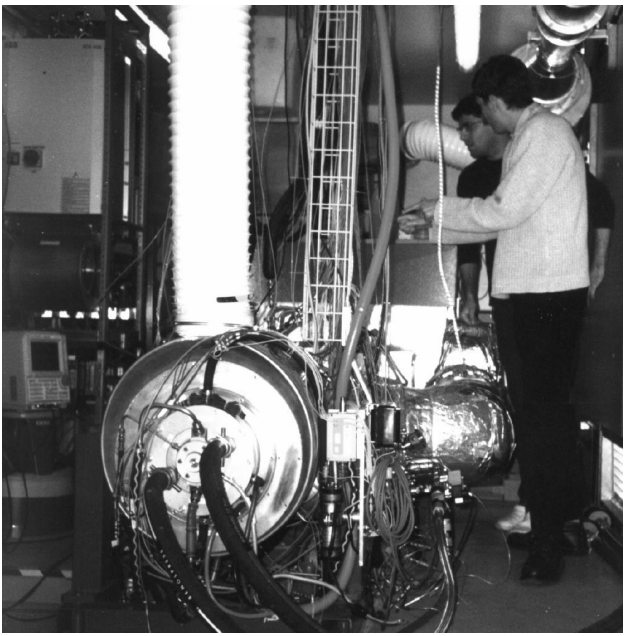

Figure 1 Alec is taking measurements on the micro-turbine unit.

power sources normally do not operate at grid frequency, and must be connected to the distribution grid via power electronics. Introduction of power electronic converters, which are very powerful actuators where power flows can be changed in a fraction of a second, implies that the influence and behavior of DPG units is highly dependent on good control. Additionally the switching nature of converters implies that harmonics are introduced into the grid. These harmonics can propagate through the grid and in worst case scenarios cause the grid to oscillate. The oscillations can trip protection systems causing wide spread electricity loss. Such a scenario is not unheard of; the Swiss national railway power grid suffered two such events during 1995 [Meyer, 1999]. The introduction of distributed power generation thus leads to a change in perspective where numerous technical business and regulatory questions [Schweer, 1999], [Hadjsaid *et al.*, 1999] arise. Primary among these questions is the impact of DPG units on the distribution system to which the unit is attached. Questions such as the effect of the unit on frequency and voltage stability, the effect on grid current and voltage harmonics, and the effect of the unit on grid power flows and grid protection need to be analyzed. To overcome these problems design and control of these systems must focus on robustness. The performance of the DPG unit has to be guaranteed under uncertain and distorted conditions — simulation alone cannot guarantee stable operation.

This paper provides a foundation for future work in this area by presenting a modeling approach of modern power systems that facilitates efficient simulation, systematic control design, and robustness analysis. In particular the focus is on replacing the traditional controller by a controller with clearly structured feedback and feedforward loops. This simplifies analysis and opens possibilities to take advantage of modern optimization and robust design techniques.

2. Converter Modeling

A power converter is a nonlinear coupling between two electric systems. Most common is that the converter is used to connect an ac system to a dc system. Linear models of the ac side and dc side dynamics respectively, are generally straightforward to derive, the problem is to get a good description of the coupling between the two sides, that facilitates analysis and design of the complete system. It is common practice to consider only the coupling between the fundamental signals, that is, to assume that dc signals are constant and ac signals are sinusoidal and symmetric [Kundur, 1994]. These assumptions may be appropriate for converters connected to a high voltage transmission network, but for small convert-

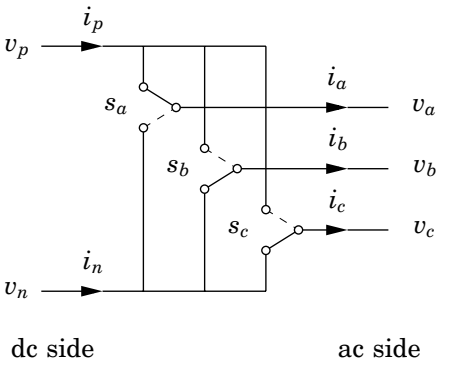

Figure 2 An ideal converter. The switch functions s_a, s_b, and s_c are used to control the power flow through the converter, and the reactive power generated on the ac side.

ers, connecting DPG units directly to a low voltage distribution system, it is not reasonable to assume that systems are balanced and free from harmonic distortion. We will therefore take an approach to modeling of the converter that facilitates a way to take such non-ideal conditions into account.

An Ideal Converter

An ideal three phase converter is shown in Fig. 2. The ideal converter has no losses and no energy storage. The converter has five terminals, two on the dc side and three on the ac side. It is normally assumed that $i_n = -i_p$. This property is not inherent to the converter, but depends on the rest of the system, so in order to get a general model, this cannot be assumed. To simplify the analysis, the dc signals are transformed as

$$\begin{aligned} v_{dc} &= v_p - v_n, \\ v_m &= (v_p + v_n)/2, \\ i_{dc} &= (i_p - i_n)/2, \\ \Delta i &= i_p + i_n. \end{aligned} \tag{1}$$

Note that $i_n = -i_p$ is equivalent to $\Delta i = 0$.

The basic goal of the converter control is to shape the ac voltage so that the generated power is fed into the grid. This is done by proper switching of the converter. From Fig. 2 and (1) it can be concluded that

$$\begin{bmatrix} v_a(t) \\ v_b(t) \\ v_c(t) \end{bmatrix} = \begin{bmatrix} s_a(t) \\ s_b(t) \\ s_c(t) \end{bmatrix} v_{dc}(t) + \begin{bmatrix} 1 \\ 1 \\ 1 \end{bmatrix} v_m(t), \tag{2}$$

where the switch functions, $s_a(t)$, $s_b(t)$, and $s_c(t)$ can be assigned the values $\pm 1/2$ if we assume infinately fast switching. This means that we do not consider the commutation of the switches. Since the ac voltages only can be assigned discrete values, smooth voltages must be approximated. Using for instance pulse width modulation, the phase voltages can approximate any signal with amplitude less that $1/2$.

The switch functions also gives a relation between ac current and dc current:

$$\begin{aligned} i_{dc}(t) &= s_a(t)i_a(t) + s_b(t)i_b(t) + s_c(t)i_c(t), \\ \Delta i(t) &= i_a(t) + i_b(t) + i_c(t). \end{aligned} \tag{3}$$

Since an ideal converter has no losses and no energy storage, the instantaneous power on the dc side and the ac side must be equal, that is,

$$\begin{aligned} P_{dc} &= v_p i_p + v_n i_n = v_{dc} i_{dc} + v_m \Delta i \\ &= v_a i_a + v_b i_b + v_c i_c = P_{ac}. \end{aligned} \tag{4}$$

The current relation (3) can also be derived from this power balance.

The $dq0$-frame

Ac systems are conveniently analyzed in the rotating $dq0$ reference frame. Three phase ac currents, ac voltages, and switch signals are transformed to the $dq0$ by a linear time periodic state transformation, which for the current becomes

$$\begin{bmatrix} i_d \\ i_q \\ i_0 \end{bmatrix} = \sqrt{\frac{2}{3}} \begin{bmatrix} \cos\omega_0 t & \cos(\omega_0 t - \frac{2\pi}{3}) & \cos(\omega_0 t + \frac{2\pi}{3}) \\ -\sin\omega_0 t & -\sin(\omega_0 t - \frac{2\pi}{3}) & -\sin(\omega_0 t + \frac{2\pi}{3}) \\ \sqrt{\frac{1}{2}} & \sqrt{\frac{1}{2}} & \sqrt{\frac{1}{2}} \end{bmatrix} \begin{bmatrix} i_a \\ i_b \\ i_c \end{bmatrix},$$

where ω_0 is the grid frequency, which has to be estimated by, for instance, a phase locked loop.

For balanced steady-state operation, i_d and i_q are constant. Hence, sinusoidal signals in the abc reference frame appears as constants in the $dq0$ reference frame [Kundur, 1994]. If on the other hand the phase signals are not symmetric, or contain harmonics, the transformed signals becomes time-varying. Therefore, for linear analysis of converter systems, the common approach is to assume symmetric ac signals, free from harmonics. The model developed here is not restricted to such conditions.

By proper grounding, it can be assured that $\Delta i = 0$. This will be assumed in the rest of the paper. Then (3) implies that $i_0 = 0$, and the converter equations (2) and (3) simplify to

$$\begin{aligned} V_{ac}(t) &= S(t) v_{dc}(t), \\ i_{dc}(t) &= S(t)^T I_{ac}(t), \end{aligned} \tag{5}$$

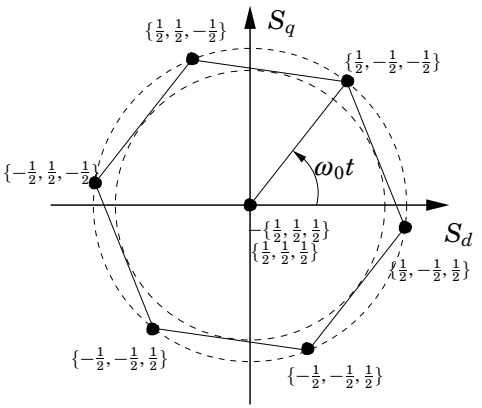

Figure 3 The seven possible values for the switch function in the dq reference frame. All values inside the inner circle can be approximated with pulse width modulation.

where

$$V_{ac}(t) = [\, v_d(t) \quad v_q(t) \,]^T,$$
$$I_{ac}(t) = [\, i_d(t) \quad i_q(t) \,]^T,$$
$$S(t) = [\, s_d(t) \quad s_q(t) \,]^T.$$

Note that even though there is no zero component in the current, both the ac voltage and the switch function, as well as the dc voltage can have non-zero zero components, $v_0(t) = \sqrt{3} v_m(t)$. However, this does not affect the power balance of the converter as in $dq0$ reference frame $p_{ac} = v_d i_d + v_q i_q + v_0 i_0$, and $i_0 = 0$.

The switch function $S = [s_d \quad s_q]^T$ can in each instant be assigned 7 different values, as shown in Fig. 3. Hence, $S(t)$ can approximate, at least, any function with

$$|S(t)| = \sqrt{s_d^2 + s_q^2} \leq \frac{\sqrt{3}}{2} \cdot \sqrt{\frac{2}{3}} = \frac{1}{\sqrt{2}} \approx 0.7.$$

If the switch signal is derived in the dq reference frame, it must be transformed back to phase values

$$\begin{bmatrix} s_a \\ s_b \\ s_c \end{bmatrix} = \sqrt{\frac{2}{3}} \begin{bmatrix} \cos \omega_0 t & -\sin \omega_0 t \\ \cos(\omega_0 t - \frac{2\pi}{3}) & -\sin(\omega_0 t - \frac{2\pi}{3}) \\ \cos(\omega_0 t + \frac{2\pi}{3}) & -\sin(\omega_0 t + \frac{2\pi}{3}) \end{bmatrix} \begin{bmatrix} s_d \\ s_q \end{bmatrix}.$$

Linearizing the Converter

The local behavior of the converter in the neighborhood of a periodic solution $\{v_{dc\,nom}(t), I_{ac\,nom}(t), S_{nom}(t)\}$ is well described by a linear approximation:

$$\begin{aligned} \Delta V_{ac}(t) &= S_{nom}(t)\Delta v_{dc}(t) + \Delta S(t) v_{dc\,nom}(t), \\ \Delta i_{dc}(t) &= S_{nom}(t)^T \Delta I_{ac}(t) + \Delta S(t)^T I_{ac\,nom}(t), \end{aligned} \tag{6}$$

By defining the vectors

$$z = \begin{bmatrix} \Delta V_{ac} \\ \Delta i_{dc} \end{bmatrix} \in R^3, \qquad x = \begin{bmatrix} \Delta I_{ac} \\ \Delta v_{dc} \end{bmatrix} \in R^3, \tag{7}$$

this can be written

$$z(t) = S_0(t)x(t) + X_0(t)\Delta S(t), \tag{8}$$

where

$$S_0 = \begin{bmatrix} 0 & 0 & s_d^{nom} \\ 0 & 0 & s_q^{nom} \\ s_d^{nom} & s_q^{nom} & 0 \end{bmatrix}, \quad X_0 = \begin{bmatrix} v_{dc}^{nom} & 0 \\ 0 & v_{dc}^{nom} \\ i_d^{nom} & i_q^{nom} \end{bmatrix}.$$

If the ac phase currents are sinusoidal and symmetric, the dc voltage is constant, and $S_{nom}(t)$ is constant in the dq reference frame, then the nominal solution $\{v_{dc}^{nom}(t), I_{ac}^{nom}(t), S_{nom}(t)\}$ becomes constant in the dq reference frame. The linearized converter (6) is then described by the constant gain matrices, S_0 and X_0. If the rest of the system is linear, analysis can be performed using standard methods for linear time invariant (LTI) systems. The case where the ac currents are not sinusoidal and symmetric, and the dc voltage is not constant is discussed in Section 5 below.

A State Space Model of the DPG System

The linearized converter is now used to derive a state space model of the DPG unit. This can be used for linear control design and analysis. A simplified model of the DPG unit is shown in Fig. 4. The converter is connected to the grid via a smoothing inductor. This can in the dq reference frame be written (neglecting the zero components)

$$\frac{dI_{ac}}{dt} = \begin{bmatrix} 0 & \omega_0 \\ -\omega_0 & 0 \end{bmatrix} I_{ac} + \begin{bmatrix} 1/L & 0 \\ 0 & 1/L \end{bmatrix} (V_{ac} - V_{grid}). \tag{9}$$

The dc side is just a current source and the dc link capacitor.

$$\frac{dv_{dc}}{dt} = \frac{1}{C}(i_{gen} - i_{dc}). \tag{10}$$

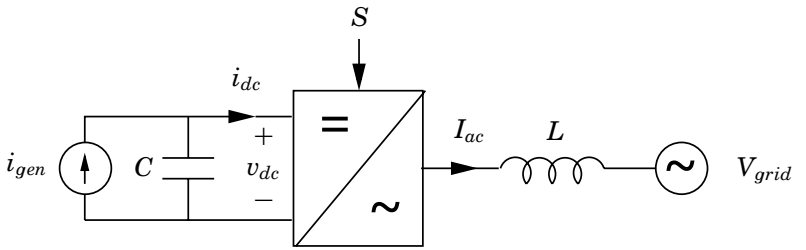

Figure 4 A simplified DPG system. The generator dynamics and the grid dynamics are neglected. A model is developed for the simplified system, treating variations in generator current and grid voltage as disturbances.

This simple description of the dc side dynamics is motivated by the fact that the dc link capacitor is chosen large to obtain decoupling of the ac side and the dc side. Following the notation in (7) with $x = [\Delta I_{ac}^T \, \Delta v_{dc}]^T$ and $z = [\Delta V_{ac}^T \, \Delta i_{dc}]^T$, the dynamic equations (9) and (10) can be written

$$\frac{dx}{dt} = A_o x + B_o(z - l),$$

where

$$A_o = \begin{bmatrix} 0 & \omega_0 & 0 \\ -\omega_0 & 0 & 0 \\ 0 & 0 & 0 \end{bmatrix}, \qquad B_o = \begin{bmatrix} \frac{1}{L} & 0 & 0 \\ 0 & \frac{1}{L} & 0 \\ 0 & 0 & -\frac{1}{C} \end{bmatrix}, \qquad l = \begin{bmatrix} \Delta V_{grid} \\ \Delta i_{gen} \end{bmatrix}.$$

Combining this with the linearized converter model (8) gives the total linearized system

$$\frac{dx}{dt} = Ax + B\Delta S + B_l l, \tag{11}$$

with

$$A = A_o + B_o S_0, \qquad B = B_o X_0, \qquad B_l = -B_o.$$

We thus have a state space description of the system linearized around the nominal solution. This will be used to design a feedback controller for the converter.

The disturbance, $l = [\Delta V_{grid}^T \quad i_{gen}]^T$, is often measurable, and can be compensated for by feedforward, but with more information about the system, it is straightforward to extend the model with states l_x, that depend on x. This gives the possibility to include the impact of a weak grid, where a deviation in current, I_{ac}, affects the grid voltage, V_{grid}, and that the generated current, i_{gen}, depends on the dc link voltage, v_{dc}.

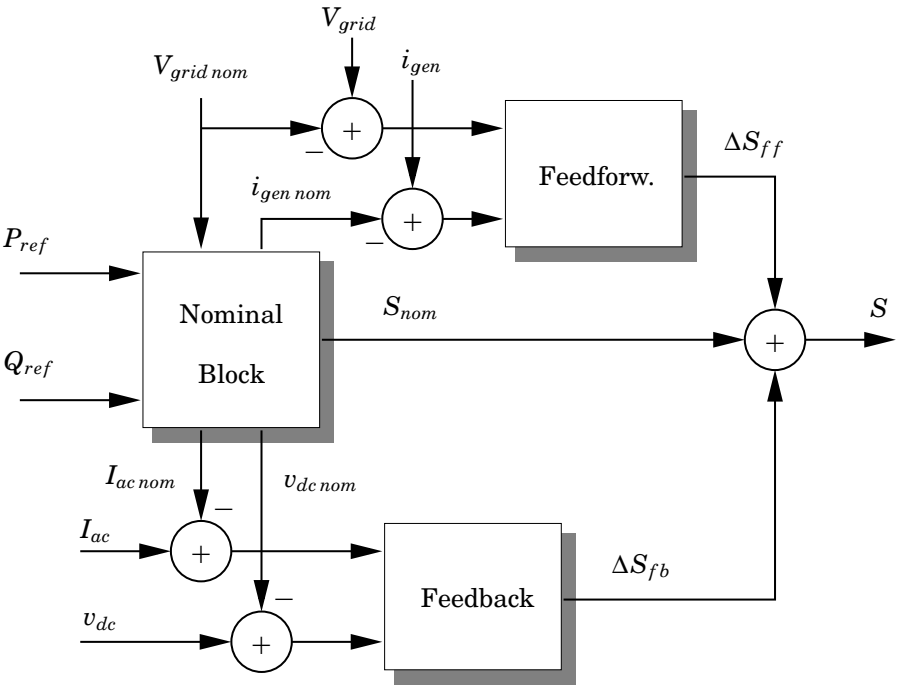

Figure 5 A controller structure with well defined feedback and feedforward paths. The nominal block determines a nominal solution based on reference values for active power P, which is the desired output power of the generator, and reactive power Q, which is determined by the grid operator. The feedback controller adjusts the nominal switch signal, S_{nom}, if the states $x = [\Delta I_{ac}^T\, \Delta v_{dc}]^T$ deviates from their nominal values, and the feedforward controller compensates for measurable disturbances $l = [\Delta V_{grid}^T\, \Delta i_{gen}]^T$.

3. A Suggested Structure for DPG-controllers

The primary goal of the converter controller is to switch the converter so that the power generated by the micro turbine, P_{gen}, is injected into the grid in a stable manner. The converter can also be used for power conditioning, with both active and reactive power injected into the grid. Hence, the converter should be switched so that

$$\begin{aligned} P_{grid} &= P_{gen}, \\ Q_{grid} &= Q_{ref}. \end{aligned} \tag{12}$$

Traditionally, converter controllers are very complex, and include a number of cascaded proportional–integral (PI) controllers and numerous

feedback and feedforward paths. Controller tuning is based on ad hoc tuning rules and experience, verified by simulation and linear analysis. However, it is not certain that traditional tuning rules are well suited for new applications, like distributed power generation. The complexity of the controllers makes proper analysis extremely complicated. Furthermore, as DPG units are to be connected anywhere in the system using pretuned controllers, a robust approach has to be taken.

To simplify design and analysis, the controller must be clearly structured, with a clear definition of feedforward and feedback loops. A proposed structure is shown in Fig. 5. The controller consists of three parts, a nominal block, a feedback controller, and a feedforward block.

The nominal block derives nominal signals based on the nonlinear model and reference values for active and reactive power. The nominal switch signal corresponding to the nominal solution is also derived.

The feedback controller adjusts the nominal switch signal by means of feedback of the deviations from the nominal measured states (dc voltage and ac current). The need for a robust controller and the control objectives to keep a constant dc voltage under desired reactive power injection, makes linear quadratic (LQ) control suitable.

The feedforward block is used to quickly react to measurable disturbances, in this case disturbances in grid voltage, V_{grid}, or generated current, i_{gen}.

The Nominal Block

If all ac signals are symmetrical with nominal amplitude and frequency, and all dc signals are constant at the nominal level, it is straightforward to derive a switch signal which results in desired power injection into the grid, see Fig. 6. The nominal switch signal is based on reference values for injected active and reactive power and dc link voltage, and nominal values of grid voltage. The nominal solution is time-varying if, for instance, P_{ref} is varying, but we will treat the inputs to the nominal block as not being time-varying. This is a good approximation if the time scales can be separated.

In the dq reference frame, nominal sinusoidal ac signals are conveniently described by complex vectors, or phasors,

$$\mathbf{v} = v_d + jv_q, \qquad \mathbf{i} = i_d + ji_q, \qquad \mathbf{s} = s_d + js_q, etc.$$

The active and reactive power injected into the grid is then given by

$$P_{grid} + jQ_{grid} = \mathbf{v}_{grid}\mathbf{i}_{ac}^{*}, \tag{13}$$

where * denotes complex conjugate. From this, the desired ac current

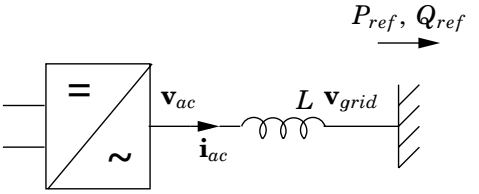

Figure 6 The nominal switch signal results in a converter ac voltage that gives a desired injection of active and reactive power into the grid under nominal conditions.

becomes

$$\mathbf{i}_{ac\,nom} = \left(\frac{P_{ref} + jQ_{ref}}{\mathbf{v}_{grid\,nom}} \right)^{*}.$$

According to Fig. 6, the nominal ac voltage should be chosen

$$\mathbf{v}_{ac\,nom} = \mathbf{v}_{grid\,nom} + j\omega_0 L \mathbf{i}_{ac\,nom},$$

since the nominal signals are assumed sinusoidal. This gives the nominal switch signal

$$\begin{aligned} \mathbf{s}_{nom} &= \frac{1}{v_{dc\,ref}} \mathbf{v}_{ac\,nom} \\ &= \frac{1}{v_{dc\,ref}} (1 + j\omega_0 L) \frac{P_{ref} - jQ_{ref}}{|\mathbf{v}_{grid\,nom}|^2} \mathbf{v}_{grid\,nom}. \end{aligned}$$

Note that if a high reactive power level is desired, the switch signal might saturate, that is, $|\mathbf{s}| > 1/\sqrt{2}$. One way to get around this is to increase the dc link voltage $v_{dc\,ref}$.

Linear Control Design

The nominal switch signal is derived for a system under ideal conditions. For a real system, with fluctuations in generation, disturbances, varying grid voltage, harmonics and unsymmetrical signals and switching converter dynamics, this nominal signal cannot be guaranteed to result in stable operation or acceptable performance. The performance and stability of the system must be improved by means of feedback. If all states are measurable, a linear state feedback controller can be used

$$\Delta S = \Delta S_{fb} + \Delta S_{ff} = -L_x x + L_l l. \tag{14}$$

The control objectives (12) can be used to derive the feedback gain L_x and the feedforward gain L_l. A mismatch in active power, $P_{grid} \neq P_{gen}$,

results in energy storage in the dc link capacitor, and thus affects the capacitor voltage. The active power can thus be controller by controlling the dc voltage, v_{dc}.

To control the reactive power, the model is extended by an extra state

$$\frac{dx_q}{dt} = Q_{grid} - Q_{ref}. \tag{15}$$

The reactive power is given by (13)

$$\begin{aligned} Q_{grid} &= \mathrm{Im}(\mathbf{v}_{grid}\mathbf{i}_{ac}^{*}) = v_{grid}^{q} i_{ac}^{d} - v_{grid}^{d} i_{ac}^{q} \\ &= \begin{bmatrix} v_{grid}^{d} & v_{grid}^{q} \end{bmatrix} \begin{bmatrix} 0 & -1 \\ 1 & 0 \end{bmatrix} \begin{bmatrix} i_{ac}^{d} \\ i_{ac}^{q} \end{bmatrix} = V_{grid}^{T} J I_{ac} \end{aligned}$$

To avoid taking the imaginary part, the complex vectors are replaced by vectors of the real and imaginary parts. Multiplication with $j = \sqrt{-1}$, is then equivalent to multiplication with the matrix $J = \left[\begin{smallmatrix} 0 & -1 \\ 1 & 0 \end{smallmatrix}\right]$. Linearizing (15) gives

$$\begin{aligned} \frac{dx_q}{dt} &= \Delta Q_{grid} \approx \Delta V_{grid}^{T} J I_{ac\,nom} + V_{grid\,nom}^{T} J \Delta I_{ac} \\ &= \begin{bmatrix} -(JV_{grid\,nom})^{T} & 0 \end{bmatrix} x + \begin{bmatrix} (JI_{ac\,nom})^{T} & 0 \end{bmatrix} l = A_q x + B_{lq} l. \end{aligned}$$

The extended system is obtained from (11)

$$\begin{aligned} \frac{dx_e}{dt} &= \frac{d}{dt}\begin{bmatrix} x \\ x_q \end{bmatrix} = \begin{bmatrix} A & 0 \\ A_q & 0 \end{bmatrix}\begin{bmatrix} x \\ x_q \end{bmatrix} + \begin{bmatrix} B \\ 0 \end{bmatrix}\Delta S + \begin{bmatrix} B_l \\ B_{lq} \end{bmatrix} l \\ &= A_e x_e + B_e \Delta S + B_{le} l. \end{aligned} \tag{16}$$

The extended system has four states, and thus $A_e \in R^{4\times 4}$, $B_e \in R^{4\times 2}$, and $B_{le} \in R^{4\times 3}$.

The control objectives are now to keep the state x_3 (dc voltage deviation) and x_4 (integrated reactive power error) close to their nominal values. This can be formulated as a linear quadratic (LQ) design problem, where the optimal feedback gain L_x minimizes the quadratic loss function

$$J = \int x^T R_x x + \Delta S^T R_s \Delta S \, dt, \tag{17}$$

with

$$R_x = \begin{bmatrix} 0 & & & \\ & 0 & & \\ & & \rho_1 & \\ & & & \rho_2 \end{bmatrix}, \qquad R_s = \begin{bmatrix} 1 & 0 \\ 0 & 1 \end{bmatrix}$$

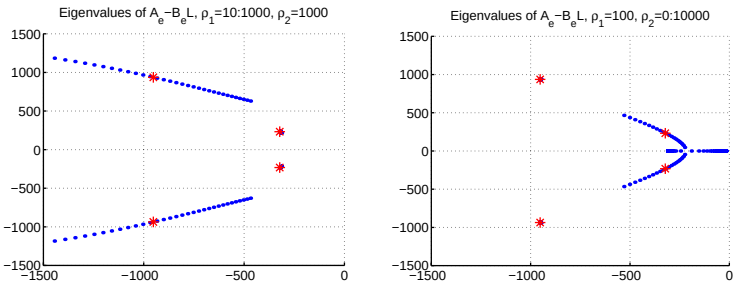

Figure 7 The closed loop poles when ρ_1 is varied (left plot) and when ρ_2 is varied (right plot). There is a clear decoupling between the weights and the pole pairs. The poles marked with stars (*) correspond to $\rho_1 = 100$ and $\rho_2 = 1000$.

The optimal feedback gain L_x, which minimizes the loss function (17) is given by

$$L_x = R_s^{-1} B S,$$

where S is the positive definite solution of the Riccati equation

$$0 = SA_e + A_e^T S - SB_e R_s^{-1} B_e^T S + R_x.$$

The positive weights ρ_1 and ρ_2 are tuning knobs to be chosen to give suitable tradeoffs between small x_3, x_4, and ΔS.

Closed Loop Poles

The closed loop poles are given by the eigenvalues of $A_e - B_e L$. The pole locations depend on the choice of weights, ρ_1 and ρ_2. In left plot in Fig. 7, ρ_1 is varied between 10 and 1000, whereas ρ_2 is kept constant (=1000). In the right plot ρ_1 is constant (=100), and ρ_2 is varied between 0.1 and 10000. It is clear that there is a decoupling between the two weights and the two pole pairs. The poles for $\rho_1 = 100$ and $\rho_2 = 1000$ are marked with stars in the two plots.

A Kalman filter has been used to filter the measured signals. The poles are chosen in order to make the Kalman filter 1.5 times faster but equally damped as the closed loop system, see Fig. 8, which shows the poles of $A_e - B_e L$ (*) and $A - KC$ (o).

Feedforward Control

To get a faster response to disturbances, a feedforward path can be introduced from a measurable disturbance, l. Ideally, this should totally

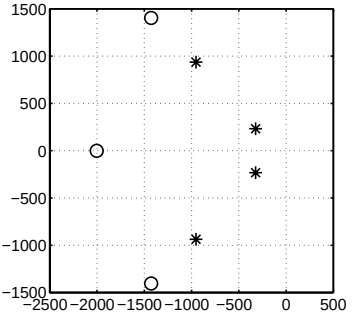

Figure 8 Poles of $A_e - B_e L$ (*) and $A - KC$ (o). The Kalman filter is made 1.5 times as fast and equally damped as the closed loop system.

compensate for the disturbance, but that generally leads to improper controllers. A static feedforward gain L_l that gives $x_3 = x_4 = 0$ in steady state is obtained from the equation

$$A_e \begin{bmatrix} x_1 \\ x_2 \\ 0 \\ 0 \end{bmatrix} + B_e \Delta S_{ff} + B_{le} l = 0,$$

which gives

$$\begin{bmatrix} x_1 \\ x_2 \\ \Delta s_d^{ff} \\ \Delta s_q^{ff} \end{bmatrix} = -\left[A_e(1:2) \quad B_e \right]^{-1} B_{le} l,$$

where $A_e(1:2)$ are the first two columns of A_e.

The closed loop system is shown in Fig. 9

4. Simulation Results

The nonlinear converter system including the controller is simulated using Simulink. The system is disturbed by a 10% increase in grid voltage amplitude after 0.02 s, a grid voltage phase shift of 10 degrees after 0.04 s, and a 10% increase in generated current after 0.06 s. In the simulations, $L = 0.12$ p.u., $C = 0.003$ p.u. $P_ref = 1$ p.u., $Q_{ref} = 0$, $V_{grid}^{nom} = [1 \quad 0]^T$ p.u., and $v_{dc}^{nom} = 1.925$ p.u.. Fig. 10 shows the result of the simulation with the nominal controller ($\rho_1 = 100$ and $\rho_2 = 1000$), but without feedforward.

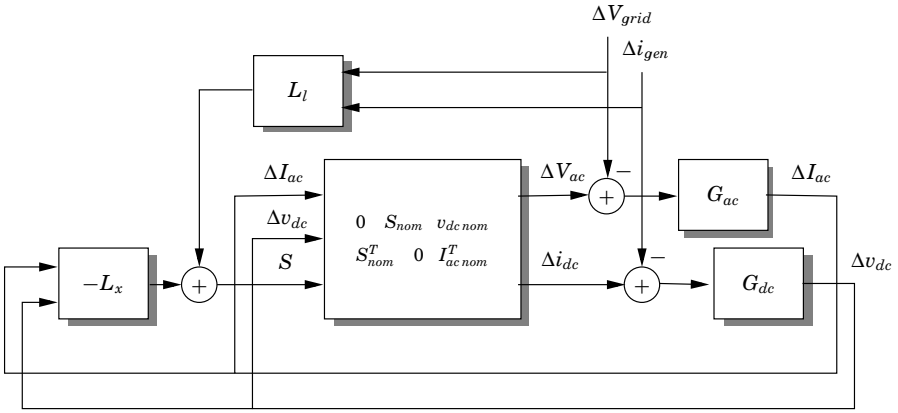

Figure 9 The closed loop system, linearized around the nominal solution.

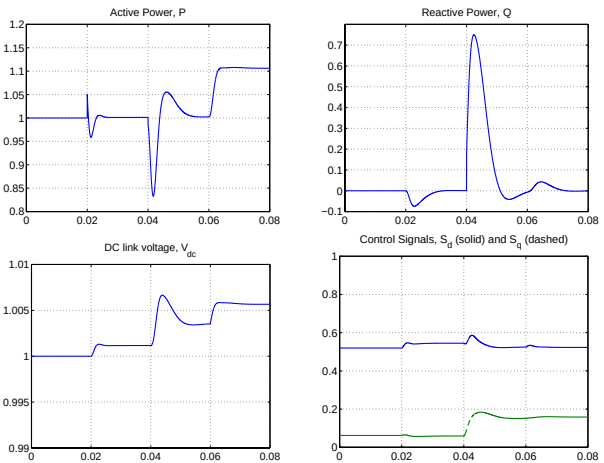

Figure 10 Simulation results of a controller with $\rho_1 = 100$ and $\rho_2 = 1000$, but without a feedforward path. The plots show good performance. There is a small error in dc voltage, because there is no integral action on the dc voltage error.

The plots show a good performance, Because there is no integral action on the dc voltage error, there is a small stationary error, note that the dc voltage is normalized in the plot. The performance is improved significantly using the proposed feedforward gain. This is shown is Fig. 11.

By changing ρ_1, the dc voltage error is affected. This is shown in Fig. 12, where ρ_1 is reduced to 10. The design weight ρ_2 affects the error

in reactive power. By increasing this weight, the error will be damped out faster. In Fig. 13 $\rho_2 = 10000$. The reactive power is damped very quickly and settles at its reference value.

In the design and analysis so far, the effects of measurement noise has not been considered. In Fig. 14, the switch signal, $S(t) = [S_d\, S_q]^T$ is plotted when the controller inputs are disturbed with band limited white noise with standard deviation $\sigma = 0.1\%$. The design weights are $\rho_1 = 100$ and $\rho_2 = 1000$. The result is terrible. It is clear that in the presence of measurement noise, the controller has to be retuned. In Fig. 15 $\rho_1 = 0.1$ and $\rho_2 = 10000$. The plots clearly shown improvement. However, this leads to larger deviations in dc voltage v_{dc}.

5. Robustness Analysis of the Converter Controller

The final choice of converter controller depends on a lot of things. It must quickly react to changed conditions and disturbances, but the bandwidth of the controller is limited by hardware. Also too fast converter switching results in too high losses. Furthermore, the controller should not be sensitive to measurement noise. The approach taken in this paper facilitates a way to perform systematic controller design and analysis of the closed loop system.

In the above analysis, simple models and simplifying assumptions have

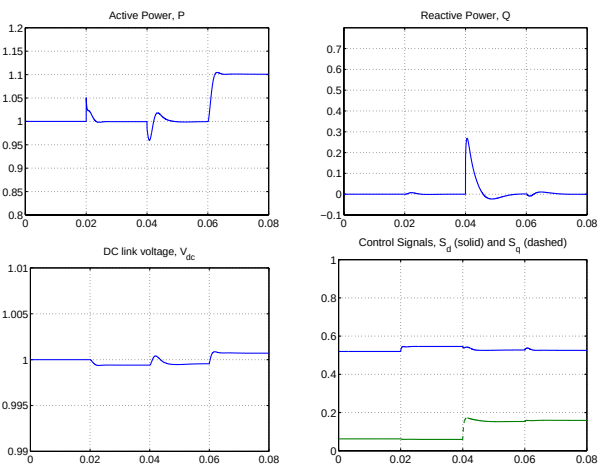

Figure 11 With feedforward, the controller reacts quicker to disturbances. This clearly affects the result, compare with Fig. 10.

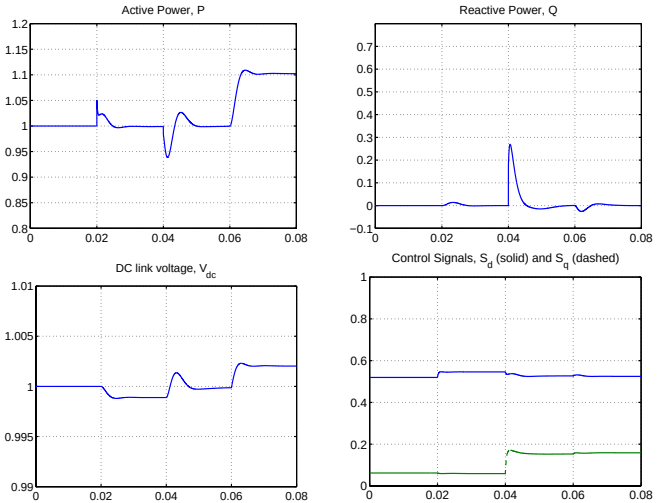

Figure 12 If the design weight ρ_1 is reduced, the dc voltage error will be larger. Here, $\rho_1 = 10$ and $\rho_2 = 1000$.

been used. The question now arises as to how to relax these assumptions, that is, how can stability and performance be guaranteed in presence of

- grid dynamics in a weak net
- generator dynamics
- other power electronic devices
- harmonics
- unbalanced loads
- non-ideal converter switchings

The approach proposed is to treat these effects as uncertainties in the system dynamics. The question can then be posed in a classical control framework of investigating system robustness with respect to uncertainties.

In robustness analysis, an uncertain system is often described as a feedback connection of a nominal system, H_{nom}, and an uncertainty block, Δ, see Fig. 16. The nominal system contains everything that is known, for instance all blocks in Fig. 9. Robust performance analysis can give the maximum norm of the uncertainty for which performance and stability are guaranteed. To view the stability conditions of the micro turbine as a robustness problem can give ideas about what has to be fulfilled by the

system to obtain stability and performance. This can give many useful ideas on how to write norms and standards for connections of DPG units to the grid. A good reference on robust analysis is [Zhou *et al.*, 1995].

Effects of Disturbances in Linearizing Trajectory

There are at least two good reasons for making robustness analysis of the model and controller constructed in the previous sections. First of all we have assumed constant $\{v_{dc\,nom}(t), I_{ac\,nom}(t), S_{nom}(t)\}$ in Section 2. The effect of harmonics, unbalance and converter switching is that this assumption no longer holds, in particular the linearized converter model is no longer constant but periodic, that is, the gain matrices $S_0(t)$ and $X_0(t)$ in (8) varies periodically. The influence of this should be studied. The second reason is that we constructed an LQG-controller. The guaranteed stability margins with full state knowledge for LQ-controllers are not valid for systems with output feedback, see [Doyle, 1978]. Thus a designer of an LQG-controller should always check robustness afterwards.

In our example we choose an uncertainty block of the type $\Delta(t) \in R^{3\times 5}$, see Fig. 17. When the trajectory we are linearizing along is perturbed, the linear model will change. If we assume the perturbation is periodic $\Delta(t)$ will be periodic. $\Delta(t)$ has five independent components: $\delta_k(t)$, $k = 1, \ldots, 5$.

It is interesting to see what happens when the nominal LQG-controller is attached to the perturbed system. Questions we would like to answer

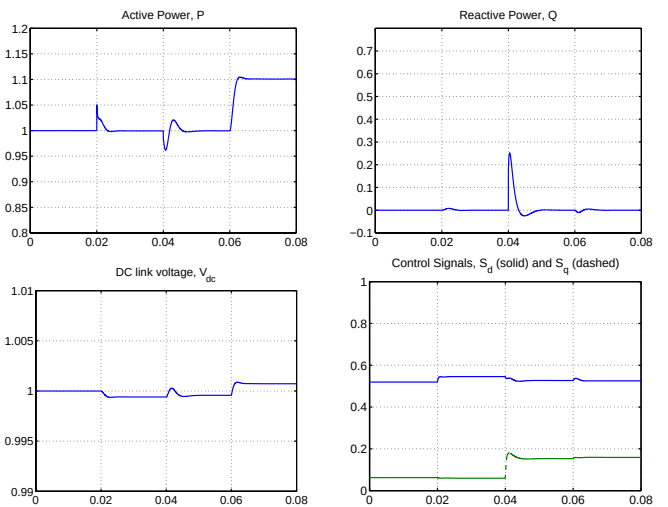

Figure 13 If the design weight ρ_2 is increased, the reactive power will faster go back to its reference value after a disturbance Here, $\rho_1 = 100$ and $\rho_2 = 10000$.

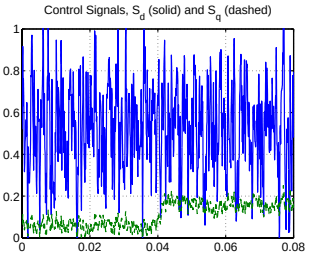

Figure 14 The switch signal for the design with $\rho_1 = 100$ and $\rho_2 = 1000$ in the presence of measurement noise. The result is terrible.

are: Is the perturbed system stable? Is the performance still good? Often the norm of disturbance attenuation is used as performance measure. This is not ideal here as will be discussed later.

Robustness analysis is often made with H_∞- and μ-analysis. Here we will use a more general approach using Integral Quadratic Constraints (IQC), see overview article [Megretski and Rantzer, 1997]. The methods are implemented in the toolbox IQCβ, [Megretski *et al.*, 2000] with a Simulink interface.

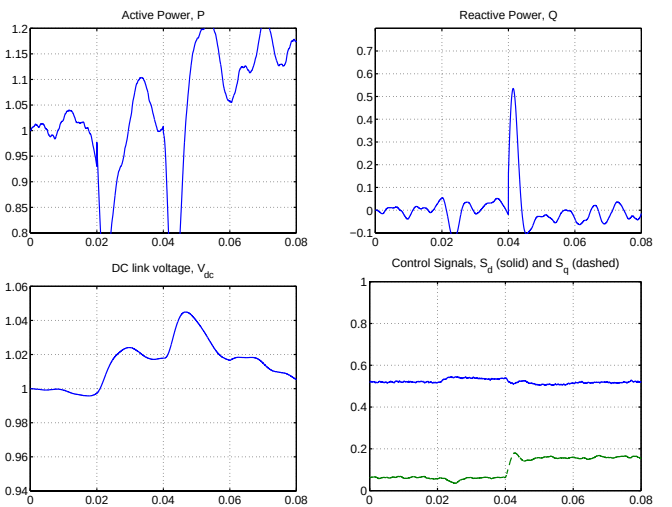

Figure 15 With measurement noise, the controller has to be retuned. Here $\rho_1 = 0.1$ and $\rho_2 = 10000$.

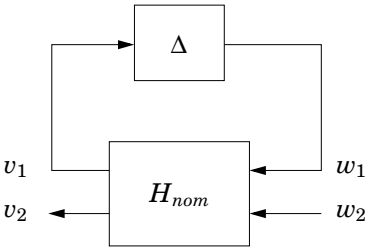

Figure 16 The uncertain system is written as a feedback connection between a nominal system and an uncertainty block. Robust performance is measured as the gain from w_2 to v_2.

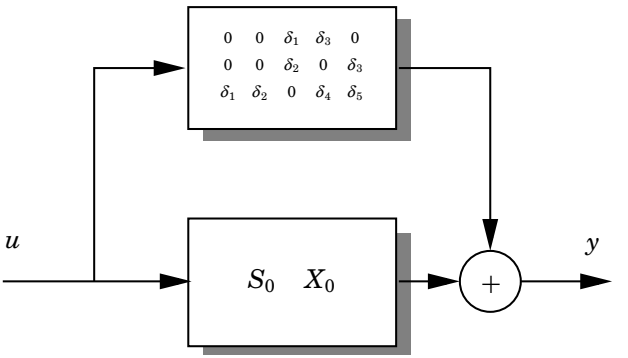

Figure 17 The periodic part of the converter gain matrix is placed in an uncertainty block Δ.

Definition 1.1 The stable and causal operator[1] Δ satisfies the IQC defined by Π if and only if

$$\frac{1}{2\pi}\int_{-\infty}^{+\infty}\begin{bmatrix}\hat{y}(j\omega)\\ \hat{x}(j\omega)\end{bmatrix}^{*}\Pi(j\omega)\begin{bmatrix}\hat{y}(j\omega)\\ \hat{x}(j\omega)\end{bmatrix}d\omega \geq 0 \tag{18}$$

for all $x, y \in L_2[0,\infty)$ where $x = \Delta y$. Here $\hat{x}$ represents the Fourier transform of x.

By finding IQC:s that are fulfilled by the uncertainties we can turn the robust performance problem into a finite dimensional Linear Matrix Inequality, [Megretski and Rantzer, 1997]. These can be solved efficiently in polynomial time, see [Nesterov and Nemirovski, 1993]. The more IQC:s

[1]Stable operator means here that it has finite L_2-induced gain.

Table 1 The upper bounds of the energy norm of disturbance attenuation for different choices of the weights ρ_1 and uncertainty bound D, $\rho_2 = 1000$.

	ρ_1		
D	10	100	1000
0.00	2.61	2.31	2.21
0.10	3.74	3.23	3.28
0.20	6.67	6.44	8.02
0.30	203.14	infeas.	infeas.
0.33	infeas.	infeas.	infeas.

we can find that are satisfied by Δ, the less conservative the result becomes. The result is an upper bound of the energy norm of the disturbance attenuation.

We will choose an IQC that is fulfilled by real periodic scalars $-1 \leq \delta(t) \leq 1$, [Willems, 1971; Megretski and Rantzer, 1997], for which Π has the structure

$$\Pi = \begin{bmatrix} X(j\omega) & Y(j\omega) \\ Y(j\omega)^* & -X(j\omega) \end{bmatrix}$$

with X, Y being bounded and measurable satisfying

$$X(j\omega) = X(j(\omega + 2\pi/T)) = X(j\omega)^* \geq 0$$
$$Y(j\omega) = Y(j(\omega + 2\pi/T)) = -Y(j\omega)^*$$

where T is the period of the scalar. In our problem we will choose constant real matrices X, Y. This adds conservatism to the problem because any time-varying scalar $-1 \leq \delta(t) \leq 1$ will satisfy this IQC. For algorithms using the periodicity see [Jönsson *et al.*,]. Another approach is to lift the entire system to a discrete time invariant system and then use constant X, Y.

We will choose $l = [\Delta V_{grid}^T \, \Delta i_{gen}]^T$ as input disturbance in this example. The measured output is $x = [\Delta I_{ac}^T \, \Delta v_{dc}]^T$. If we can get an upper bound on the energy norm bound between these signals we know the system is stable. Now let $|\delta_k(t)| \leq D$ for all t, k. With $D = 0$ we have the nominal system without perturbation. By running the optimization program with different values of D, we can find the largest perturbations, for which stability can be guaranteed.

We can introduce another degree of freedom by varying the controller. In Table 5 ρ_1 is varied. Bounds of the energy bound for different D and

Table 2 The upper bounds of the energy norm of disturbance attenuation for different choices of the weights ρ_2 and uncertainty bound D, $\rho_1 = 100$.

	ρ_2			
D	100	1000	10000	100000
0.00	2.34	2.31	2.25	2.20
0.10	3.69	3.23	3.06	2.96
0.20	15.04	6.44	4.87	4.60
0.30	infeas.	infeas.	14.89	10.56
0.33	infeas.	infeas.	47.40	17.81
0.35	infeas.	infeas.	infeas.	33.12
0.40	infeas.	infeas.	infeas.	infeas.

ρ_1 are shown. 'Infeasible' means we cannot prove stability for this combination of controller and disturbance.

Not surprisingly we see that when the uncertainty is increased the performance deteriorates until we cannot prove stability any more. It can be seen that the best disturbance rejection is not achieved by keeping the dc voltage as constant as possible.

In Table 5 ρ_2 is varied instead. It is shown that the more integral action, the better disturbance rejection. The choice of ρ_2 is limited by the controller hardware.

One could ask the fully justified question: Is it really the energy norm from l to x we would like to minimize, and what is the interpretation? What we really are interested in are particular frequencies and coupling. For example, a constant rise in ΔV_{grid} would ideally be followed by a drop in ΔI_{ac}, as we would like the generator to deliver constant power. A norm of 0 is thus not optimal. Instead we should compare to the case $D = 0$, which is the one we get when we use linear time invariant methods for analysis, and see how much the figures changes for different D. Small changes in the bounds indicates that the performance is roughly the same.

To analyze the influence of some frequencies we can introduce input and output filters on the signals w_2 and v_2. By letting through some frequency bands we can study the important regions. For example a 50 Hz disturbance should not spread out too much in other frequency regions.

6. Conclusions

It is well documented that introduction of distributed power generation poses challenging technical questions relating to power stability, protection and quality. To this end the paper has described the development of a model of a line side converter of a micro-turbine that will facilitate investigation of these issues. Additionally a generalized converter controlled framework enabling generalization of different converter control algorithms has also been introduced. Finally an approach to handling converter non-linearities and harmonic effects based on robustness analysis has been proposed, in particular it is noted that harmonic effects can be modeled by introducing periodic uncertainties into the developed models. Much of this work is ongoing and future research will show how these results can be used to guarantee stable operation of distributed power generation systems.

Acknowledgments

The work was supported by ABB Corporate Research, Baden-Dättwil, Switzerland, and Elforsk AB, Sweden.

7. References

Doyle, J. C. (1978): "Guaranteed margins for LQG regulators." *IEEE Transactions on Automatic Control*, **23**, pp. 756–757.

Hadjsaid, N., J. Canard, and F. Dumas (1999): "Dispersed generation impact on distribution networks." *IEEE Computer Applications in Power*, **12:2**, pp. 23–28.

Jönsson, U. T., C.-Y. Kao, and A. Megretski "Robustness analysis of periodic systems."

Kundur, P. (1994): *Power System Stability and Control*. McGraw-Hill Inc., USA.

Megretski, A., C. Y. Kao, and U. Jönsson (2000): *A Guide to IQCβ:software for robustness analysis*. `www.mit.edu/~cykao/home.html`.

Megretski, A. and A. Rantzer (1997): "System analysis via integral quadratic constraints." *IEEE Transactions on Automatic Control*, **42**, pp. 819–830.

Meyer, M. (1999): "Netzstabilität in grossen Bahnnetzen." *Eisenbahn-Revue*, **No 7-8**, pp. 312–317.

Nesterov, Y. and A. Nemirovski (1993): "Interior point polynomial methods in convex programming." *Studies of Appl. Math, SIAM*, **13**.

Schweer, A. (1999): "Impact of increasing contribution of dispersed generation on the power system." Technical Report 137. CIGRE Working Group 37.23.

Willems, J. C. (1971): *The Analysis of Feedback Systems*. MIT Press, Cambridge, MA, USA.

Zhou, K., J. Doyle, and K. Glover (1995): *Robust and Optimal Control*. Prentice-Hall, Inc., New Jersey, U.S.A.